

**PERFORMANCE EVALUATION OF FIBREGLASS REINFORCED POLYMER  
RESINS IN HYDROMETALLURGICAL PROCESS SOLUTIONS**

By

Muinul Hasan Banna

A THESIS SUBMITTED TO THE SCHOOL OF GRADUATE STUDIES  
IN PARTIAL FULFILMENT OF THE REQUIREMENTS FOR THE DEGREE OF  
MASTER OF ENGINEERING

FACULTY OF ENGINEERING AND APPLIED SCIENCE

MEMORIAL UNIVERSITY OF NEWFOUNDLAND

ST. JOHN'S, NEWFOUNDLAND

AUGUST, 2010

## Table of Contents

LIST OF TABLES .....	i
LIST OF FIGURES .....	ii
LIST OF ACRONYMS AND SYMBOLS .....	x
ABSTRACT .....	xiv
ACKNOWLEDGMENT .....	xvi
Chapter 1 .....	1
INTRODUCTION AND OBJECTIVES .....	1
1.1 The Use of FRP .....	1
1.2 Objectives .....	2
Chapter 2 .....	4
LITERATURE REVIEW .....	4
2.1 Structure of FRP Material and its Composition: Background on Mechanical Properties:.....	5
2.1.1 Resin and Hardener:.....	6
2.1.2 Fibres.....	11
2.1.3 Types of FRP .....	13
2.2 Construction of FRP Tanks, Pipes and Components .....	14
2.2.1 Filament Winding: .....	15
2.2.2 Custom Contact Moulding:.....	16
2.2.3 Spray-up Moulding: .....	17
2.2.4 Bag Moulding and Autoclaving.....	17
2.2.5 Vacuum Moulding .....	18
2.2.6 Hot Press and Cold Press moulding.....	18

2.3	Standard Tests to Characterize FRP Resins and their Composites .....	18
2.4	Deterioration of FRP Tanks due to Process condition .....	20
2.4.1	Application of FRP in Highly Corrosive environment .....	20
2.4.2	Effect of Moisture, Temperature and Exposure time.....	23
2.4.3	Deterioration of FRP Tanks due to Heat and Fire .....	25
2.5	Mechanism of Failure.....	26
2.5.1	Tensile Strength of Composites .....	27
2.5.2	Failure of Fibre .....	28
2.5.3	Failure of Resins .....	28
2.5.4	Failure Criteria for Composites .....	29
2.5.5	Fracture of FRPs .....	31
2.6	Deterioration of FRP Tanks in Hydrometallurgical Process condition.....	32
2.6.1	Nickel Extraction Process .....	32
2.6.2	Probable Factors of Degradation when Exposed to Hydrometallurgical Process Condition.....	39
2.7	Microstructure .....	44
2.8	Expected Outcome .....	44
Chapter 3	.....	46
STRATEGY AND SELECTION OF TESTS	.....	46
3.1	Available Material and Selected Tests .....	46
3.1.1	Standard Tests.....	46
3.1.2	Developed Test Method.....	47
3.2	Evaluation of the Tests .....	47
3.3	Strategy.....	48

Chapter 4.....	49
EXPERIMENTAL SPECIMENS AND TESTS .....	49
4.1 Preparation of Test Specimens .....	49
4.1.1 Specimens Made from Resin .....	50
4.1.2 Specimens Made from Tube .....	51
4.1.3 Specimens Made from FRP Plates.....	52
4.2 Materials Available/ Used.....	52
4.2.1 Resins:.....	52
4.2.2 Commercially Available FRP Tubes .....	52
4.2.3 FRP Sheets .....	54
4.3 Exposure:.....	54
4.3.1 Liquid Used and Temperature of Exposure .....	55
4.3.2 Methods of Exposure .....	55
4.4 Number of Specimens Tested: .....	56
4.5 Conditioning of Test Specimens: .....	56
4.6 Atmospheric Condition of the Test Room: .....	57
4.7 Tests on Resins.....	57
4.7.1 Tensile Test (ASTM D638) .....	57
4.7.2 Bending Test (ASTM D790) .....	60
4.7.3 Micro Hardness Test (Vickers).....	64
4.7.4 Heat Deflection Temperature (ASTM D648).....	67
4.8 Tests on Tube Sections.....	70
4.8.1 Tensile Test on Lateral Loaded Tube Sections.....	70
4.8.2 Compression Test on Axial Loading Test Sections.....	73

4.8.3	Three Point Load Bending for Tube Sections.....	75
4.9	Examination of FRP Structure and Effect of Exposure on Resins.....	78
4.9.1	Optical Microscopy.....	78
4.9.2	Scanning Electron Microscopy.....	80
Chapter 5	.....	81
RESULTS AND DISCUSSION	.....	81
5.1	Tensile Test ASTM D638:.....	81
5.1.1	Repeatability of the Test.....	82
5.1.2	Effect of Exposure Duration on Stress Strain Curve.....	83
5.1.3	Effect of Different Resins and Solutions on Stress Strain Curve.....	86
5.2	Bending Test (ASTM D790).....	89
5.2.1	Phase 1 Bending test.....	90
5.2.2	Repeatability of Test.....	91
5.2.3	Effect of Exposure Duration.....	93
5.2.4	Effect of Resins and Solution.....	96
5.2.5	Effect of Temperature of Exposure.....	96
5.2.6	Test for FRP Samples.....	99
5.3	Micro Hardness Test:.....	101
5.3.1	Repeatability of the Test.....	103
5.3.2	Effect of Duration of Exposure and Surface Preparation.....	104
5.3.3	Effect of Resin and Solution.....	105
5.3.4	Effect of Temperature.....	106
5.3.5	Effect of Exposure on Microhardness at Different Depth of Penetration.	107
5.4	Heat Deflection Temperature ASTM D648.....	110

5.5	Tensile Test on Laterally Loaded Pipe Section.....	111
5.5.1	Repeatability of Test.....	112
5.5.1	Effect of Exposure Duration .....	115
5.5.1	Effect of Resins and Solution .....	118
5.6	Compression Test on Axially Loaded Pipe Section.....	120
5.6.1	Repeatability of the Test .....	121
5.6.2	Effect of Duration of Exposure.....	123
5.7	Three Point Bending Test on FRP Pipe Section .....	125
5.7.1	Repeatability of the Test .....	125
5.7.2	Effect Exposure Duration .....	126
5.7.3	Effect of Resins and Solution .....	128
5.7.4	Effect of Temperature and Exposure .....	129
5.8	Microstructure Assessment .....	131
5.8.1	Optical Microscopy.....	132
5.8.2	Scanning Electron Microscopy.....	136
Chapter 6	.....	142
CONCLUSIONS	.....	142
6.1	Test on Resins .....	142
6.2	Tests on FRP Tube Sections.....	144
6.3	Study of Microstructure .....	144
Chapter 7	.....	145
RECOMMENDATION FOR FUTUTRE WORK	.....	145
REFERENCES	.....	- 147 -
APPENDIX 1: TEST RESULT	.....	- 154 -

APPENDIX 2: SAMPLE RAW DATA .....- 160 -

## LIST OF TABLES

Table 2-1 Fatigue values of GFRV2 composite for Dry heat-70°C exposed for 300 hours (Shafeeq, 2006) .....	43
Table 5-1 Tensile test results of unexposed polyester for testing repeatability ....	82
Table 5-2 Bending test result (phase 1) .....	91
Table 5-3 Results of bending test ASTM D790.....	98
Table 5-4 Result for ASTM D790 test for fibre reinforced polymers .....	101
Table 5-5 Heat deflection temperature results .....	111
Table 5-6 Tube section tensile test results of unexposed H150 and P150 pipe sections for testing repeatability .....	114
Table 5-7 Result for tensile test on laterally loaded pipe sections.....	119
Table 5-8 Compression test result for the on axially loaded pipe.....	124
Table 5-9 Three point bending test results for FRP pipe sections .....	131

## LIST OF FIGURES

Figure 2-1 Synthesis of polyester (Mallik, 1988).....	8
Figure 2-2: Bisphenol-A epoxy based acrylate vinyl ester resin (Mallick, 1988)...	10
Figure 2-3 Diglycidyl ethers of bisphenol-A (DGEBA) (Bunsell & Renard, 2005).. .....	10
Figure 2-4 Manufacturing process of glass fibre (Mallick, 1988).....	12
Figure 2-5: Filament Winding ( <i>Reinforced Plastic</i> , 2010).....	16
Figure 2-6 Custom Contact Moulding ( <i>Reinforced Plastic</i> , 2010) .....	16
Figure 2-7 Flowsheet for Nickel extraction (Snow, 2005).....	33
Figure 4-1 Mould made of ABS material fabricated using rapid prototype machine and a polyester specimen made from that mould. ....	50
Figure 4-2 Preparation of room temperature vulcanized rubber mould for preparing bending test specimen.....	51
Figure 4-3 FRP pipes used to prepare tube samples.....	53
Figure 4-4 Two sides of FRP sheets.....	54
Figure 4-5 Exposure of specimens .....	56
Figure 4-6: Casting of Tensile test specimen .....	57
Figure 4-7: Tensile test specimen.....	58
Figure 4-8: Tensile test experiment setup .....	59
Figure 4-9: Extensometer and the grip of the jig.....	59

Figure 4-10 Preparation of bending test samples .....	60
Figure 4-11: Bending test frame- phase 1 .....	61
Figure 4-12 Bending test rig (phase 1).....	62
Figure 4-13 Bending test specimen .....	62
Figure 4-14 Phase 2 bending test apparatus .....	63
Figure 4-15 Bending test apparatus: supports and loading bar .....	64
Figure 4-16 Schematic diagram of the Vickers Hardness testing apparatus from Instruction for Micromet hardness tester (manual) .....	65
Figure 4-17 Microhardness test apparatus.....	66
Figure 4-18: 40X magnification of an indentation in the resin .....	66
Figure 4-19 Preparation of HDT mould (a) Mould is assembled with side and bottom support (b) Disassembled support mould and specimen.....	67
Figure 4-20 Exposed heat deflection temperature test specimen exposed to 1M H <sub>2</sub> SO <sub>4</sub> for 4 weeks.....	68
Figure 4-21: Heat deflection temperature measuring apparatus.....	69
Figure 4-22 Apparatus for heat deflection test.....	70
Figure 4-23 Unexposed FRP specimen .....	71
Figure 4-24 H150 specimens prepared for exposing in 1M H <sub>2</sub> SO <sub>4</sub> acid solution...	71
Figure 4-25 Design of jig for laterally loaded tubular test specimen .....	72
Figure 4-26 Tensile test rig for laterally loaded pipe sections .....	73
Figure 4-27 Compression test samples.....	74
Figure 4-28 Self aligning plate for compression test.....	74

Figure 4-29 Compression test rig .....	75
Figure 4-30 Bending test specimen after test .....	76
Figure 4-31 Design for three point bending test jig for FRP section .....	77
Figure 4-32 Three point bending test apparatus for FRP samples .....	77
Figure 4-33 Specimen preparation for microstructure examination (a) before polishing (b) after polishing (thin section) .....	79
Figure 4-34 Microscope and camera used for analysing the microstructure of the FRP pipes.....	79
Figure 5-1 Tensile stress versus strain for four polyester specimens .....	83
Figure 5-2 Effect of duration of exposure on exposed polyester specimen (a) when exposed to acid (b) when exposed to Cobalt spent electrolyte at 75°C.....	84
Figure 5-3 Effect of exposure duration on bisphenol A epoxy vinyl ester to (a) 1M H <sub>2</sub> SO <sub>4</sub> and (b) Hydrometallurgical solution at 75°C. ....	85
Figure 5-4 Effect of different resins on tensile stress strain curve when the specimens are exposed to (a) 1M H <sub>2</sub> SO <sub>4</sub> and (b) Cobalt spent electrolyte solution at 75°C.....	87
Figure 5-5 Effect of different resins on tensile stress strain curve exposed to 1M H <sub>2</sub> SO <sub>4</sub> at 75°C.....	88
Figure 5-6 Effect of exposure (exposed to 1M H <sub>2</sub> SO <sub>4</sub> ) and different resin on flexural stress strain curve .....	90
Figure 5-7 Repeatability of bending test specimen for (a) unexposed polyester and (b) bisphenol A epoxy vinyl ester exposed to 1M H <sub>2</sub> SO <sub>4</sub> at 75°C for 1 week.....	92

Figure 5-8 Flexural stress strain curve for unexposed and exposed bisphenol A epoxy vinyl ester to 1M H <sub>2</sub> SO <sub>4</sub> and cobalt spent electrolyte .....	93
Figure 5-9 Flexural stress strain curve for unexposed and polyester to 1M H <sub>2</sub> SO <sub>4</sub> and cobalt spent electrolyte at 75°C for 1 week .....	94
Figure 5-10 Flexural stress strain curve for unexposed and exposed poly ester to 1M H <sub>2</sub> SO <sub>4</sub> and cobalt spent electrolyte at 75°C for 4 week .....	94
Figure 5-11 Flexural stress strain curve for unexposed and exposed bisphenol A epoxy vinyl ester to 1M H <sub>2</sub> SO <sub>4</sub> and cobalt spent electrolyte .....	95
Figure 5-12 Effect of exposure duration on modulus of flexural stress versus strain curve for different resins and exposure condition when exposed to 1 M H <sub>2</sub> SO <sub>4</sub> or Cobalt spent electrolyte at 75°C. ....	96
Figure 5-13 Effect of resin and solution on the modulus of stress strain curve when exposed to 1M H <sub>2</sub> SO <sub>4</sub> and cobalt spent electrolyte for 1 week at 75°C.....	96
Figure 5-14 Flexural Stress versus strain curve for (a) polyester and (b) bisphenol A epoxy vinyl ester when exposed to 1M H <sub>2</sub> SO <sub>4</sub> and cobalt spent electrolyte at 25°C .....	97
Figure 5-15 Effect of temperature on the modulus for different resins and exposure when exposed for four weeks .....	98
Figure 5-16 Flexural stress versus strain curve for glass fibre reinforced (a) polyester (b) bisphenol A epoxy vinyl ester for different exposure conditions exposed for four weeks at 75°C.....	100

Figure 5-17 Effect of different exposure conditions for different resin on stress versus strain modulus for 4 weeks at 75°C.....	101
Figure 5-18 Repeatability of micro hardness test of unexposed polished polyester resin for different weights of indentation. ....	104
Figure 5-19 Effect of exposure duration on Vickers hardness when exposed to 1M H2SO4 at 75°C for (a) polished surface and (b) unpolished surface.....	105
Figure 5-20 Effect of solution on Vickers average micro hardness at loads 5, 10, 15, 20 and 25 gram for different resins for (a) polished and (b) unpolished surface when exposed at 75°C for 4 weeks .....	106
Figure 5-21 Effect of exposure temperature on Vickers hardness for (a) polished and (b)unpolished surface exposed for 4 weeks.....	107
Figure 5-22 Change of hardness of polished surface with depth of indentation for (a) polyester exposed at 75°C (b) bisphenol A epoxy vinyl ester exposed at 75°C (c) ) polyester exposed at 25°C (b) bisphenol A epoxy vinyl ester exposed at 25°C .	109
Figure 5-23 Change of hardness of unpolished surface with depth of indentation for (a) polyester exposed at 75°C (b) bisphenol A epoxy vinyl ester exposed at 75°C (c) polyester exposed at 25°C (d) bisphenol A epoxy vinyl ester exposed at 25°C....	110
Figure 5-24 Applied force for laterally loaded tube sections. ....	112
Figure 5-25 Repeatability of laterally loaded tube section for (a) unexposed H150 (bisphenol A epoxy vinyl ester) and (b) unexposed P150 (bisphenol A epoxy novolac vinyl ester) pipe sections.....	113

Figure 5-26 Force per unit length vs deflection curve for different exposure duration when H150 pipe sections are exposed to (a) cobalt spent electrolyte and (b) 1M H <sub>2</sub> SO <sub>4</sub> at 75°C. ....	116
Figure 5-27 Force per unit length vs Deflection curve for different exposure duration when P150 pipe sections are exposed to (a) cobalt spent electrolyte and (b) 1M H <sub>2</sub> SO <sub>4</sub> at 75°C. ....	117
Figure 5-28 Effect of exposure duration for different resins exposed to different solutions at 75°C on (a) slope of force per unit length vs deflection curve and (b) force for the first failure .....	118
Figure 5-29 Effect of solutions on different resins for different durations of exposure at 75°C on (a) slope of force per unit length vs deflection curve and (b) force per unit length for the first failure .....	119
Figure 5-30 Stress versus strain for compression for exposure to 1M H <sub>2</sub> SO <sub>4</sub> and cobalt spent electrolyte exposed for different times for (a) P150 (bisphenol A epoxy novolac vinyl ester) and (b) H150 (bisphenol A epoxy vinyl ester) FRP pipe sections exposed at 75°C .....	122
Figure 5-31 Effect of time on (a) slope of stress versus strain and (b) first failure force for different resins exposed to 1M H <sub>2</sub> SO <sub>4</sub> and cobalt spent electrolyte.....	123
Figure 5-32 Effect of resins for different duration of exposure and resins on the modulus of stress versus strain curve for (a) modulus of stress versus strain curve and (b) force per unit length for the first failure.....	124

Figure 5-33 Repeatability test of the results for 3 point bending test for FRP pipe section made of (a) P150 material and (b) H150 material.....	126
Figure 5-34 Flexural stress versus strain curve for different duration and exposure condition for (a) H150 and (b) P150 pipe sections.....	127
Figure 5-35 Effect of exposure duration on (a) modulus of stress strain curve and (b) flexural stress at 5% strain for specimens exposed at 75°C to cobalt spent electrolyte and 1M H <sub>2</sub> SO <sub>4</sub> .....	128
Figure 5-36 Effect of resins on (a) modulus of stress strain curve and (b) flexural stress at 5% strain for different resins exposed at 75°C for four weeks .....	129
Figure 5-37 Flexural stress versus strain curve for different material exposed to cobalt spent electrolyte and 1 M H <sub>2</sub> SO <sub>4</sub> for four week at 25°C .....	130
Figure 5-38 Effect of exposure temperature on (a) flexural stress at 5% strain and (b) modulus of stress strain curve for specimens exposed to cobalt spent electrolyte and 1M H <sub>2</sub> SO <sub>4</sub> .....	131
Figure 5-39 Microstructure of commercially available FRP pipes by optical microscopy at 100X magnification of (a) outer layer, (b) interphase interface between inner and outer layer and (c) inner layer. All images are of area 10 mm by 15 mm wide in the original.....	134
Figure 5-40 Polyester specimens: unexposed (left) and exposed to 1M H <sub>2</sub> SO <sub>4</sub> for four weeks at 75°C. (Magnification 32X) .....	135
Figure 5-41 Bisphenol A epoxy vinyl ester resin: unexposed (left) and exposed to 1M H <sub>2</sub> SO <sub>4</sub> for four weeks at 75°C (Magnification 32X). .....	135

Figure 5-42 Unexposed (left) and exposed (right) surfaces of H150 pipe section.	136
Figure 5-43 Fibre pull out of a bending test specimen after the test. ....	137
Figure 5-44 (a) Polyester Unexposed surface and (b) Polyester exposed surface (exposed to 1M H <sub>2</sub> SO <sub>4</sub> for four weeks).....	137
Figure 5-45 Energy dispersive spectra of a cross-section of (a) unexposed polyester (a) exposed polyester on crack (b) exposed polyester not on a crack 0.1 mm away from surface.....	138
Figure 5-46 SEM image of bisphenol A epoxy vinyl ester for (a) unexposed and (b) exposed surface to 1M H <sub>2</sub> SO <sub>4</sub> for 4 weeks .....	138
Figure 5-47 Energy dispersive spectra of unexposed (left) and exposed (right) bisphenol A epoxy vinyl ester at 0.1 mm inside of outer surface. ....	139
Figure 5-48 SEM image of H150 pipe inner surface for (a) unexposed and (b) exposed surface to 1M H <sub>2</sub> SO <sub>4</sub> for 4 weeks .....	140
Figure 5-49 Energy dispersive spectra of (a) unexposed and (b) exposed H150 pipe section (bisphenol A epoxy vinyl ester) at 0.1 mm away from surface. ....	140
Figure 5-50 X-Ray MAP of H150 inner pipe section exposed for 4 week to 1 M H <sub>2</sub> SO <sub>4</sub> . The left side of the figure is the inner surface (total width 0.62 mm) .....	141

## LIST OF ACRONYMS AND SYMBOLS

2-D	Two Dimensional
3-D	Three Dimensional
ABS	Acrylonitrile Butadiene Styrene
AOC	Alpha Corporation of Coleirville
ASTM	American Society for Testing Material
ASTM D638	Standard test method for tensile properties of plastics
ASTM D648	Standard test method for deflection temperature of plastic under flexural load in the edgewise position.
ASTM D790	Standard test methods for flexural properties of reinforced and unreinforced plastic and electrical insulating material
ASTM D3039	Standard test method for tensile properties of polymer matrix composite material.
ASTM E399	Standard test method for the linear elastic plain strain fracture toughness $K_{IC}$ of metallic materials
a.u.	arbitrary unit
C Glass	Chemical Resistant Glass
DGEBA	Di-Glycidyl Ether of Bisphenol A
DIN	Deutsches Institut für Normung (German Institute for Standards)
DIN 53445	Testing of Polymer Materials: Torsion Pendulum Test. 1965
E Glass	Electrical Application Glass

EPC	Exposed polyester exposed to Cobalt spent electrolyte
EBC	Exposed Bisphenol A epoxy vinyl ester exposed to Cobals spent electrolyte
EPA	Exposed Polyester exposed to 1M sulphuric Acid
EBA	Exposed Bisphenol A epoxy vinyl ester exposed to 1M sulphuric Acid
FeO	Wüstite
Fe <sub>2</sub> O <sub>3</sub>	Hematite
Fe <sub>3</sub> O <sub>4</sub>	Magnetite
FRP	Fibre Reinforced Plastic
GFRV2	Glass Fibre Reinforced Vinyl Ester (Batch 2)
GPa	Giga Pascal
H150	Bisphenol A Epoxy Vinyl Ester FRP Pipe
H <sub>2</sub> SO <sub>4</sub>	Sulfuric Acid
HCl	Hydrochloric Acid
LVDT	Linear Variable Displacement Transducer
MEKP	Methyl Ethyl Ketone per Oxide
NaOCl	Sodium Hypochlorite
NaOH	Sodium Hydroxide
P150	Bisphenol A Novlac Vinyl Ester
PC	Personal Computer
RTV	Room Temperature Vulcanized

S Glass	High Strength Glass
SEM	Scanning Electron Microscopy
UP	Unsaturated Polymer
VHN	Vickers Hardness Number
$l_c$	critical fibre length
$\sigma$	Stress
$\sigma_{cl}^*$	longitudinal strength of composite
$\sigma_m'$	Ultimate tensile strength of matrix
$\sigma_f'$	Ultimate tensile strength of fibre
D	Diffusion coefficient
$D$	Deflection of the specimen due to applying load
d	diameter of the fibre
$d$	thickness of the specimen
$\tau_c$	Fibre matrix bond strength
$K_I$	Stress Intensity Factor
$\pi$	pi
a	Crack Length
$\gamma$	Geometric Factor
$V_f$	Volume fraction of glass
$E_{cd}$	Elastic modulus of composite
K	Fibre efficiency parameter that depends on $E_f/E_m$
$E_f$	Elastic modulus of fibre

$E_m$	Elastic Modulus of the matrix
Ni	Nickel
Cu	Copper
Co	Cobalt
Zn	Zinc
Pb	Lead
Cl <sub>2</sub>	Chlorine

## **ABSTRACT**

Fibre reinforced plastic (FRP) tanks and pipes exposed to corrosive environment in hydrometallurgical process plants are expected to degrade. The objective of this research is to develop a series of tests which are sensitive to the exposure and will be able to distinguish different materials used for this purpose. In this study both FRP material (pipes and plates) and resins were exposed to different acidic solutions at different temperatures, exposure durations. They were tested by the help of standard ASTM and developed test methods to study whether these tests are sensitive indicators of exposure and if these tests could be used for distinguishing between different materials in their susceptibility to exposure. Microstructure assessment included tests only on resins, a tensile test (ASTM D638), a bending test (ASTM D790), a microhardness test and a heat deflection temperature test (ASTM D648). Among these tests the bending test and the microhardness test showed sensitivity to change of exposure conditions (solution, temperature, duration) and material (polyester and vinyl ester). Commercially available FRP tubes were used as samples for the tests on FRPs. Tests on FRP tube section included a tensile test on laterally loaded tube sections, a compression test and a bending test.

The bending test and the tensile test on laterally loaded tube sections were the more sensitive among the tests done on the FRP tubes. Microstructure analysis of resins and FRPs before and after exposure showed the effect of exposure on the surface of

different resins and provided indication regarding the penetration of the acidic fluid into the material. The tests were carried out after four weeks of exposure which limits the tests results to predict failure due to hydrometallurgical applications of the FRP components. The tests which are more sensitive to the exposure should be carried out for a longer period of time to predict the lifetime of the fibre reinforced plastic pipes and tanks.

## ACKNOWLEDGMENT

The contribution of the individuals who were directly or indirectly associated with this research work are worth much more than the word itself can express.

My first appreciation is for Dr. John Shirokoff and Dr. John Molgaard, who were directly associated in introducing a recent topic of the use of FRP tanks in hydrometallurgical process. I really acknowledge their contribution in guiding me in the design and develop of a series of tests and analyze the results. Dr. Shirokoff and Dr. Molgaard have been really good mentors throughout this time. They did not only guide me throughout this research technically, they also spurred my ability to accommodate myself in a new environment, here in Canada. It had been a great honour to work with such great persons, who were humble even during the hard times, to show me the right track and boost up my confidence in this research.

I would also like to acknowledge Atlantic Canada Opportunity Agency (ACOA) and Vale for their support in funding the project and Institute of Ocean and Technology (IOT), National Research Council (NRC) and Reinforced Plastic Systems (RPS) for their donation of materials.

I am also delighted to acknowledge Michael Shaffer, Steeve Steel and Matt Curtis, who were directly involved in performing different tests on FRPs.

There are many other people who have triggered my enthusiasm since the beginning. I greatly appreciate the contribution of my beloved parents Khawaja Muyeenuddin and Laila Khairun Nahar, who deserve the real honours for this

achievement. Their love and guidance assisted in making my dream come true. It cannot adequately express the contribution of my beloved wife, Shirmin Sultana. Endless support from my friends is greatly appreciated. Their company assisted me in going through the challenging situations.

## **Chapter 1**

### **INTRODUCTION AND OBJECTIVES**

This chapter introduces the use of FRPs, sets up the background of the research and defines the objectives or goals that were set for the research.

#### **1.1 The Use of FRP**

The use of fibreglass reinforced plastic (FRP) tanks is playing an increasingly important role in processes involving highly corrosive environments. A more complex structure with a total reduced maintenance cost can be achieved by using reinforced plastic. The use of the FRP tanks in hydrometallurgical process plants or other components is becoming common. Though the use of FRPs started with the military aircraft, FRPs are now being used in boats, automobiles, electronics, buildings and civil engineering applications. This is a study of ways to test FRPs and the resin used in FRPs for suitability in hydrometallurgy equipment.

“Fibre reinforced composite material consists of fibres of high strength and modulus embedded in or bonded to a matrix with a distinct interface (boundary) between them.” (Mallik, 1988, p 96). Both the resin and the fibre have their own physical and chemical properties but in combination produce a new material which shows such properties that none of its components could have achieved alone. In general, the fibres carry the load and the resin or surrounding matrix keeps the fibre at desired location and orientation, protect the fibre from harmful environment, transfer load. The most common

form of using fibre reinforced composite is in laminates. The laminate is obtained by the stacking of a number of fibres and layers and consolidating them into the desired thickness. Fibre orientation in each layer and the stacking sequence of various layers can then be controlled to generate a wide range of physical and mechanical properties.

## **1.2 Objectives**

The review of literature revealed limited lab work has been conducted directly on the standardization of tests to evaluate the performance of FRP in hydrometallurgical process. A number of standard tests are recommended by ASTM but it is not clear that how sensitive these tests are to exposure for short duration when exposed to hydrometallurgical solution. If these tests are not sensitive to short term exposure it will be difficult, if not impossible, to evaluate the performance with the recommended tests.

The focus was on developing a series of tests which could be easily performed in common facilities mostly based on standard ASTM tests modified as necessary. The scope is to explore ways of testing FRP materials for use in hydrometallurgical processes and to provide guidance in selection of most suitable material. The specific objectives are listed below.

1. To develop a series of tests which are reproducible and sensitive to short term exposure to hydrometallurgical solutions.
2. To understand the mechanism of failure of the FRP materials due to exposure.
3. To analyse the failure mechanisms of specimens during modified tests and predicting the sensitivity of the tests.

Recognizing that the ability of the resin to withstand exposure is a key aspect of the performance of an FRP (if the acidic fluid penetrates through a resin layer only then glass fibre will be affected), some tests were carried only on resin samples.

Multiple samples of FRP with identical structure can be readily obtained from commercially produced tubing. So tests based on these materials were explored.

## **Chapter 2**

### **LITERATURE REVIEW**

Fibreglass reinforced plastic (FRP) composites are a good choice for use in the process industry in terms of their expense per life cycle. But their use may present hazards in case of accidents and fire as they are obviously more susceptible to degradation from high temperature and impact loading when compared to their counterpart: higher priced metal alloys.

The deterioration of the fibre reinforced composites at high temperature has been modelled and verified by many researchers over the past few decades. Sullivan (1993) developed a model for the thermal and structural response of a polymeric composite (glass phenolic material and the design is known as H41N) during chemical degradation. He compared his results with Rammamurthy (1988) for validation. Later Feih et al. (2007) developed another model for determining the temperature and structure for a polymer composite. This validated model predicted the response of the whole body of a fibre glass vinyl ester composite at a temperature up to until the start of ignition of the sample.

A considerable number of references exist in the literature concerning the prediction of the service life of FRP material which is being exposed to the environment. This includes describing the mechanism of environmental degradation (Mills, 1993; Barkatt, 2001); models for FRP properties in exposed condition (Springer,1988); methods

for predicting the properties to the exposure of the FRPs in typical service condition and analyzing the properties after the exposure (Shafeeq, 2006).

An example is the model based on hygrothermal stress distributions reported by Springer (1988). The material swells up or changes its shape due to absorption of moisture and change of temperature. A load develops at the interface of the matrix and fibre because the change of length is different for the components of FRPs. This load is known as hygrothermal load. In this model the temperature and moisture distribution inside the material are determined through analysis, then the hygrothermal stress and strain is calculated, and lastly the change of performance of the material is evaluated from the stress-strain. Ngoy et al. (2009) established a model considering the chemical degradation, physical degradation and mechanical degradation of the composite and the stress is modified considering the effect of hygrothermal stresses. All the factors considered result in a mathematical model representing the change of the chemical and mechanical structure and properties of the FRP.

## **2.1 Structure of FRP Material and its Composition: Background on Mechanical Properties:**

The structure of the FRP material is a complicated one because it is a combination of two materials. Depending upon the structure the mechanical properties will vary. As has been mentioned before, the composite material is built up in layers or laminates. The variables in each laminate are numerous, for example, the type of resin, the type of hardener, proportion of the resin and hardener, type of fibre, length of fibre, orientation of fibre, etc. The arrangement or orientation of the laminates may also vary. In this section

the main variation of the components i.e. the resin and the fibre reinforcement will be discussed.

### **2.1.1 Resin and Hardener:**

One of the main advantages of using a composite material is that it can be designed as needed for the particular application. For example if an FRP has to be chosen for body parts its resin has only to be able to stand against hot and humid conditions which may be well served by polyester. If it is a tank used in highly corrosive environment different types of epoxy vinyl ester resin may be used. Typically, the resin component of most common composite materials with fibreglass, carbon fibre, and Kevlar, are formed from at least two parts, the catalyst and the resin. Different types of resins and their properties are discussed here in more detail. As this research involves the testing of polyester and bisphenol-A epoxy vinyl ester resins and their composites, their properties are discussed here in more detail. The types of the resins may be classified on the basis of the change of mechanical properties with temperature (thermosetting and thermoplastic), depending on their use (flame-retardant polymer, chemically inert polymer) and depending on the composition of the monomer (poly ester, epoxy vinyl ester). In this section various widely used resins are described. If we want to categorize the basis of these resins, which are discussed in this section, they may fall under "Commercial Thermoset Polymers".

#### **2.1.1.1 Polyester:**

Polyesters are heterochain macromolecular substances and they are characterized by the presence of carboxylate ester groups (-CO-O-) in the repeating unit of the main

chains (Kulshershta & Vasile, 2002). A wide variety of polyesters are available nowadays. Similar to the use of composite material, polyester is gaining increased importance in the last few decades due to a wide range of application in all major industries such as textile fibres (Bansal, Mittal & Sing, 1989), paints, varnishes, printing inks, adhesives (Japan Patent No JP05148379, 1993), wire insulation, moulding, packaging, laminate coating, composites (Weng, Hiltner & Baer, 1989), production of boats, bath, shower units, etc.

An unsaturated polyester resin that contains a number of C=C double bonds is the starting material for a thermoset polyester. The reaction between maleic anhydride and ethylene glycol produces it. To modify the chemical structure between the cross linking sites, saturated acid is added. The resultant liquid is diluted by a polymerizable substance (styrene). A very small amount of inhibitor is also added to inhibit polymerization while it is stored. The curing reaction for polyester resin starts when a small amount of catalyst (i.e. organic peroxide methyl ethyl ketone peroxide (MEKP)) is added. This catalyst breaks the unsaturated C-C bonds in the styrene and in turn styrene reacts and apparently joins the polyester molecules as follows.

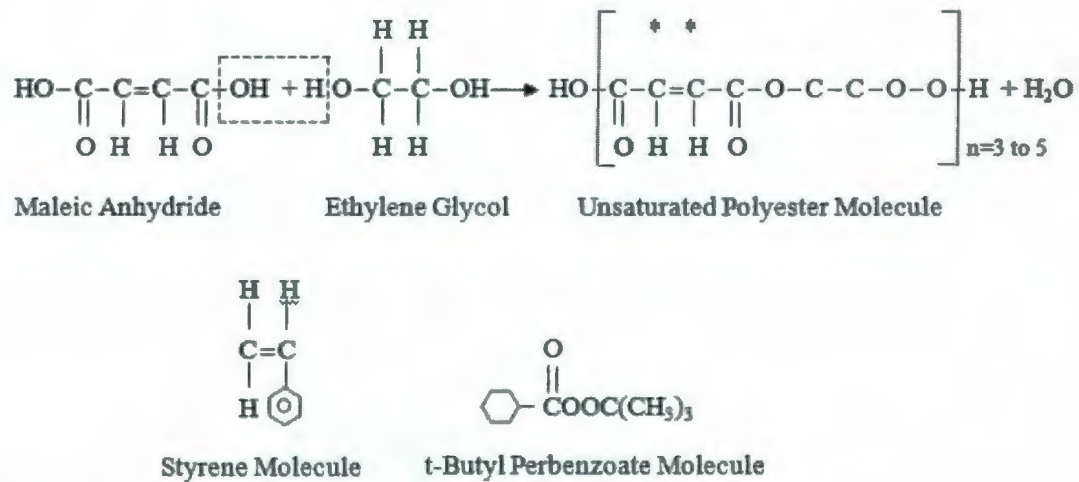


Figure 2-1 Synthesis of polyester (Mallik, 1988)

The color of the polyester resin is yellowish and semitransparent. Its low cost and ease of application made it suitable for most of the backyard projects. But due to its sensitiveness to UV rays, it usually requires a protective coating. Its hardener or the catalyst is usually MEKP as discussed earlier. Polyester resin can have a wide range of properties depending on its curing process. Therefore they can be hard and brittle or soft and flexible; however their properties are usually lower than the epoxies. The principle disadvantage of polyester as compared to the epoxies is its high shrinkage rate upon curing. But the low cost and excellent quality in normal condition has made polyester the most widely used resin in FRP components.

#### 2.1.1.2 Vinyl Ester

Vinyl ester resins are thermoplastic and they consist of a polymer which terminates with R-CH<sub>2</sub>-CH<sub>3</sub>. The vinyl ester resin is derived from polyester or epoxy

resin. After curing vinyl ester resins transform into thermosetting resins forming a 3-D network structure. Vinyl-ester resin tends to have a purplish to bluish to greenish tint (Composite material, 2010). The viscosity of this resin in the liquid form is much lower than polyester resin, and it is more transparent. This resin is often termed as being fuel resistant, but it will liquefy when in contact with gasoline. This resin is more resistant over time to degradation than polyester resin and it is more flexible. The catalyst or hardener, the mix ratio of hardener to resin and the chemical cost is almost the same as the polyester resin for common vinyl ester resin.

Vinyl ester resin can be divided into two classes (i) the epoxy vinyl ester resins and the non epoxy vinyl ester resins. Those with epoxy structure are of commercial significance (Kulshershta & Vasile, 2002). In the experiments reported in this thesis bisphenol-A epoxy vinyl ester resin was studied so it is important to provide some background information on this particular resin. The epoxy vinyl ester resins have mainly a backbone of epoxide resulting from the reaction of bisphenol-A and epichlorohydrin and terminated at both ends by acrylate or methacrylate functions; they are named as bisphenol-A epoxy based acrylate or methacrylate vinyl ester resin. Some of these resins may be produced from the phenol resin which have been modified by the acrylic or methacrylic acids and are called phenolic novolac epoxy based vinyl ester resin. Epoxy vinyl ester resins can be produced from any epoxy resins depending on the properties needed. The bisphenol-A epoxy resin has excellent mechanical properties as well as good thermal resistance.

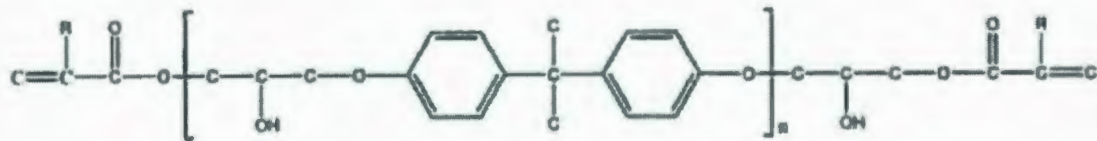


Figure 2-2: Bisphenol-A epoxy based acrylate vinyl ester resin (Mallick, 1988).

Epoxy vinyl ester resins are based on the epoxy resins. Same as unsaturated polyester resins, they are modified in such a way that they can be cured via free radical mechanism with styrene as a co-occurring monomer.

### 2.1.1.3 Epoxy

Epoxy resins are generally considered with better properties than polyester resins. The molecular structure of epoxy resins is based on the epoxy or oxirane group as shown in the Figure 2-3. The commercially most important epoxy resin is known as diglycidyl ethers of bisphenol-A (DGEBA) (Bunsell & Renard, 2005).

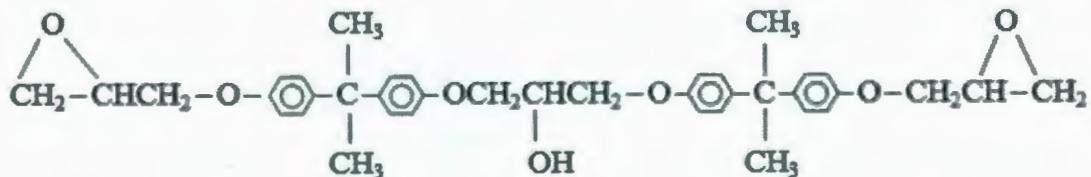


Figure 2-3 Diglycidyl ethers of bisphenol-A (DGEBA) (Bunsell & Renard, 2005)

Curing of epoxies is carried out usually by amine, anhydrides or catalytic agents. Epoxy resin is almost totally transparent when cured. In the aerospace industry, epoxy is used as a structural matrix material or as structural glue.

### **2.1.2 Fibres**

The manufacturing of a composite structure starts with the incorporation of a large number of fibres into a thin layer of matrix to form a lamina or ply. Continuous fibres that are used in making lamina may be arranged either in a unidirectional or in a bidirectional orientation. For a lamina containing unidirectional fibres the composite material will have highest tensile strength along the direction of the fibres. Proper selection of the type, quantity and orientation of fibres is very important because it controls the specific gravity, tensile strength and modulus, compressive strength and modulus, compressive strength and modulus, fatigue strength, electrical and thermal conductivity and cost. Fibres can carry a huge load before fracture provided there is no flaw present.

#### **2.1.2.1 Glass Fibres**

Glass fibres are most common of all the reinforcing fibres for polymeric (plastic) composites. The principle advantage of glass fibres are low cost, high tensile strength, when undamaged, high chemical resistance and excellent insulating properties. The disadvantages are low tensile modulus, relatively high specific gravity sensitive to abrasion with handling relatively low fatigue resistance and high hardness. The two types of glass fibres most commonly used are E glass and S glass. In chemical applications another type of glass fibre, called C glass, is usually used. The manufacturing process of glass fibre is shown in the figure 2-4. The basic principle involves drawing molten glass through a designed nozzle. The form of the glass fibres used in the composite material are different i.e. continuous strand roving, woven roving, chopped strand, chopped strand

mat and woven roving mat. The average tensile strength of freshly drawn glass fibres may exceed 3.45 GPa. However, surface flaws produced by abrasion arise either by rubbing against each other or against the process equipment tends to reduce its values to 1.7 GPa. Surface flaws increase under the presence of cyclic load, exposure to chemicals, water and so on.

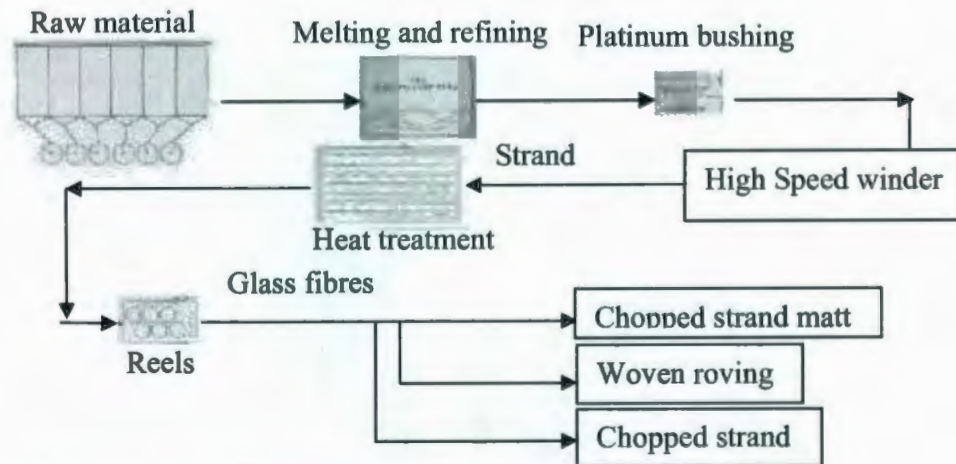


Figure 2-4 Manufacturing process of glass fibre (Mallick, 1988)

#### 2.1.2.2 Carbon Fibres

The tensile modulus of commercially available carbon fibres varies from 270 GPa to 517 GPa. The high tensile strength-to-weight ratio and tensile modulus-to-weight ratio, very low coefficient of linear thermal expansion and high fatigue strength are common properties of carbon fibres. In addition, they are known to have low impact resistance and high electricity conductivity. Carbon fibres are manufactured from textile precursors (starting material: most common polyacrylonitrile) and pitch precursors. The basic form in which carbon fibres are available is called "tow". It is a bundle of up to 160,000 parallel filaments (Mallick, 1988).

### **2.1.2.3 Kevlar Fibres**

Kevlar is a highly crystalline aramid (aromatic polyamide) fibre. The repeating unit in Kevlar is an amide group and an aromatic ring. Kevlar is manufactured by extruding an acidic solution of a proprietary precursor from a spinneret. These fibres are available as yarns, roving and fabrics (Mallick, 1988).

### **2.1.2.4 Other fibres**

Boron fibre, silicon carbide and aluminum oxide are also fibres of varying importance and properties. For example boron fibre has extremely high tensile modulus, which is in the range of 379 - 414 GPa. Silicon carbide retains its tensile strength above 650°C and aluminum oxide has an excellent strength retention up to 1370°C (Mallick,1988).

## **2.1.3 Types of FRP**

Fibre reinforced plastics can be categorized depending upon the types of fibre, resin, and application. Categories based on fibre type include glass fibre reinforced plastic, carbon fibre reinforced plastic and boron fibre reinforced plastic. Categories depending upon resin involve polyester, vinyl ester, etc. Finally, various FRP types that are based on applications that are known include fire resistant, heat resistant and corrosion resistant. The purpose of our research is to evaluate the performance of various FRPs suitable for corrosive environment, reinforced by glass fibres. Therefore after defining several important categories (corrosion resistant, glass fibre reinforced polymers) we should recognize that the fibre length is one of the criteria that govern the properties of the FRPs.

The mechanical characteristics of a fibre reinforced composites not only depends on the properties of the fibre but also the on the degree to which an applied load is transmitted to the fibres by the matrix phase. There is no load transmittance from the matrix at the end of each fibre under any applied load, only along the length of the fibre, limited over each unit area of interface to the strength of the bond between the two materials, or the strength of the resin. Therefore the total force transmitted between the two materials increases with the length of the fibre up to a critical fibre length ( $l_c$ ) as in equation (2-1)

$$l_c = \frac{\sigma_f^* d}{2\tau_c} \quad (2-1)$$

where,  $d$  is the diameter of the fibre,  $\sigma_f^*$  is its ultimate strength  $\tau_c$  is the fibre matrix bond strength (or the shear yield strength of the matrix, whichever is smaller) (Callister, 2005). A composites containing fibres much greater than  $l_c$  (usually 15 times  $l_c$ ) is called continuous or long fibre FRP and if it has smaller sized fibres are called discontinuous type. In application for tanks usually chopped (short fibre) strand mat is used for preparing FRPs.

## 2.2 Construction of FRP Tanks, Pipes and Components

Hand lay-up, filament wound or a combination of these methods is usually involved in tank construction. The finished laminate has a single generic type of thermoset resin throughout and usually does not contain dyes, fillers or pigment unless specified (*Product information Vipel, 2010*). For highly corrosive environments, the inner surface of the tank or pipe consists of a resin rich layer. The outer portions of the pipes

and tanks provide most of the strength and consist of laminates with the same resin and reinforcing glass fibre with increased volume fraction of the glass fibres. Additional reinforcement is provided as necessary to support the required accessories. For instance, the top of the tank has to be reinforced in accordance with the requirement of the applicable governing standard. The surface of a domed top has to be provided with a non-slip finish. Bracketed flat surfaces are provided with each tank so that a liquid level gauge, name plate, certification plate can be installed. Again, a variety of techniques using varying degree of automation are used to fabricate the various components. Each technique or combination of techniques produces a product with unique characteristics.

#### **2.2.1 Filament Winding:**

The filament winding process involves pulling glass fibres under controlled tension, through a catalyzed resin bath. The resin bath travels back and forth past a rotating mandrel, with the angle of fibre placement determined by the translational speed of the resin bath relative to the rotational speed of the mandrel (*Reinforced Plastic*, 2010). Through this motion a pattern is established and maintained until the required thickness is achieved (*Vipel corrosion*, 2010).

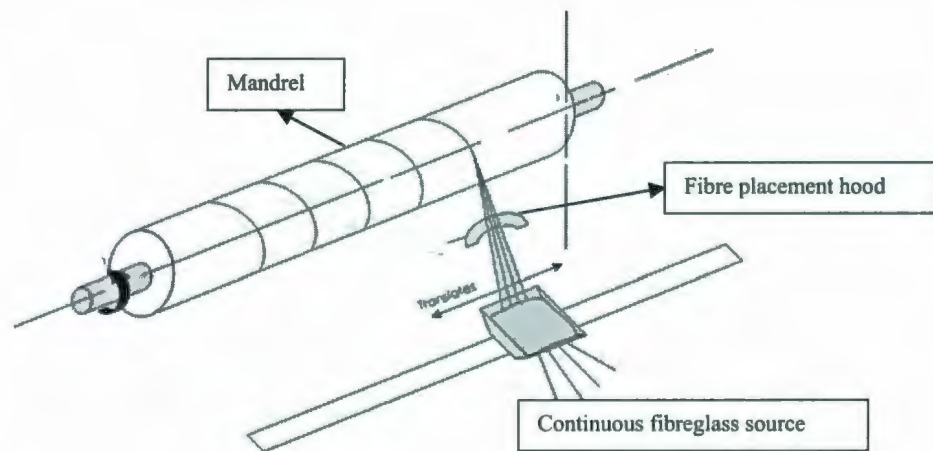


Figure 2-5: Filament Winding (*Reinforced Plastic*, 2010)

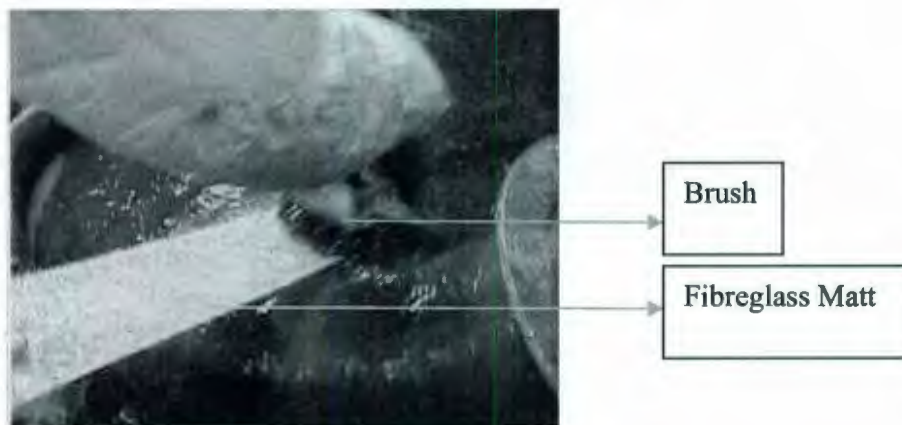


Figure 2-6 Custom Contact Moulding (*Reinforced Plastic*, 2010)

### 2.2.2 Custom Contact Moulding:

In this approach resin and glass fibre is sprayed by spray gun or applied by hand on to stationary or rotating moulds. The resin, reinforcement combination is rolled out to remove entrapped air, compact the layers and ensure complete wetting of the glass fibres. The number of layers that can be continuously applied to the mould is limited since the

heat generated by the resin cure can create blisters in the part. To prevent this laminates are built in stages, which are allowed to cool and cure before the next stage of reinforcement is applied. Each sequence of reinforcement must begin and end with a layer of chopped strand glass to provide proper adhesion (*Vipel corrosion, 2010*).

### **2.2.3 Spray-up Moulding:**

In this application the reinforcing fibre (usually in the chopped form) and the resin is sprayed through a gun into the mould with help of compressed fluid. A handheld spray gun is usually used for this purpose. A continuous fibre from the ribbon is fed to the gun, the fibre is chopped automatically and then sprayed along with the resin on the mould surface. Like the other types of moulding of composite material, for spray-up moulding the entrapped air bubbles has to be removed by the help of a roller brush. Contact moulding and spray up moulding can be used together for fabricating complex composite structure (*Reinforced Plastic, 2010*).

### **2.2.4 Bag Moulding and Autoclaving**

In this method pressure is applied during the cross linking process. A flexible sheet is used to cover the composite lay-up and the edges are sealed. Air is removed from the cover so that the flexible sheet pressurizes the resin and a controlled temperature is maintained with the help of an oven. Moulding in an autoclave is done primarily for the production of a small number of high performance composite structures. It also has the same principle as bag moulding. Typical autoclave moulding consist of a bleeder material to absorb excess resin, a barrier film, breather material to allow uniform pressure over the

composite material and the vacuum bag as employed in case of bag moulding. Similarly, when using autoclaving air is removed from the bag as in the bag moulding process (Mallick, 1988).

### **2.2.5 Vacuum Moulding**

The mould is first filled with the fibre reinforcement and then the resin flows into the evacuated mould via the vacuum pressure involved in the process. The air is removed at the extreme points of the composite material and whenever the resin shows up at any of these points the air removal is stopped. There are several drawbacks of this type of method. The reinforcement can be displaced due to the movement of the viscous resins and the composite can have some porosity due to trapped air (Mallick, 1988).

### **2.2.6 Hot Press and Cold Press moulding**

In this process male and female moulds are fitted together into a hydraulic press which then forms the specified shapes in the heated or unheated resin into the fibre reinforcement which is already inside the mould. Large structures like trucks, cabs (taxi, compartment of trucks, vehicles and trains), roofs for caravans and mobile homes are made by hot press and cold press moulding.

## **2.3 Standard Tests to Characterize FRP Resins and their Composites**

Several American Society for Testing Material (ASTM) standard tests were initially chosen as listed below and evaluated for their suitability for hydrometallurgical applications. As described later, modified versions of several of these tests were used in this work.

a. Standard Mechanical Properties

Tensile Strength

For Resins: ASTM D638-00. Title: Standard Test Method for Tensile Properties of Plastics

For FRPs: ASTM D3039/ D 3039M-00. Title: Standard Test Method for Tensile Properties of Polymer Matrix Composite Materials

Flexural Modulus

ASTM D790. Title: Standard Test Methods for Flexural Properties of Unreinforced and Reinforced Plastics and Electrical Insulating Materials

b. Thermal Properties:

Heat Deflection Temperature:

ASTM D648. Title: Standard Test Method for Deflection Temperature of Plastics Under Flexural Load in the Edgewise Position

Glass Transition Temperature:

DIN 53445. Title: Testing of Polymer Materials; Torsion Pendulum Test

c. Crack Propagation Property:

Stress intensity ASTM E399. Title: Standard Test Method for Linear-Elastic Plane-Strain Fracture Toughness  $K_{IC}$  of Metallic Materials

## **2.4 Deterioration of FRP Tanks due to Process condition**

FRP components are used in many process engineering applications mainly as pipes, storage tanks, and process tanks. The effect of exposing to the solutions of process conditions had been investigated for the past few decades (Mallick, 1988). Most of the literature deals with the most common phenomenon i.e. exposure to water of FRPs or the polymers used as its matrix to water.

### **2.4.1 Application of FRP in Highly Corrosive environment**

Plastics, synthetic resins and reinforced plastics have been playing an extraordinary role in last few decades such that these nonferrous materials are being used more widely with a greater market share each year in the economy. The use of these polymeric reinforced materials reduces labour, enables the operational products to be improved and the dependence on high quality alloys is reduced. Also the fabrication and implementation of FRP tanks for corrosive environment has taken place in recent years (Severov, Posyosoeva, & Litvinenko, 1982; Marsh, 1992).

Consequently research has been going on over the past few decades on the probable failure and means of damage detection in FRP materials. Sprague, Hira and Ahluwalia (2000) devised a way of introducing a conductive veil into the fibre laminated FRPs to detect the electrical conductivity as a function of penetration for various solutions (HCl, Ethylene dichloride, Nitric Acid, NaOCl, NaOH). For HCl there were no change in the conductivity for 15 months and after that an abrupt increase of resistance took place. Though the experiment was meant to devise a new methodology to determine penetration it is to be noted that there was little change in their meter reading up to 15

months. Also, the change of flexural modulus, weight gain, retention of hardness, impact absorption capability due to exposure of polyester to strong acid was investigated by Mahmoud, & Tantawi (2003) to be discussed in section 2.6.2. Determination of diffusion rate in the resins by the percentage of weight gain gives us only an idea about the amount of the fluid absorbed by specimen not the depth up to which the specimen is affected. A method of determining the diffusion of acid into the polymer matrix was pioneered by Marshall, J. P., Marshall, G. P., & Pinzell (1982). The method involves slicing of the samples and determination of the concentration of tritium (isotope of water) in that slice by scintillation counting (radioactive tracer method). The application of this method of measurement has given a clear picture of the way in which water diffuses into glass-reinforced laminates. With the help of the developed method Marshall, J. P. (1982) determined the diffusion coefficient of hydrochloric acid and water into the glass reinforced vinyl ester. The effects of stress and damage on this diffusion of acid and water were also determined. The presence of stress increases the rate of diffusion and it further increases with stress concentration. But his research suggested that there was no wicking (capillary motion) of liquid along the fibres. The depth of penetration for both hydrochloric acid and water after 720 hour was approximately 2.5 mm. It has also been found that the diffusion rate for hydrochloric acid was less than that of water. Another important observation in this study (which is important for this research) is the lower absorption of acid (0.25% by weight) compared to water (0.45% by weight). Specimens exposed to HCl at 50°C gained weight up to 500 hours exposure and then the weight decreased with time. The weight loss is explained by the loss of species from the sample

by the attack of acids. Furthermore this indicates that the acid is attacking glass because vinyl ester resin when exposed alone to the acid with same concentration did not lose weight (Marshall, et al., 1982). Caddock, Evans, & Hull (1987) modified the radioactive tracer method (Marshall, 1982) and investigated the diffusion of hydrochloric acid in polyester thermosetting resins. Water diffuses freely in the resin with a diffusion coefficient,  $D = 3 \times 10^{-9} \text{ cm}^2\text{s}^{-1}$  (at 25°C) for unstressed polymer resin and its saturation concentration is 1 to 2 wt% which is much higher than the hydrochloric acid. Chloride ion did not penetrate through the polymer network (Caddock, Evans & Hull, 1987). Later on Caddock (1989) investigated the effect of applied tensile stress on the diffusion of hydrochloric acid in polyester resins and found the diffusion rate increases for water and hydrochloric has a small increase of diffusion rate due to the effect of stress on the specimens. Hydrogen ion diffusion was measured experimentally through polyester composites exposed to 5%  $\text{H}_2\text{SO}_4$  and 15%  $\text{HCl}$  at 100°C by Regester, (1969). Even after an exposure period of six months no evidence of such diffusion was found.  $\text{H}^+$  ion mobility is restricted by the anion mobility to preserve electrical neutrality within the laminate (Regester, 1969).

Hogg & Hull (1983) found that glass fibre reinforced polyester resin composites may be subject to failure by stress corrosion cracking under the simultaneous effects of low applied stresses and a corrosive environment. Chemical corrosion of the primary load bearing glass fibres was found to be the principal cause of failure (Metcalfe & Schmitz, 1972). Due to fibre failure, stresses increase locally and sharp cracks propagate through

the composite proceeding at an increasing rate as the stress intensity at the crack tip increases. The resulting fracture surface is remarkably smooth in cases of the presence of acidic environment (Hogg & Hull, 1983; Price & Hull, 1983) at low loads. To establish criteria for the long-term service life of pipes and vessels the low stress regime is of particular interest. For these low stress regions it is known (Metcalfe & Schmitz, 1972; Scrimshaw, 1980; Proctor, 1984) that failure of the glass reinforcement may occur if the aggressive agent can gain access to the fibres. Two processes may be liable through which the agent can have access to fibres. Microcracks, or flaws, in the resin can allow passage of the corrosive medium to the fibres by a percolation process. Even in the absence of load, this can be a way of acid penetration (Jones, Mulheron & Bailey, 1983) and is particularly prevalent in crossply laminates due either to residual thermal stresses or to the swelling associated with the uptake of water by the polymer. It can also be assumed that the agent can also pass through the undamaged matrix of FRP.

#### **2.4.2 Effect of Moisture, Temperature and Exposure time**

Fibre reinforced resins, as we have seen earlier, are used not only for their good mechanical strength and light weight but also for their inertness to many environments. However, the absorption of water or moisture into the FRP can lead to observable changes of the properties of the FRPs. Storage tanks and process tanks of other materials are being replaced by FRP tanks. Therefore, the penetration of the water molecule into the matrix can result into the debonding of the fibres and the matrix. The water molecule acts as a lubricant between the polymeric matrix and fibre interfaces. Once the water has reached the glass fibres it travels along the fibres, reduces the strong bond between matrix

and the fibre and ultimately leads to failure (Mallick, 1988). When this absorption interrupts the bonding, i.e. the load transferring capability of the composites, it can reduce the performance of the composite parts. Another two effects of absorbing moisture is the lowering of glass transition temperature and the hydrolysis deterioration of the resin. The dependency on temperature and time varies with the type of resin, fibre and hardener. There are three ways water can affect FRP which are discussed in the following articles.

#### **2.4.2.1 Dependence of Physical and Chemical Composition of FRPs on Absorption**

Water molecules tend to be absorbed by resins, depending upon the chemical composition of the resin. Resins are mixed with hardener which in turn produces a cross-linked structure and provides many sites for hydrogen bonding of the water molecules. These sites are usually created from the presence of hydroxyl, phenol, amine or sulfone groups. If the water can create a bond with these groups, hydrolysis takes place and the resin degrades. The composition of the fibre, i.e. carbon fibre, glass fibre, boron fibre, determines whether there will be any effect of moisture or water. Carbon fibres are not affected by the presence of water but glass fibre can be degraded if there is any presence of water on the surface of the fibres. The presence of alkali metal oxides is the main reason for the absorbing of water by glass and the absorption is characterized by the hydration of these oxides (Bunsell & Renard, 2005).

#### **2.4.2.2 Degradation of Mechanical Properties due to Absorption of Water:**

Due to absorption of water molecules, the glass transition temperature is lowered. If in any case the glass transition temperature goes well below atmospheric temperature

then the whole resin may become liquid. Softening of the matrix is a common phenomenon if the specimen absorbs water. Some mechanical properties may increase such as an increase in modulus (Bunsell & Renard, 2005).

#### **2.4.2.3 Effect of Hardener on the absorption**

The hardener also plays an important role not only for the mechanical properties but also its ability of absorbing water or moisture. For example bisphenol-A epoxy ester resin reinforced by glass fibres and hardened by diamine gains weight in as proportion to the square root of time when the composite is exposed to humid condition. And later it reaches an equilibrium condition (Bunsell & Renard, 2005).

#### **2.4.3 Deterioration of FRP Tanks due to Heat and Fire**

FRP tanks containing corrosive liquid present hazards for the environment as well as to humans. The assessment of risk of using these composites involves determination of the behaviour of the material during accidental cases of high heat or even fire. Feih et al. (2007) developed a model to predict the tensile strength and time to failure in case of high temperature or fire. The model predicts the tensile strength very accurately up to the ignition of the fibre reinforced plastic, in which case rapid degradation of all the mechanical properties takes place. Feih et al. (2007) also showed (in order to compare the model with the experimental result) that the rate of change of the tensile strength of vinyl ester and glass fibre composites are low up to 150°C. He also exposed the specimen to 650°C in which case the change of strength is very rapidly decreased.

## 2.5 Mechanism of failure

Composites can fail on the microscopic or macroscopic scale. Microscopic failure refers to the failure (i.e. debonded, cracked, sheared) of a single fibre. The glass fibres have high modulus of rigidity compared to the plastic resin.. Compression failures can occur at both the macro scale or at each individual reinforcing fibre in compression buckling. Tension failures can be the result of net section failures of the part or degradation of the composite at a microscopic scale where one or more of the layers in the composite fail in tension of the matrix or failure at the bond between the matrix and fibres. FRP laminates can be separated by shock, impact, or repeated cyclic stresses at the interface between two layers, which is known as delamination. Individual fibres can therefore separate from the matrix as in the case of fibre pull-out (Composite material, 2010).

Some composites may fail just after the initial onset of failure. They are brittle and have little reserve strength after the initiation of failure. The other FRPs may have large reserve energy absorbing capacity even after the onset of damage. A very large range of properties can be obtained by varying the type of fibres, resins as well as the mixtures that can be made with blends. Therefore the properties of composite materials may be designed into its composition. One example is the failure of a brittle ceramic matrix composite occurred when the carbon-carbon composite tile on the leading edge of the wing of the ``Space Shuttle Columbia`` fractured when impacted (experienced an impact load) during take-off. Later on it led to catastrophic break-up of the shuttle when

it re-entered the Earth's atmosphere on February 1, 2003 (Composite material, 2010). Compared to metals, composites have relatively poor bearing strength.

### 2.5.1 Tensile Strength of Composites

If any load is applied to the material above its tensile or compressive strength, by definition that material is bound to fail. In this section the relationship of tensile strength of the composite to the tensile strength of its components and volume fraction of fibres is discussed.

**Longitudinal Tensile Strength:** For continuous and aligned fibre reinforced composites loaded in the longitudinal direction, strength is usually taken as the maximum stress in the stress versus strain curve. Failure of these types of composite material is complicated and several modes of failure are possible. Modes of fracture or failure will depend on the type / strength of the fibre and the matrix and the nature and strength of the bond between the fibre and matrix. The longitudinal strength  $\sigma_{cl}^*$  of the composite with continuous fibres can be expressed by the following equation (2-2):

$$\sigma_{cl}^* = \sigma_m'(1 - V_f) + \sigma_f^* V_f \quad \dots \quad \dots \quad \dots \quad (2-2)$$

where  $\sigma_m'$  is the ultimate tensile strength of the matrix,  $\sigma_f^*$  is the ultimate tensile strength of the fibre and  $V_f$  is the volume fraction of the fibre (Callister, 2005).

**Transverse Tensile Strength:** The transverse tensile strength (perpendicular to the direction of the fibres) is much lower compared to the longitudinal tensile strength; in fact it is lower than the matrix because it depends on the strength of bonding between the fibre and the matrix. For example the typical longitudinal strength for unidirectional glass fibre reinforced polyester is 700 MPa whereas its transverse tensile strength is only 20

MPa. That is why the FRPs are designed in such a way to experience loads along the fibres (Callister, 2005).

Both the longitudinal and transverse tensile strength is different for discontinuous fibres. For discontinuous and randomly oriented fibres the elastic modulus may be expressed as follow in the equation (2-3):

$$E_{cd} = KE_f V_f + E_m V_m \dots \dots \dots \dots \quad (2-3)$$

Where K is the fibre efficiency parameter that depends on  $V_f$ , fibre orientation and the  $E_f/E_m$  ratio (Callister, 2005).

### 2.5.2 Failure of Fibre

Fibre is the main load carrying element of the FRPs and failure of fibre, in most cases, corresponds to the last stage of life of FRPs. The onset of failure and the failure properties of fibres show a large variability in the experimental results. In order to mitigate this variability safety of factor is used in the design (Bunsell, 2005). It has also been evident that for a particular elongation of the composite material glass phase or the bonding between the two phases will fail.

### 2.5.3 Failure of Resins

Resin phase of composite material used in process conditions of hydrometallurgical plants may fail due to exposure of the components to various conditions. Degradation of the resin due to abrasion, increase in hardness, increase in brittleness, absorption of the solutions is evident from previous research (Sjorgen & Gamsted, 1999; Mahmoud & Tantawi, 2003, Shafeeq, 2006) which is also a part of

elaborated discussion of degradation of FRP in hydrometallurgical process conditions in article 2.6.2.

#### **2.5.4 Failure Criteria for Composites**

The failure criteria of composites are described by many models for a single ply. The ply strength constants are five independent ply failure modes i.e. tensile and compressive breaking strength in fibre direction, tensile and compressive breaking strength transverse to fibre direction and shear breaking stress. Maximum stress criteria assumes if any of the stresses crosses these breaking stresses then the failure would occur. Various ply failure criteria are used in the failure analysis of laminates. Failure in a laminate may occur when a weaker ply fails first while the rest of the plies in the laminate carries the load. The failure of the composites which deals with the interplay delamination cannot be described by these criteria.

##### **2.5.4.1 Physical Failure Mechanisms in composite materials**

Many processes which can absorb energy during failure governs the fracture toughness of a composite material, such as matrix cracking, fibre fracture, failure of the fibre matrix interface, inter laminar delamination. Different composite material exhibit different modes of failure, and some composites can be analyzed based on the fracture mechanics but it is not so in all cases. The original work of Inglis (1913) was concerned with the isotropic material containing holes and it was clear that the stress concentration described above was the determining factor in crack development. Cook and Gordon considered the whole stress field around a crack. If a stress was applied at right angles to

the crack axis then the stress concentration at the crack tip produced a maximum of stress at right angle to the crack and that at the point the stress along the crack axis was zero. However the stress along the axis increased from zero and passed through the maximum just ahead of crack tip (figure 7.28, Bunsell & Renard, 2005). Extending this argument to anisotropic material if the difference in strength in two right orthogonal directions is great a crack at right angles to the initial crack will be created. However, in spite of crack initiation, the composite has its own crack progress inhibitors, and these are the laminate fibre the layers. Layers of a composite laminate are highly anisotropic and the fibre matrix interface is usually a weak discontinuity which can separate and blunt the developing crack.

Composite material can develop three kind of damage depending on the applied load. Ply cracking or transverse cracking, debonding between the plies or delamination and failure of fibres, and these will be considered next.

#### **2.5.4.2 Intra Ply Cracking**

Different laminates or ply are joined together to fabricate a composite material. When load is applied to the composite material the ply which creates the largest angle ( $90^\circ$ ) with the applied stress fails first. Calculation for the  $[0/90_n/0]$  laminates show that the first crack occurs suddenly and across the whole width of the  $90^\circ$  layer specimen.

#### **2.5.4.3 Delamination**

Delamination or inter ply cracking is the failure of bonds between two laminates. When  $[25/-25/90/-25/25]$  laminates are loaded under uniaxial tension, transverse cracking appears in the  $n-90^\circ$  plies. In this case the 3-D stresses close to the laminate free edges

are predominant compared to 2-D inplane stress inside the laminate i.e. the stress rise sharply between the plies sharply. Thus the first and main mode of degradation in such a laminate is an interply crack, known as free edge delamination, which is mainly initiated by out of plane stresses close to the edge. Observations, of specimens with different lay ups, by optical and (scanning electron microscopy (SEM) as well as x-radiography, after tensile test allow the physical damage mechanism which occur to be observed. Depending upon the orientation of plies the possible failure mechanism can be very different.

#### **2.5.5 Fracture of FRPs**

The fracture behaviour of the material deals with the initiation and increase of cracks that may cause failure of the structure. The fracture in thermosetting polymers is usually brittle but it may also be ductile especially when the temperature of the polymer is near or above its glass transition temperature. The fracture, in general, is associated with the formation of localized stress concentration points (i.e. scratches, notches). Though the fracture in the resin does not mean the failure of the composite material but the degradation of the matrix often leads to the rapid change of the properties of the whole material due to the exposure of the fibres to the environment from those fractures. A mechanism for this process described by Callister (2005) is the formation of microvoids due to much localized yielding. If the tensile strength is sufficient these micro voids coalesce and initiates fracture. Many investigators (Gaggar, 1975; Mandal, 1975; Harris 1985) used linear elastic fracture mechanics approach for studying the crack growth

resistance of FRPs. In this approach the Stress Intensity Factor  $K_I$  is expressed by the following equation:

$$K_I = \sigma_o \sqrt{\pi a} Y \quad \dots \quad \dots \quad \dots \quad \dots \quad (2-4)$$

where  $K_I$  is mode I stress intensity factor,  $\sigma_o$  is the applied stress,  $a$  is the crack length and  $Y$  the geometric function that depends on the crack length, crack location and mode of loading.

## **2.6 Deterioration of FRP Tanks in Hydrometallurgical Process condition**

### **2.6.1 Nickel Extraction Process**

There are several processes (grinding concentrating, matte roast smelting, hydrometallurgy etc.) for treating nickel ores (laterite-nickel oxide, nickel sulphide etc.). The following section will discuss several of the processes as a background for potential uses of FRPs in nickel extraction processes, since for each ore body or mine site there is a particular flow sheet (extraction process) to efficiently recover metals from ore. One nickel extraction process essentially consists of subjecting ore, which is reduced to slurry, to different treatments, through the addition of water, using an acid solution to extract from it nickel transformed into nickel oxide and cobalt, transformed into cobalt carbonate (Hydrometallurgy-Vale-Inco-New Caledonia, 2010).

#### **2.6.1.1 The Vale Inco Process flow sheet for Voisey's Bay**

Nickel is extracted by either pyrometallurgy or hydrometallurgical process. Most sulphide ores have traditionally been processed using pyrometallurgical techniques to produce a matte for further refining. Recent advances in hydrometallurgy have resulted in

recent nickel processing operations being developed using these processes. Even the hydrometallurgical process of extracting Nickel from ore varies with type of ore (Ni-sulphide, Ni-oxide (laterite)), availability of the resources and the nickel producing company. The flowsheet for Voisey's Bay nickel production plant of Vale Inco is shown for a better understanding of the chemical composition of the hydrometallurgical fluid contained by the FRP tanks.

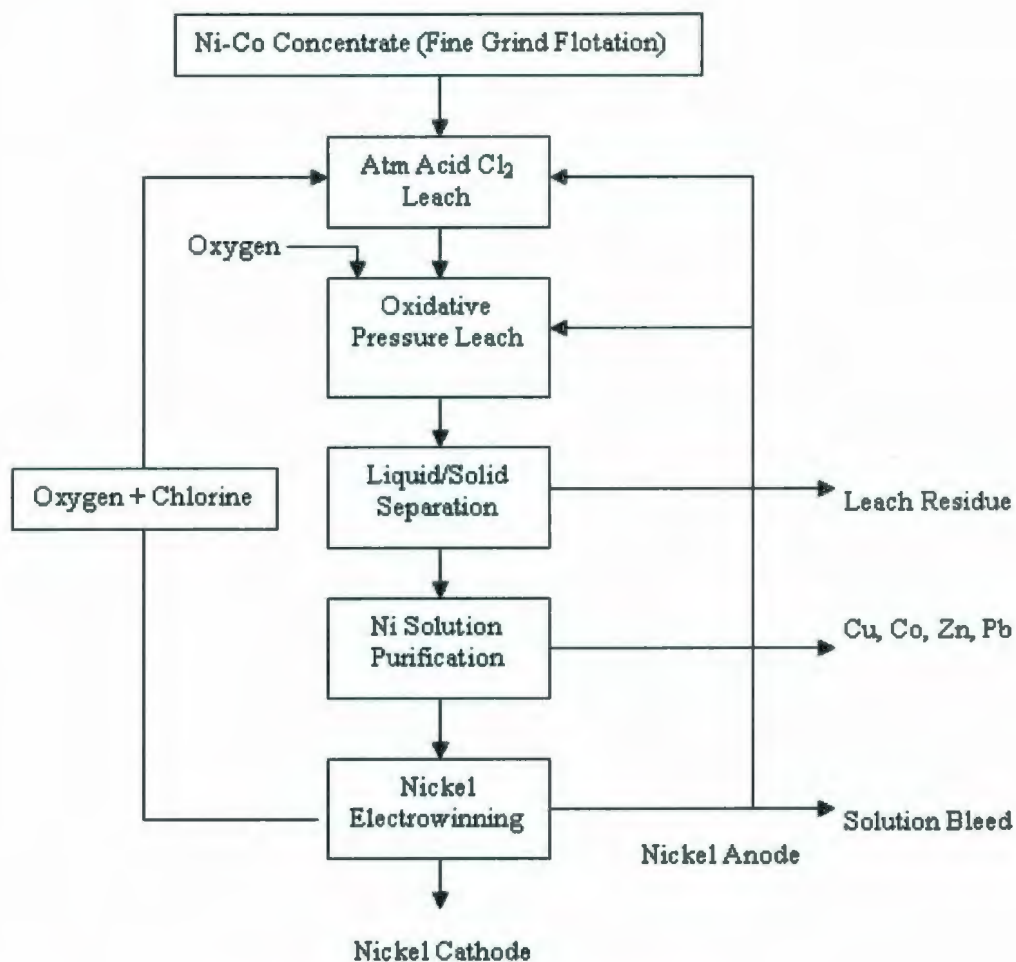


Figure 2-7 Flowsheet for Nickel extraction (Snow, 2005)

The whole process consists of more than thirty complicated steps. The detail of these steps may vary from plant to plant. FRP tanks and pipes can be used in many steps after the pressure leaching. The major common steps in nickel extraction process are briefly discussed in the following articles.

#### **2.6.1.2 Preparation of the ore**

The ore preparation plant is usually located very close to the mine. The laterite ores (*limonite*) and saprolite ores (*garnierite*) are mixed with water, sifted and ground to form a sludge known as slurry. This slurry is piped to the treatment plant.

#### **2.6.1.3 Leaching**

The slurried ore is preheated by steam and injected continuously into an autoclave with sulphuric acid. Leaching once again 'washes' the ore with sulphuric acid. The role of the acid is to dissolve certain metals which are extracted in this way from the solid ore and transferred into the liquid solution. The high temperature in the autoclave (270°C) permits the acceleration of this extraction and therefore allows a greater quantity of ore to be processed in a small autoclave. However, this high temperature requires operation under high pressure so as to prevent the liquid from boiling.

The 'leached' slurry thus obtained contains solids (mainly iron oxide) and a liquid solution containing the dissolved metals including nickel and cobalt but also metals not recoverable for exploitation (magnesium, aluminum, chromium, zinc, copper, etc.). This slurry is then cooled again and depressurised. This operation generates steam which is

recycled upstream in the slurry heating circuit before its injection into the autoclave (Hydrometallurgy-Vale-Inco-New Caledonia, 2010).

#### **2.6.1.4 Counter Current Decantation**

The leached and cooled slurry passes through a decantation circuit designed to separate and wash the solid residues from the liquid solution called 'mother liquor'. In other words, the solids settle at the base of the decanter from which they are pumped (the underflow), while the excess liquid is collected (overflow).

To wash the solids well, the operation is repeated six times in six successive decanters. By the end of the operation, the mother liquor has recovered 98% of the nickel and cobalt contained in the leached slurry. The solids are sent in the form of a thick paste to the unit for treating solid residues, where they are neutralised (Hydrometallurgy-Vale-Inco-New Caledonia, 2010).

#### **2.6.1.5 Partial Neutralization**

The mother liquor contains not only cobalt and nickel, but also other metals, present in the original ore (aluminum, iron, chromium, zinc, silica, copper and manganese), considered impurities (since not destined to be recovered and processed), as well as sulphuric acid not used up during the leaching process. The acid and some of the metal impurities are eliminated through the addition of limestone and lime to form solid gypsum (plaster), separated from the solution by decantation and filtration operations.

The gypsum and metal hydroxides form a thick paste which is sent to the waste processing plant. Copper is removed by precipitation then by absorption in an ion

exchange circuit to remove the last traces. It is, in its turn, sent to the waste processing plant.

#### **2.6.1.6 Extraction by Solvent**

When aluminum, iron, chromium, silica and copper have been removed from the mother liquor, but, as well as nickel and cobalt, it still contains zinc and manganese, as well as magnesium and calcium, major components of the limestone and lime used to neutralise the acid.

It is injected into a first extraction circuit in which an organic solvent captures the nickel, cobalt and zinc, leaving manganese, magnesium and calcium in the liquor. This solution is sent to the liquid residue processing unit. A second extraction, on contact with a small quantity of hydrochloric acid, releases the nickel, cobalt and zinc. This solution, whose volume is between 20 and 30 times less than that of the mother liquor, gives a concentrate of nickel, cobalt and zinc chlorides. The solvent, with the three metals removed, is introduced again into the extraction cycle.

Passage through a selective resin enables the zinc to be retained. Finally, a concentrated hydrochloric solution is obtained, cleansed of nickel and cobalt.

The last part of this stage consists of the separation of cobalt from the nickel, thanks to another solvent extraction circuit which extracts just the cobalt. Two pure solutions are created in this way: one of nickel chloride and one of cobalt chloride. The solvent, with the nickel, cobalt and zinc removed, is now available for another extraction cycle – recycled in a closed circuit.

#### **2.6.1.7 End Process**

The nickel chloride solution is processed in a fluidized bed oven, heated to a high temperature (800°C) through the combustion of a mixture of air and natural gas. The nickel chloride is then broken down into nickel oxide and hydrochloric acid which is reconstituted and recycled for the extraction process.

The particles of nickel oxide thus formed are in the form of spherical granules, comprising successive layers, something like pearls, producing small grey balls, round and solid. The hydrochloric acid is recycled to the first solvent extraction stage (Hydrometallurgy-Vale-Inco-New Caledonia, 2010).

#### **2.6.1.8 Electrowining Process**

Nickel can be electrowon from hydrometallurgical solution using electrolytes which are produced by many steps of purification from leached liquor of ore. Solution purification depends on impurity department for each individual flowsheet, as well as on the relative abundance of the impurity in the matte feed. Hofirek and Halton (1990) provided an excellent description of the purification operations at a commercial plant. A major impurity in all above operations is cobalt. Cobalt is separated either by precipitation with electrolytic nickelic hydroxide or it is removed by solvent extraction with Cyanex 272. Pavildes, A.G. (2006) showed a few case studies of electrowining process in nickel tank houses in Africa. Some of the plants make use of boric acid, which acts as a pH buffer, limiting the formation of nickel hydroxide at the cathode surface. Sodium lauryl sulphate is also added as a second reagent which reduces unwanted surface pitting. Solution surrounding the cathodes is separated from the adjacent anodes in the cell using a cloth of suitable permeability which means that nickel is electrowon in

divided cells. In many plants, each cathode slots into a suitable frame, over which a woven Terylene (trade name for polyester fibre also known as Dacron) bag is stretched at the cell. Each cathode compartment gets advance electrolyte (specially treated electrolyte) at a fixed rate. The diffusion rate of acid formed at the anode into the cathode compartment is reduced by a positive hydrostatic head developed across the cathode bag at the cell. As a result the pH in the cathode compartment is maintained and controlled to approximately 3.5. Operation at higher pH limits the amount of hydrogen produced, because the evolution of hydrogen competes with nickel reduction at the cathode surface which in turn increases current efficiency and reduces deposit pitting. The cathode quality, i.e. the quality of nickel production will largely depend on the control of the rate of electrolyte introduction to each cell and on the solution head developed across each cell unit. The flow rate of the electrolyte is controlled by using a glass orifice installed in the electrolyte feed tube. It is often difficult to control bag permeability, which is maintained by quality assurance technique (purchase, repair and replacement) of the polymer bag on a regular basis. Spent nickel electrolyte flowing through the cathode bags, leaves the cells via an end overflow box, and gravitates to a collection tank or sump. In our research the FRPs are exposed to these nickel spent electrolytes. The threshold limit value of the sulphuric acid is approximately 10% of the airborne acid. The sides of the tank house are enclosed with suitable sheeting and fans are used to draw the air from the tank. The sheeting around the tank house is not used in other plants where natural ventilation is possible (Pavildes, 2006).

## **2.6.2 Probable Factors of Degradation when Exposed to Hydrometallurgical Process Condition**

The effect of application of the FRPs in highly corrosive environment has already been discussed in article 2.1. This article discusses the factors that will affect the FRPs. In other words the parameters whose effects we should consider in exposing the FRPs in different environments. For example if abrasive particle is considered as a major factor for the degradation of FRPs in case of hydrometallurgical nickel extraction process experiments should be designed to determine the effects of abrasion on the FRPs. Some factors that were considered to be key cause for the degradation of FRPs were analyzed with the help of previous research and a decision was made whether to proceed with the determination of the effects of these factors.

### **2.6.2.1 Abrasion**

The hard residue can cause abrasive effects on the surface of the FRP. The iron oxide present in the residue is one of the hardest and may be the main cause for any sort of abrasion. The iron oxides present in the liquid may consist of wüstite (FeO), hematite (Fe<sub>2</sub>O<sub>3</sub>), magnetite (Fe<sub>3</sub>O<sub>4</sub>), iron oxide hydroxide (FeOOH). The presence of abrasive particles in a corrosive environment can result in catastrophic wear in the case of metal where the layers created due to corrosion are swept away by abrasion providing new space for contact between the surface and the fluid. Abrasion can be a problem of fibre glass reinforced plastics especially when they are used for ash handling and salt crystallization. Due to abrasion the thickness of the material (FRP) may reduce as well as cracks may form. Obviously abrasion depends on the kinetic energy of the particles as

well as the angle of impinging on the surface. Mallison, J. H. (1982) described case studies where commercially available FRPs were exposed to corrosive and abrasive environments and the effect of velocity, size, shape and hardness of the abrasive particle was analyzed. Small particles are not a problem even if the particle is hard. In case of hydrometallurgical extraction of nickel the ore is finely ground to 10 to 20  $\mu\text{m}$  using attritor grinders after which it looks like an ink. So the abrasive effect of the particles in hydrometallurgical was not investigated in this research. Mallison also suggested that extra allowance of material should be provided depending upon the rate of abrasion of the FRPs.

#### **2.6.2.2 Fatigue**

Due to cyclic loading and unloading, due to changes in pressure and temperature, for instance in a batch process, fatigue failure can occur. Cyclic loading also takes place due to filling and emptying of the process engineering tanks. This could lead to delamination, failure of the matrix as well as the failure of the fibre. The mechanism is described as initiation and propagation of fracture. Microscopic examination has shown that the transverse cracks are initiated from the coalescence of the fibre-matrix debond for both static and cyclic loading (Sjorgen & Gamstedt, 1999). Though fatigue failure was not investigated in this research, the effect of loading and unloading of the FRP tanks must have an influence on the deterioration of the properties of the tanks used in highly corrosive environments such as hydrometallurgical processes.

#### **2.6.2.3 Increase in Brittleness**

The brittleness or the hardness changes with the exposure of resins to hydrometallurgical solution which can be compared in terms of change in hardness (Mahmoud & Tantawi, 2003). The brittleness of the resins may increase or decrease depending upon duration of exposure, exposure duration, type of solution they are exposed to and temperature of exposure.

#### **2.6.2.4 Decrease in Strength**

The failure strength for the FRP specimens also changes depending on the resins, solution, duration and temperature of exposure. Due to the exposure of the FRPs to the hydrometallurgical solutions, which is highly acidic, the material degrades at long exposure. When the glass reinforced polyester is exposed to sulphuric acid the flexural modulus decreases by 15% in 90 days and when the same specimen is exposed to hydrochloric acid the decrease of flexural modulus is 10% (Mahmoud & Tantawi, 2003).

#### **2.6.2.5 Change in Hardness**

The above three properties of the material may be expressed as a function of tensile strength. By measuring the tensile strength we can have some idea about these properties of the materials. Mahmoud & Tantawi (2003) investigated the effects of hydrochloric acids, sulfuric acids, nitric acids and phosphoric acids on the physical and mechanical properties of glass fibre polyester composite pipes internally lined with C glass. The specimens were exposed for 90 days. It was found that the retention of Barcol hardness was approximately 85% after three months for the specimens exposed to  $H_2SO_4$  and HCl.

The retention or the change of hardness by the resins used to prepare FRP tanks are determined by the manufacturer (Curry, 2005) as well as available in the literature (Mahmoud, & Tantawi, 2003). Mahmoud et al. Found that when exposed to strong acid the hardness decreases. Curry (2005) exposed the laminates made with vinyl ester (Vipel F010) to methanol and air at different temperature. For each of the case Barcol hardness and the percentage retention of hardness increased rather than decreasing. But the hardness at different depth of the specimen is not described in any of the papers. Barcol hardness may be considered as an average hardness of a thick layer of the specimen.

#### **2.6.2.6 Separation of the Fibre from the Matrix:**

Separation of fibres from matrix material can be caused by fatigue and mechanical forces. Sjorgen & Gamstedt (1999) detected failure (transverse crack) due to cyclic or static loading that initiates from the debonding of the fibre and the matrix. The separation of the fibres at the surface of the tanks enhances the penetration of the fluid into the matrix. Also, the diffusion of the moisture through the debonded area becomes faster.

#### **2.6.2.7 Delamination**

Delamination can occur due to cyclic loading and unloading. After this occurs the separation of the layers will then lead to failure, by allowing the fluid to penetrate into the material. It is really necessary to check out whether delamination or interply failure should be considered as one of the key probable failure causes. Shafeeq (2006) determined the effect of environmental exposure on the fatigue and tensile properties of FRPs.

Table 2-1 Fatigue values of GFRV2 composite for Dry heat-70°C exposed for 300 hours (Shafeeq, 2006)

<b>% of tensile strength</b>	<b>P amp (kN)</b>	<b>Stress amplitude (MPa)</b>	<b>Life(cycles)</b>
50%	10.0	54.5	2377
40%	7.6	43.6	17,402
40%	8.1	43.6	13,970
30%	5.7	32.7	71,876
30%	5.6	32.7	94,151
20%	3.9	21.8	2,000,000

Shafeeq tested FRP tubes at different temperature (up to 70°C) and different duration of exposure (up to 1000 hours). He showed that an increase of dry heat temperature for 70°C produces a noticeable effect with fatigue life improving by a factor of 4 in low cycle and high stress regions for 300 hours. Though we have considered fatigue may be one of the cause of failure, from Shafeeq's result it is observed that it takes 2,000,000 cycles for the failure of the FRPs at 21.8 MPa of stress amplitude. The cyclic loading and unloading should not create a problem for the reduction of life in case of its use in hydromtallurgical process.

#### **2.6.2.8 Degradation of the matrix**

Degradation of the matrix is expected for various environmental exposure (i.e. acid) conditions. These conditions will result in to the hardness, tensile strength and compressive strength of the matrix being reduce. To measure the degradation of the FRP components different tests are carried out before and after the exposure of the specimens in hydrometallurgical solution.

## **2.7 Microstructure**

Analyzing the microstructure of the FRPs is a common way of understanding the mechanism of failure, diffusion of the fluid into FRPs, degradation of the matrix, etc. Hammami & Al-Ghuilani (2004) determined the environmental degradation of vinyl ester composite. They exposed the glass-vinyl ester composite for 3 month and 6 month and compared the result with virgin (unexposed) specimens. They analyzed the fractured surface of the scanning electroscopy microscope and found out that the decrease of flexural and tensile strength for six month acid exposure is due to the debonding of the fibre matrix interface and the increase of strength for dry and hot exposure is the better bonding between the fiber and the matrix. Failure during the test occurs due to delamination (Hammami & Al-Ghuilani, 2004).

Shafeeq (2006) during the determination of tensile and fatigue behaviour of FRP exposed to oil and environment used optical and electron microscopy to evaluate the microcracks growth in the matrix and in the fibre due to exposure.

## **2.8 Expected Outcome**

Initial target was to determine the best quality of FRPs in hydrometallurgical processes. Due to large variability of available FRP material determination of the best of its kind is not possible. The variation occurs due to infinite possible combination of resins, fibres, layup, strengths and bonding. For example resins vary with composition (Example polymer: Bisphenol A Epoxy vinyl ester, polyester), amount of catalyst, composition of catalyst and cross linking. Also glass fibre varies with size and orientation.

The outcome of the thesis is aimed at developing some tests which will be able to distinguish between different qualities of resins.

Different tests were selected to be performed on unexposed and exposed samples. The results of these tests will allow us to compare among the tests in terms of sensitivity to exposure. That in turn will help to decide which tests should be carried out in future.

The test result after exposure will also help to determine the suitability of the resins to be used in hydrometallurgical processes. The properties determined by the tests will be a standard to compare different glass reinforced fibre materials.

## **Chapter 3**

### **STRATEGY AND SELECTION OF TESTS**

This chapter deals with the selection of various tests carried out during the thesis and justifies the preliminary selection of the tests. The choice of test methods was guided by the most readily available equipment and material following ASTM tests which lead to the development of several methods or tests to determine the properties of FRPs

#### **3.1 Available Material and Selected Tests**

The available material were mainly donated by Reinforced Plastic Systems (RPS) and consisted of H150 and P150 FRP pipes, bisphenol A epoxy vinyl ester resins and polyester resins.

The resins were used to prepare ASTM standard plastic and fibre glass reinforced plastic specimens. For testing the commercially available FRP pipes new methods were developed which were assumed to be sensitive to the change of exposing environment. The tests which are carried out are listed and discussed in this section.

##### **3.1.1 Standard Tests**

The ASTM tests that were carried out are tensile test (ASTM D638), bending test (ASTM D790) and heat deflection temperature test (ASTM D 648). These tests were mainly done only on the resins. ASTM bending tests (D790) were carried out on a few FRP samples which were prepared by cutting of FRP plate.

### **3.1.2 Developed Test Method**

FRP samples to be tested should preferably be repeatable in terms of dimensions, ratio of the resins, and orientation of the fibres and so on. It was considered difficult in the laboratory, if not impossible, to produce FRP specimens identical in all respect, in particular in the quantity and arrangement of fibres. It should be possible to cut specimens of identical shape and structural from commercially produced products such as tubes. However, the commercially available FRP products do not correspond to the ASTM specifications of shape and dimensions. Some tests were developed to determine the effect of the hydrometallurgical process conditions on specimens made from these commercially available products. These include significantly modified ASTM tests that have been given new names.

1. Tensile test on lateral loaded tube sections.
2. Compression test on axial loaded test sections
3. The three point load bending for tube sections.
4. Micro hardness test.
5. Micro structural assessment of the fibre reinforced plastic.

Cylindrical pipe samples were donated by Reinforced Plastic Systems, Inc.

### **3.2 Evaluation of the Tests**

The tests to be carried out determine the mechanical properties (tensile, compressive, bending stress-strain, hardness), thermal property (heat deflection temperature) and microscopic study.

The sensitivity of the properties due to the exposure must be high for the tests and the parameters (for example modulus of strain curve, force for breaking of specimen) must be repeatable. Among the mechanical property tests the bending test should be the most sensitive to the exposure because for a particular deflection of the loading bar the outer and inner layer of the specimens experiences the most stress for a particular strain.

### **3.3 Strategy**

The availability of material and the availability of the equipment in turn led to a strategy of focusing on two manufacture's grade resins (bisphenol A epoxy vinyl ester and polyester), on ASTM tests (tensile, bending and heat deflection temperature) and on modified ASTM tests with short duration of exposure to sulphuric acid, cobalt spent electrolyte and water for varying temperature and time.

## **Chapter 4**

### **EXPERIMENTAL SPECIMENS AND TESTS**

This chapter describes the experimental methods and setups that have been designed to determine the quality of the FRPs and resins that are used in hydrometallurgical processes. For the studies of possible degradation the specimens were exposed to two different environments i.e. hydrometallurgical solutions donated by the Vale Inco and prepared solutions. These specimens were also tested unexposed to compare between exposed and unexposed specimens. As noted above, these tests were done on two types of samples: i) standard ASTM samples (ASTM D638, ASTM D648 and ASTM D790) prepared by casting and ii) specimens cut from commercially available tubing tested using an approach developed in this laboratory.

This chapter consists of two parts. From section 4.1 to 4.6 it deals with the common features of the tests and the later articles describes these tests in detail.

#### **4.1 Preparation of Test Specimens**

It was quickly realized that the best way to produce many similar FRP test specimens was to cut from commercial tubes which also happens to have a similar structure to that of large tanks. However this kind of specimen does not appear in many, if any, useful ASTM tests. It was, however, possible to produce reproducible standard ASTM specimen shapes from just a resin.

Preparation of tests specimens from the three types of available material involved three different procedures.

#### 4.1.1 Specimens Made from Resin

In the first attempt, a rapid prototype machine was used to make up the moulds (Figure 4-1) where the acrylonitrile butadiene styrene (ABS) thermoplastic material was used. This material is quite good for preparing/casting polyester samples. But ABS started reacting with bisphenol-A epoxy vinyl ester and became soft at the surface contact with the resin. A silicon based rubber was chosen for the moulds which were prepared by casting using the polyester specimens as a core print while the mould was prepared (Figure 4-2).



Figure 4-1 Mould made of ABS material fabricated using rapid prototype machine and a polyester specimen made from that mould.

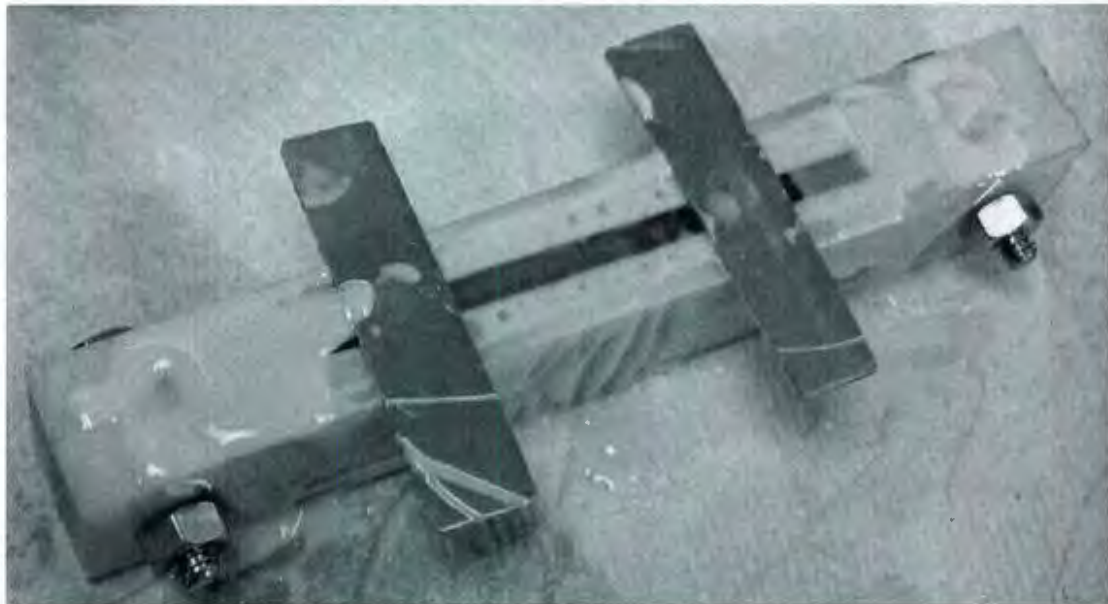


Figure 4-2 Preparation of room temperature vulcanized rubber mould for preparing bending test specimen

Standard specimens were prepared by casting polymers (polyester, bisphenol-A epoxy vinyl ester). The moulds were made of silicon based room temperature vulcanized (RTV) rubber (Figure 4-10, Figure 4-10, Figure 4-19). The resin and the hardener were mixed, then poured into the mould and it was placed inside a vacuum pump for 2 minutes. After the resin was hardened it was taken out of the mould and was polished wherever necessary. The shape and dimension of the specimens were according to the ASTM specifications.

#### **4.1.2 Specimens Made from Tube**

From 3 feet long pipes (Figure 4-3) specimens were cut with a hack saw. The outer diameter of the pipes was 65 mm (2.5 inch) and the inner diameter was 30.8 mm (2

inch). The cut edges were smoothed by polishing with different grit sand and emery papers as seen in Figure 4-23. The length of the each of the section was 38 mm (1.5 inch).

#### **4.1.3 Specimens Made from FRP Plates**

The ASTM standard FRP specimens were prepared by cutting off 7 mm thick FRP plates prepared by Institute of Ocean and Technology (IOT), St. John's, NL. The cut off rectangular portions were polished on the four sides to obtain smooth surfaces around the specimen.

## **4.2 Materials Available/ Used**

It should be noted that the kind of material available were resins (polyester and bisphenol A epoxy vinyl ester) and commercially available FRP pipes (H150 and P150 pipes). That was a very important consideration given the available materials for testing. The available types of material are listed below.

### **4.2.1 Resins:**

Bisphenol-A epoxy vinyl ester: Manufacturer's Code Vipel F010 ,

Polyester: Product ID0475808 .

The manufacturers of these resins were Alpha Corporation of Collierville (AOC) and Bondo Corporation respectively.

### **4.2.2 Commercially Available FRP Tubes**

Bisphenol-A epoxy vinyl ester pipe. Manufacturer's Code of the resin Vipel F010, and the code for the tubes was H150

Bisphenol-A epoxy novlac vinyl ester pipe. Manufacturer's code of the resin Vipel F080 and the manufacturer's code of the pipe was P150.

The manufacturers of these resins were Alpha Corporation of Collierville (AOC). The pipes were manufactured and donated by Reinforced Plastic Systems, Inc. The outer diameter of the pipes was 65 mm (2.5 inch) and the inner diameter was 30.8 mm (2 inch).



Figure 4-3 FRP pipes used to prepare tube samples

These commercially available FRP tubes were designed and manufactured to sustain in corrosive environment. As confirmed in our own study of the structure (see section 5.8), these pipes consists of a resin rich inner laminates and the outer laminates have higher proportion of glass fibres to plastic than that of the inner layer because they are only exposed at the inner surfaces and a resin rich layer will ensure less dissipation of fluid through the FRP while the high fibre glass contained outer layer will make tanks or pipes stronger. The glass fibre reinforced plastic pipes and tanks used in different plants

also have the same design of construction. That is why these tubes were exposed only at the inside rather than submerging these pipes into the corrosive solutions.

#### **4.2.3 FRP Sheets**

Using the resins mentioned in article 4.2.1 (bisphenol A epoxy vinyl ester and polyester) and glass fibre matt provided by RPS, Institute of Ocean Technology (IOT) prepared two sheets of FRP sheets for testing. These FRP sheets provided an opportunity to prepare the ASTM standard test specimens.

As normal for the material for boats, this FRP sheets consists of resins, glass fibre and an orange color gel coat. While the tubes for using in process plants had distinctive two layers containing low and high fraction of glass fibres, these FRP plates did not have special design for a corrosive environment rather it was designed for life boats.



Figure 4-4 Two sides of FRP sheets

#### **4.3 Exposure:**

Mechanical property tests were carried out on the exposed and unexposed test specimens. The test specimens were exposed to different conditions varying the temperature, liquids used to exposed test samples and the methods of exposure.

#### **4.3.1 Liquid Used and Temperature of Exposure**

The temperatures were 25°C and 75°C and the specimens were exposed to cobalt spent electrolyte (hydrometallurgical solution from which cobalt has been extracted, provided by the Vale Inco) and to 1M sulphuric acid for different time periods in both cases. The pH level of cobalt spent electrolyte is 2.96 and contains sulphur, cobalt, magnesium, manganese and very small amount of other elements (Rashed, 2010).

#### **4.3.2 Methods of Exposure**

Two types of specimens were tested (i) Standard test specimens prepared from resin, (ii) specimens cut off from the tube samples and (iii) standard specimens cut off from FRP sheets. The exposed surface also varied for different specimens.

Standard flat specimens (following ASTM D638, ASTM D648 and ASTM D790 specification) were completely submerged into the fluid.

The inside of the tube specimens were exposed to the acidic solution. To meet this purpose a fibre reinforced plastic plate were attached at the bottom of the each FRP tube with the help of silicone based glue. Later they were filled with acidic solutions. The specimens were kept inside an oven at 25°C (room temperature) and 75°C.

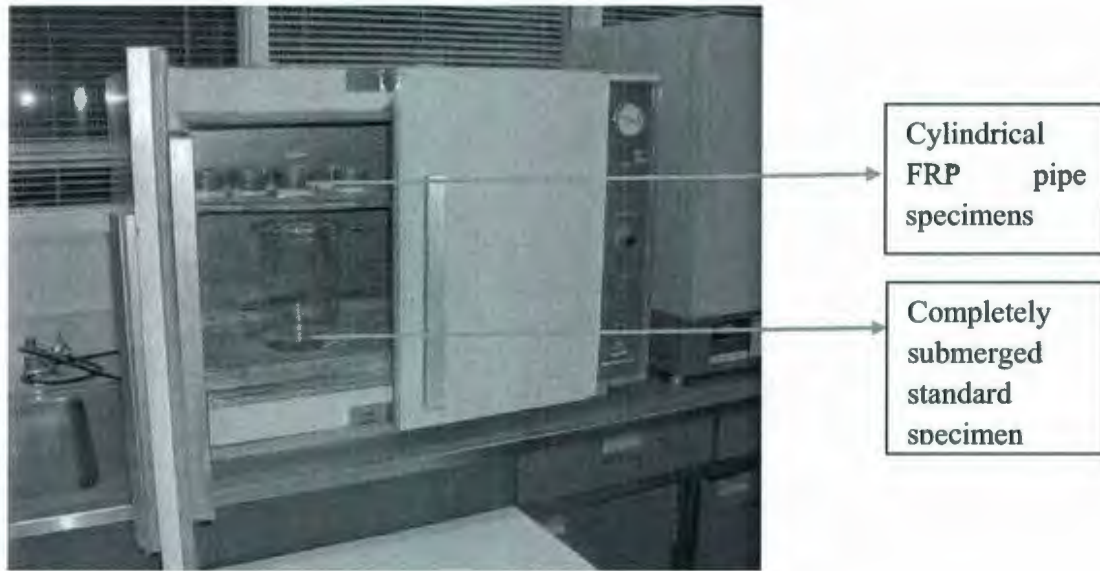


Figure 4-5 Exposure of specimens

The volume of the fluid was checked every 12 hour and was refilled if necessary. After each week the specimens were taken out to replace the fibreglass plate at the bottom and the fluid due to the change of concentration of the fluid.

#### 4.4 Number of Specimens Tested:

For each of the ASTM, modified ASTM and newly created test configurations i.e. type of material, exposure condition of the material, a minimum of two test specimens were used.

#### 4.5 Conditioning of Test Specimens:

After exposure the test specimens were kept in over 75% humidity for at least 48 hours before the test by storing in a beaker with a little amount of water at the bottom. They were exposed to room environment only just before the tests. This is carried out because exposing different specimen to different condition for a long period of time may

change their properties which would have affected the test results if different specimens were kept in different environments.

#### 4.6 Atmospheric Condition of the Test Room:

The ambient temperature of the test room was in the range of 24 to 25°C and the indoor humidity varied from 30% to 50% as measured in the engineering laboratories.

#### 4.7 Tests on Resins

Four tests were carried out on the resins, namely, tensile test, bending test, measurement of heat deflection temperature and determination of surface micro hardness. Among these tests bending test was also performed on FRP material.

##### 4.7.1 Tensile Test (ASTM D638)

Tests following the ASTM D638 standard were carried out to determine the tensile strength of the specimen as well as to see whether this test could provide us any information about the degradation of the fibre glass reinforced plastic after exposure.

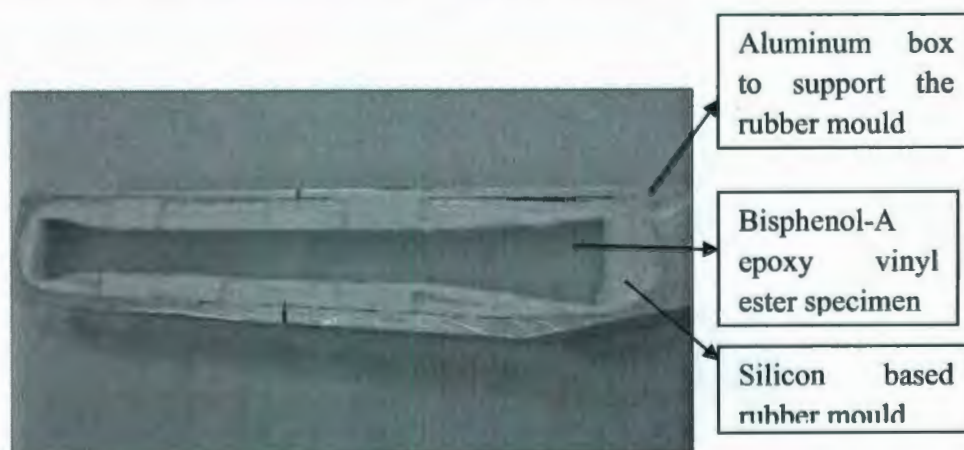


Figure 4-6: Casting of Tensile test specimen

Resins (article 4.2.1) were used to prepare the test specimens. The length of the specimens was 160 mm, thickness of the specimen was 5 mm and the smaller width of the specimens was 12.7 mm. The detailed dimension of the test specimen can be found in ASTM D638. Specimens were casted (article 4.1.1) in a rubber mould (Figure 4-6). They were completely submerged into different solution (article 4.3) for exposure.

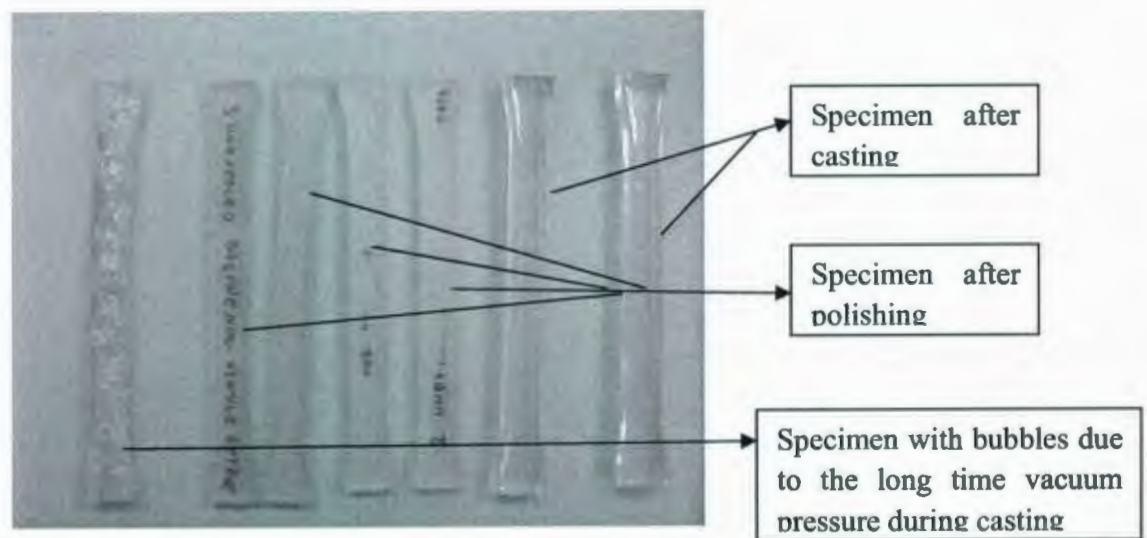


Figure 4-7: Tensile test specimen

All tensile tests were performed at a crosshead movement (speed) of 5 mm per minute. An Instron 5585H test frame (Figure 4-8 and Figure 4-9) was used to perform the tensile load versus extension and stress versus strain measurement by personal computer (PC) control. An extensometer with one inch gauge length was used for this case.



Figure 4-8: Tensile test experiment setup



Figure 4-9: Extensometer and the grip of the jig.

Care was taken to minimize slipping at the grips and the fracture of the specimen due to crack formation at the grips. During the preparation of the specimens each individual specimen was polished to obtain a flat surface. This had the effect of eliminating sample slippage in the grips. This jig did not have a procedure to govern the force that was applied at the grips. When excessive amount of force at the grip is applied

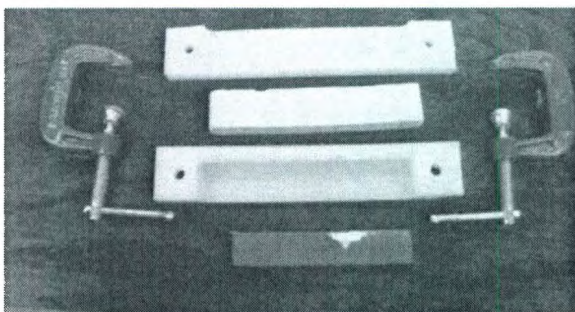
the tendency was to initiate fracture at the grips. Both problems were solved by adding additional fibre glass layers at the ends of the specimens where the grips were applied.

#### 4.7.2 Bending Test (ASTM D790)

Bending tests on samples of resin used for FRPs were done in two phases. The first phase, a test frame apparatus as seen in Figure 4-11 was used. This test frame force is applied by a hand operated hydraulic pump which leads to steps (wiggly lines) in the load versus extension data. Since this apparatus was not servo controlled the test was discontinued on FRPs. More useful results were obtained in phase two by applying the same bending test.



(a)



(b)

Figure 4-10 Preparation of bending test samples

Resins (article 4.2.1) were casted (article 4.1.1) to prepare the plastic specimens as shown in Figure 4-10. The length of the plastic specimens was 100 mm, thickness was 5 mm and the width was 10 mm. FRP specimens were prepared FRP sheets as mentioned in article 4.1.3. The length of the FRP specimens was 130 mm, thickness was 7 mm and the width was 10 mm. The specimens were tested before and after exposure article 4.3.2.

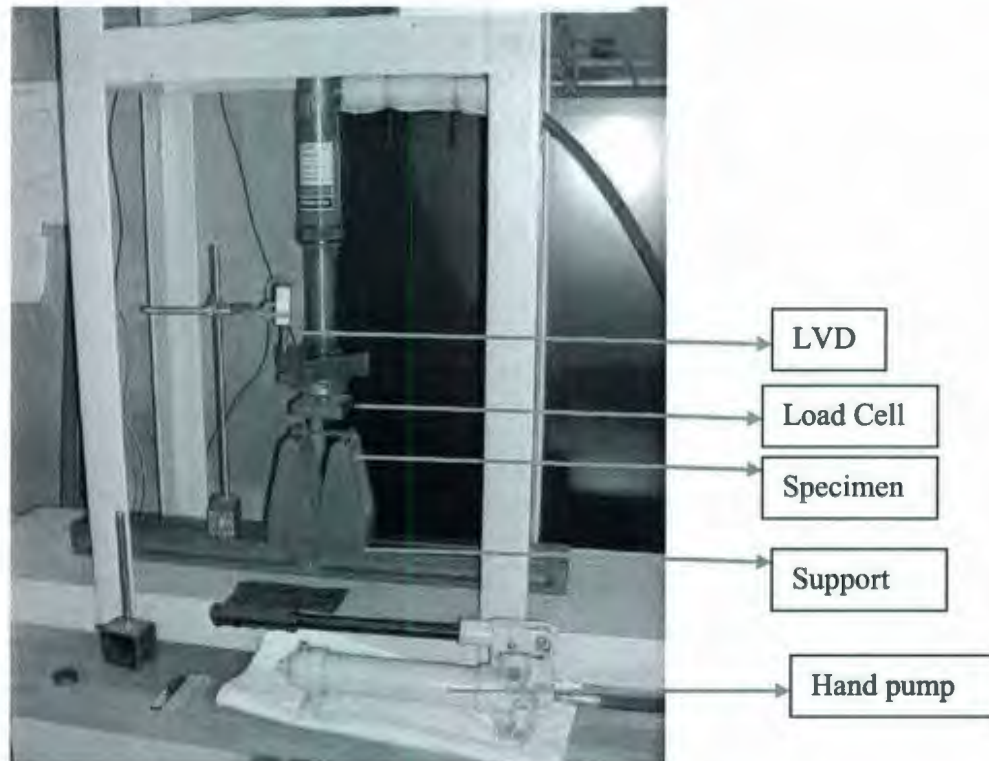


Figure 4-11: Bending test frame- phase 1

In phase one experiments the speed of cross head movement was not controlled rather a hand pump was used to move the cross head. But the cross head movement was lower than 5 mm per minute. For the second phase tests all bending test were performed at a crosshead movement (speed) of 5 mm per minute.

Phase one bending rig (figure 4-11) consisted of a load cell, a linear variable displacement transducer (LVDT) to measure the displacement of the loading bar (underneath the load cell) and a hand pump used to apply the load hydraulically.

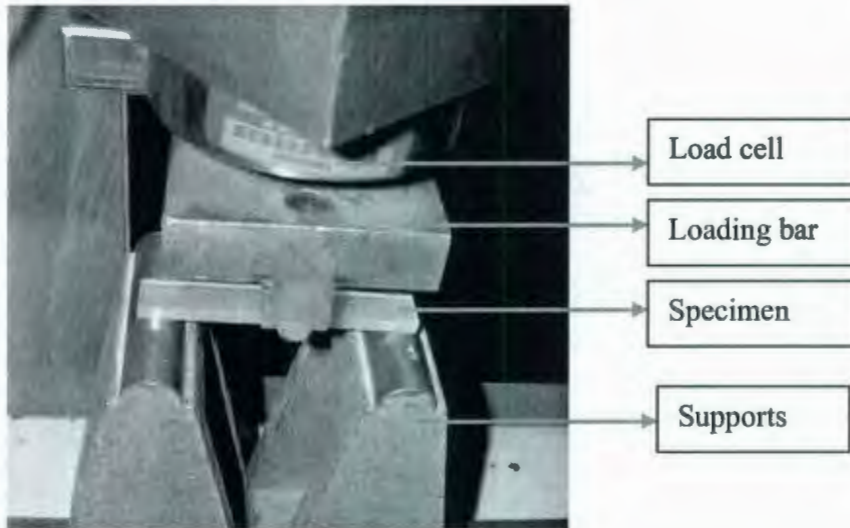


Figure 4-12 Bending test rig (phase 1)

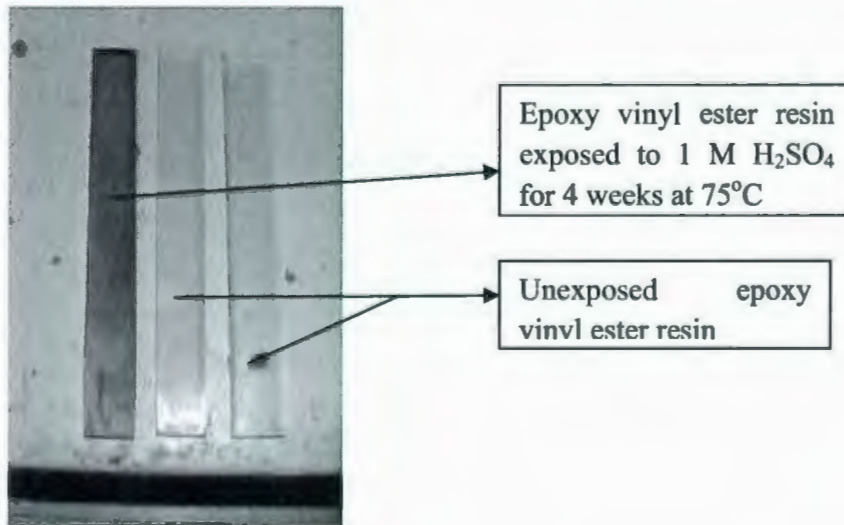


Figure 4-13 Bending test specimen

The load versus extension result for the first phase it was obvious that constant cross head movement is essential for the bending test of these plastic material as creep of the specimens are a dominant factor for this test. The same dimension and preparation method was used for the specimens tested for flexural modulus. The supports of the bending test were the same as phase-one bending test. An Instron 5847 test apparatus (Figure 4-14) was used for this purpose which is powered by hydraulic pressure. A load cell is used to measure the force and an LVDT to measure the displacement of the loading bar.

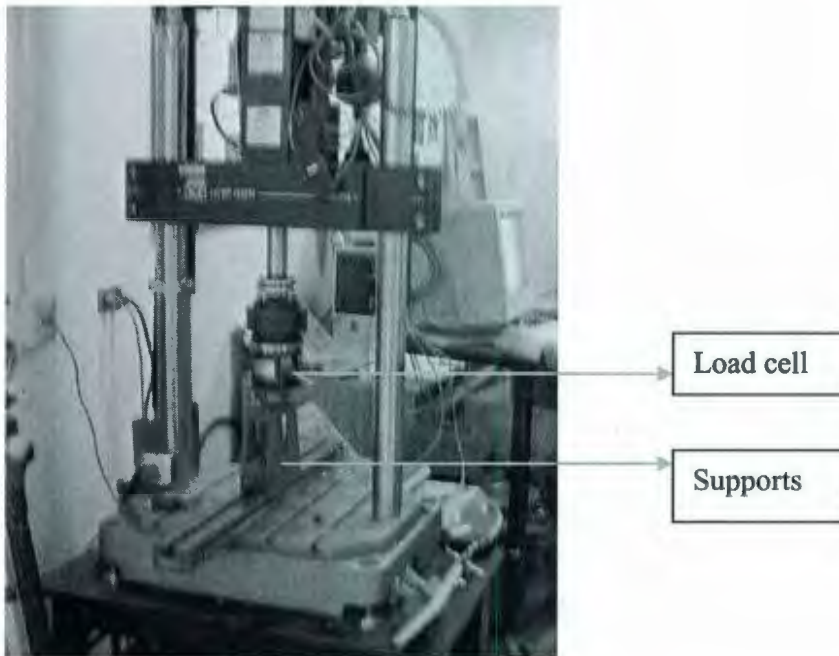


Figure 4-14 Phase 2 bending test apparatus

For both the phases the support span or the distance between the supports was 16 times the thickness of the specimen which is 80 mm. The support span was adjustable i.e.

both the supports can slide through the grooved base (Figure 4-15). The supports span for FRP samples was 126 mm which was carried out onle with phase two test rig.

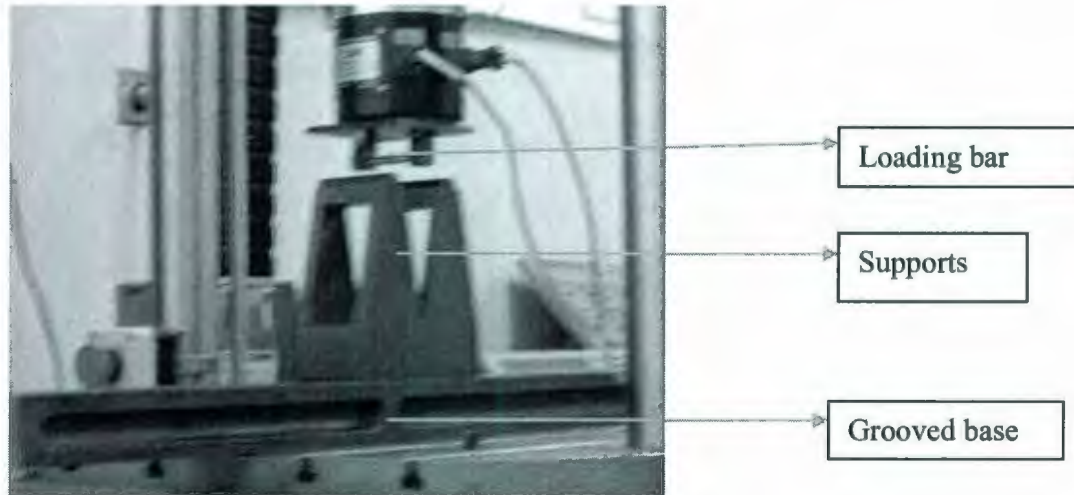


Figure 4-15 Bending test apparatus: supports and loading bar

#### 4.7.3 Micro Hardness Test (Vickers)

As noted in the literature review, other work has not consistent on the effect of exposure to acid on hardness. In this research we have used a Vickers micro-hardness tester (Micromet model) to perform the surface indentation and measurements.

Apart from the material, the hardness of the original casted surface and polished surface before and after exposing was also determined. The length of the specimens was 89 mm, thickness of the specimen was 5 mm and the width of the specimens was 10 mm.

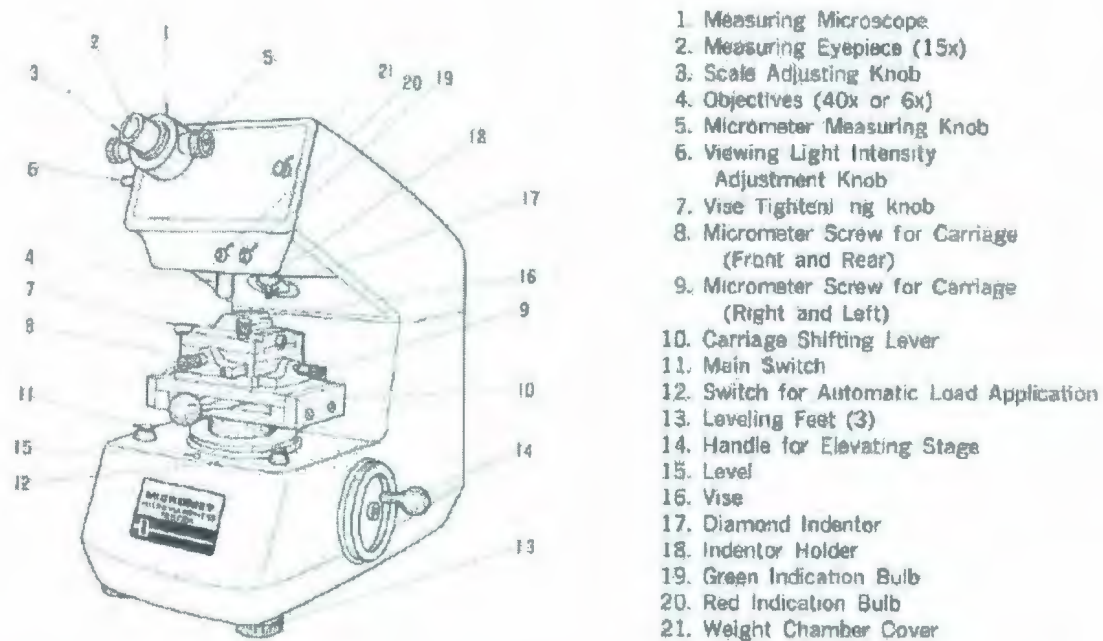


Figure 4-16 Schematic diagram of the Vickers Hardness testing apparatus from Instruction for Micromet hardness tester (manual)

The micro hardness tests are done on the metal to have an idea of the hardness at specific location. Standard hardness test (i.e. Brinell, Rockwell) produce plastic deformation in a surface layer of appreciable thickness (of the order of mm). Micro hardness tests involve much thinner surface layer (10- 100  $\mu\text{m}$ ) and may provide a useful indication of the effect of exposure to aggressive agents with limited penetration of the agent. By using different loads the micro hardness of the polymer resin may be useful for comparing the hardness at different depth for exposed and unexposed specimens. The microhardness tests were done using a Micromet hardness tester as seen in Figure 4-16 and figure 4-17. Its major parts are the microscope and the indenter. The indenter is loaded with different loads and the diagonal distance of the indent is measured to obtain the hardness value which is a function of the load and the diagonal distance of the indent.

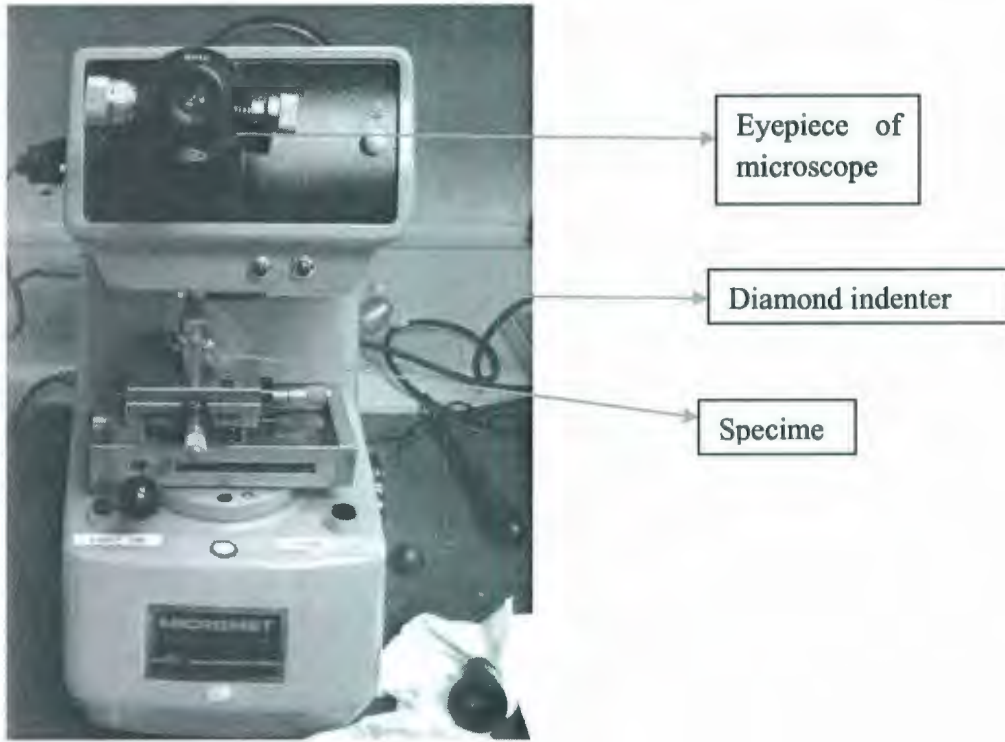


Figure 4-17 Microhardness test apparatus

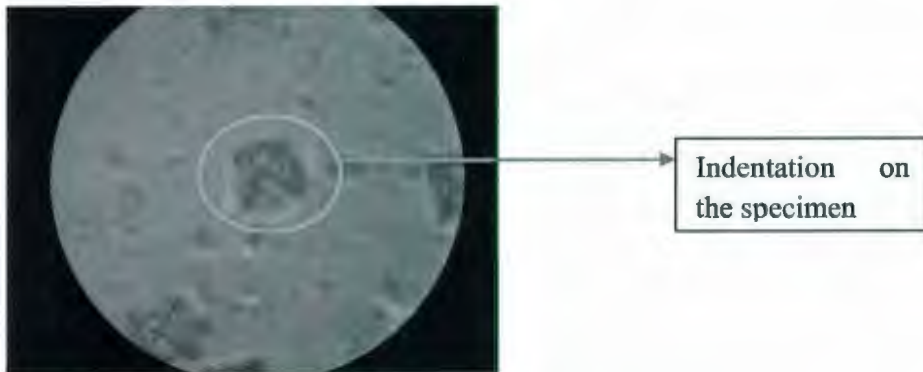


Figure 4-18: 40X magnification of an indentation in the resin

#### 4.7.4 Heat Deflection Temperature (ASTM D648)

Heat deflection temperature or heat distortion temperature is another property of the resin which is largely used by the manufacturer to describe its temperature resistance ability.

The materials mentioned in section 4.2.1 were used to cast (see article 4.1.1) the specimens as shown in Figure 4-19. The length of the specimens was 110 mm, thickness of the specimen was 13 mm and the width of the specimens was 10 mm (Figure 4-20).



(a)



(b)

Figure 4-19 Preparation of HDT mould (a) Mould is assembled with side and bottom support (b) Disassembled support mould and specimen

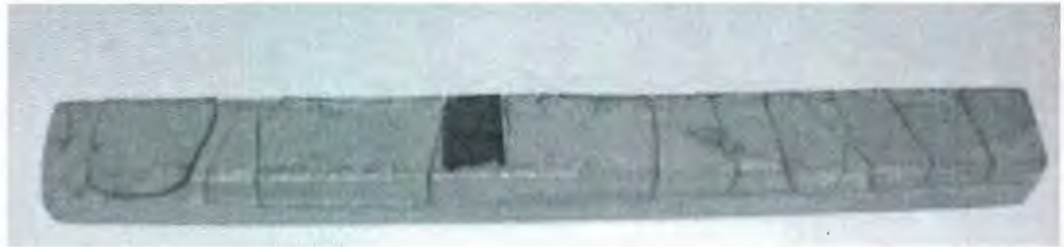


Figure 4-20 Exposed heat deflection temperature test specimen exposed to 1M H<sub>2</sub>SO<sub>4</sub> for 4 weeks

The heat deflection temperature was measured using the ASTM D648. The heat deflection temperature is the temperature at which a defined deflection in bending occurs. An apparatus was fabricated for this purpose (Figure 4-21). It consists of a loading rod, the supports for the specimens, a deflection measurement device, emersion bath and thermometers (Figure 4-22). The deflection measurement device (dial gauge) was attached with the loading bar and the relative movement of the loading bar to the upper plate of the apparatus could be readable to 0.01 mm. The target of doing this experiment was to check whether its heat deflection temperature changes due to the exposure.



Figure 4-21: Heat deflection temperature measuring apparatus

The immersion medium used for polyester was water but for epoxy vinyl ester paraffin oil was used as an immersion medium as it was assumed that the heat deflection temperature for bisphenol-A epoxy vinyl ester will be higher than  $100^{\circ}\text{C}$ . The initial temperatures of all the tests were room temperature, which is  $24\text{-}25^{\circ}\text{C}$ .

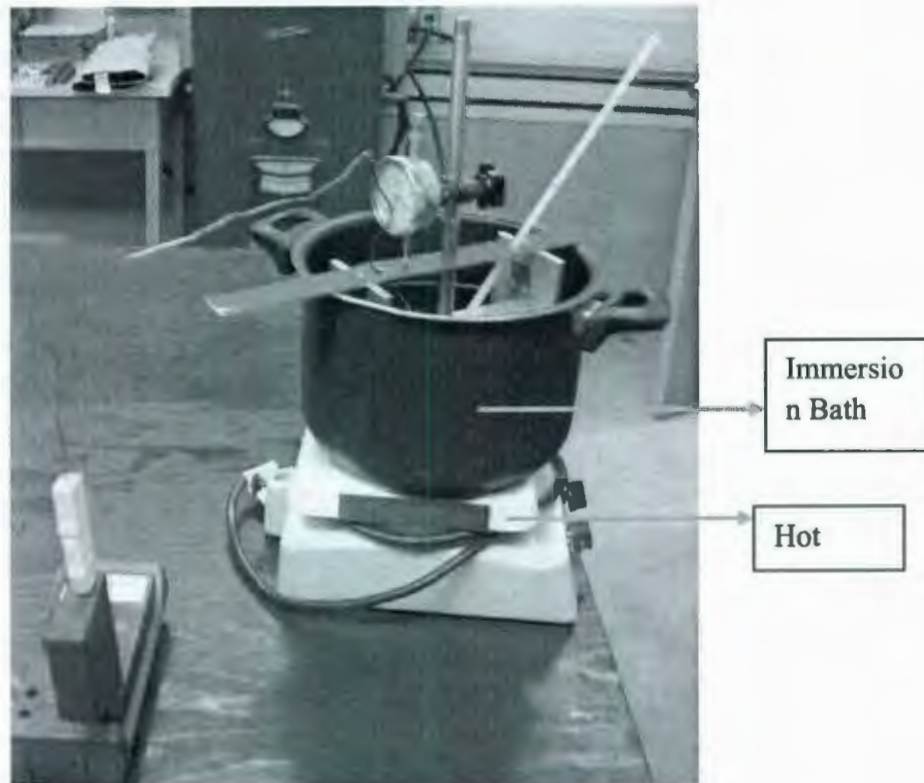


Figure 4-22 Apparatus for heat deflection test

#### **4.8 Tests on Tube Sections**

To ensure reproducible test specimens commercially available tube sections were used to produce test specimens. Three different tests were carried out which are described in the following sections.

##### **4.8.1 Tensile Test on Lateral Loaded Tube Sections**

This test was developed to obtain an easy process of testing the tube sections of a pipe which is manufactured commercially. The standard tensile ASTM test method cannot be done with these tube sections, so these new tests were developed to have an idea about the change of properties of these commercially available pipes.

The materials mentioned in section 4.2.2 were used to prepare test specimens by cutting 38 mm (1.5 inch) long sections (see article 4.1.2) as shown in Figure 4-23.



Figure 4-23 Unexposed FRP specimen

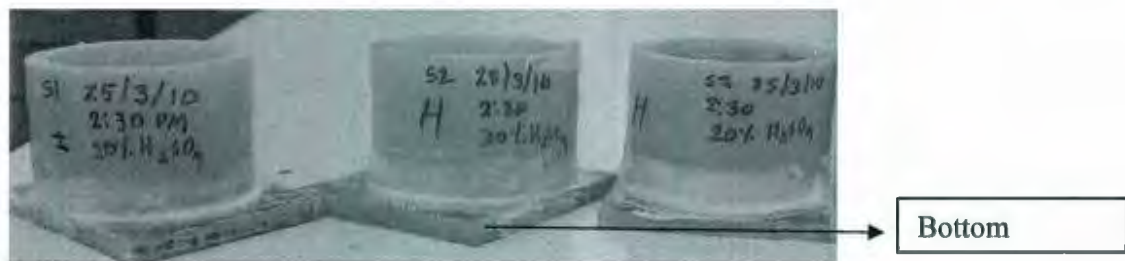


Figure 4-24 H150 specimens prepared for exposing in 1M H<sub>2</sub>SO<sub>4</sub> acid solution

All tensile tests on lateral loaded tube specimens were performed at a crosshead movement (speed) of 12 mm per minute. The hydraulic powered crosshead was set to move 0.2 mm per second. The actual and instantaneous loading rate can also be determined because time, load and position were recorded

A new experiment was designed to observe the load carrying ability of the laterally loaded specimen and compare their result with exposed and unexposed

specimen. Special test jig was designed (Figure 4-25) and fabricated to perform the test (Figure 4-26).

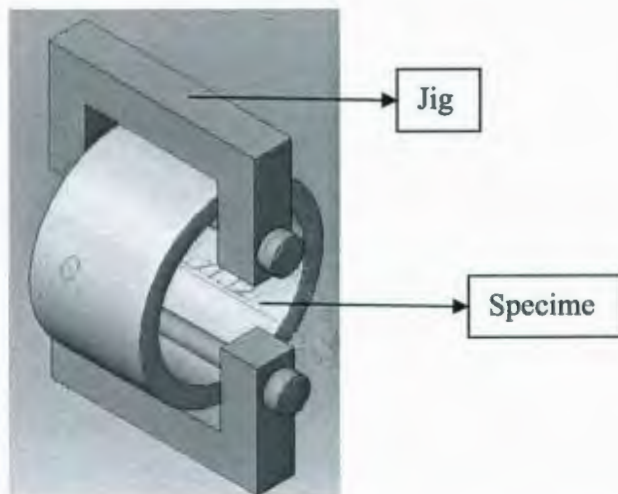


Figure 4-25 Design of jig for laterally loaded tubular test specimen

The same test rig was used as the bending test only the jig was modified. The lower part of the jig was fabricated in such a way so that it can rotate freely along an axis parallel to the axis of the specimen. Instron 5874 test apparatus was used for this test.

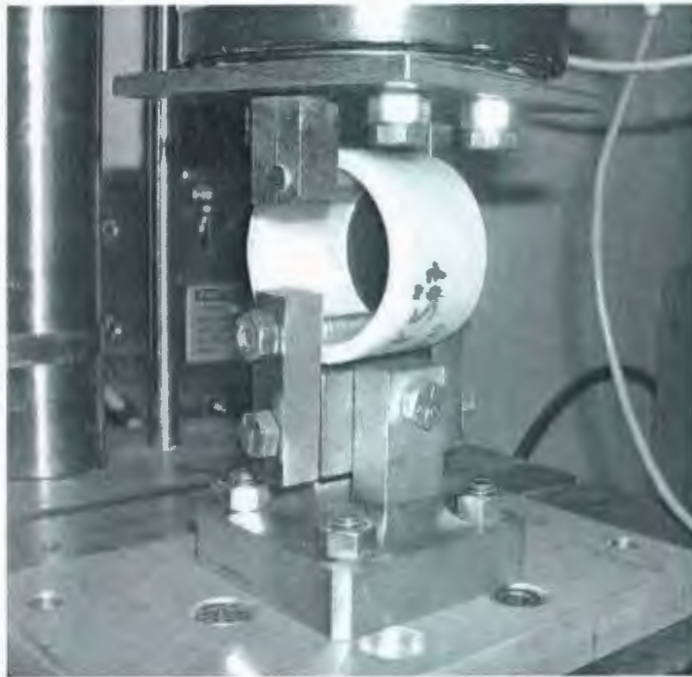


Figure 4-26 Tensile test rig for laterally loaded pipe sections

#### **4.8.2 Compression Test on Axial Loading Test Sections**

In a search for the tests, which can easily categorize the FRP or rank the FRP, compression tests were done. The standard compressive ASTM test method cannot be done with these tube sections, so new tests were developed to have an idea about the change of properties of these commercially available pipes.

The FRP pipes mentioned in article 4.2.2 were used to prepare samples for this test as shown in Figure 4-27.



Figure 4-27 Compression test samples

All compression tests on lateral loaded tube specimens were performed at a crosshead movement (speed) of 6 mm per minute. The hydraulic powered crosshead was set to move 0.1 mm per second. The actual and instantaneous loading rate can also be determined because time, load and position were recorded.

A new experiment was designed to observe the compressive load carrying ability of the axially loaded specimen and compare their result with exposed and unexposed specimen. A self aligning plate was designed and fabricated to ensure the flat surface is in touch with the plate and equally loaded at all the points of the surface (Figure 4-28).



Figure 4-28 Self aligning plate for compression test

A Tinius Olsen testing machine was used for this test. High compression force has to be applied for the failure of the specimens in axial direction. The effect of the acidic solution of the surface is appeared to have a little effect on the test result. An LVDT is used to measure the displacement and the load was measure by a load cell installed in the machine (Figure 4-29). The data was collected and recorded automatically in the computer.



Figure 4-29 Compression test rig

#### 4.8.3 Three Point Load Bending for Tube Sections

Bending tests are more sensitive to the change of the surface as the maximum strain occurs at the surface. The three point bending test was designed to determine the

effect of exposing the FRP pipe to the acidic solution. In this case, similar to laterally loaded tensile test and axially loaded compression test, the commercially available FRP pipes were used as samples.

The FRP pipes mentioned in article 4.2.2 were used to prepare samples (see article 4.1.2) for this test. The 1.5 inch long tube section was cut down at 120° angle into 3 equal width specimens as in Figure 4-30.



Figure 4-30 Bending test specimen after test

All bending tests on laterally loaded tube specimens were performed at a crosshead movement (speed) of 12 mm per minute. The hydraulic powered crosshead was set to move 0.2 mm per second. The actual and instantaneous loading rate can also be determined because time, load and position were recorded. The average rate of displacement appears constant.

This one is also a new experiment designed to observe the bending load carrying ability of the specimen and compare their result with exposed and unexposed specimen. Special test jig was designed (Figure 4-31) and fabricated to perform the test (Figure 4-32).



Figure 4-31 Design for three point bending test jig for FRP section

The same test rig was used as the ASTM bending test and laterally loaded FRP tube section, only the jig was modified. It consists of a base which consists of two supports and a loading bar.

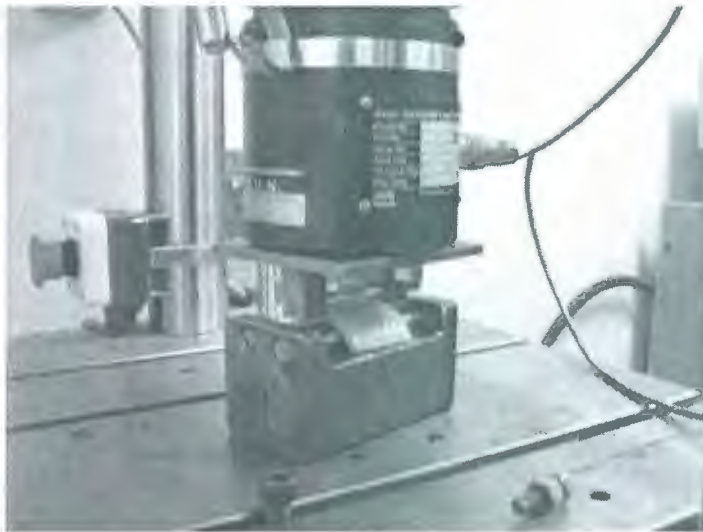


Figure 4-32 Three point bending test apparatus for FRP samples

## 4.9 Examination of FRP Structure and Effect of Exposure on Resins

Microstructure of the FRP samples was examined in order to understand the content of the material. Later on it was examined to see the depth of penetration of the acid into the resin. Microstructures were assessed with the help of optical microscope and scanning electron microscope. Along with the microscopic images electron dispersion spectra was recorded to determine any penetration of the acid or cobalt spent electrolyte.

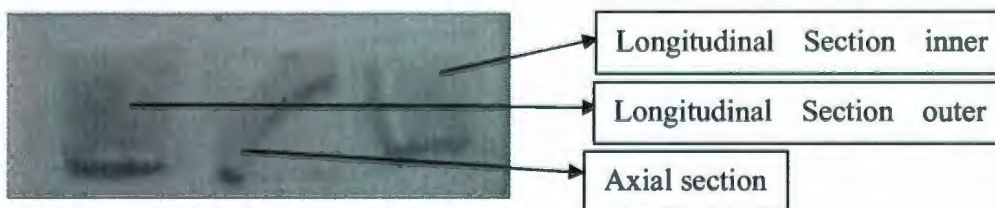
All the types of materials mentioned in article 4.2 were examined to observe and analyze the effect of exposure and the structure of different FRPs used for different tests

### 4.9.1 Optical Microscopy

For optical microscopy specimens with length 15 mm, width varied from 5 mm to 15 mm and a thin section was used for this purpose which was less than a millimetre.

The specimens prepared from the FRP pipes were cut into small pieces in longitudinal and perpendicular direction of the pipe axis. One side of the piece was attached to the glass slide as seen in the Figure 4-33 (a). Then these specimens were polished off to prepare thin sections as seen in Figure 4-33 (b)

Specimens made from only resins were examined both on the surface and along the cross-sections. The specimens prepared for analysing the surface were kept as were and the cross sections were polished.



(a)



(b)

Figure 4-33 Specimen preparation for microstructure examination (a) before polishing (b) after polishing (thin section)

A Reichert optical microscope was used for this purpose. Magnification was 32X. The photographs were taken by a digital camera fitted with a special adaptor lens (Figure 4-34).



Figure 4-34 Microscope and camera used for analysing the microstructure of the FRP pipes

#### **4.9.2 Scanning Electron Microscopy**

Approximately 5 mm by 5 mm specimens were used and the thickness varied from 5 mm to 10 mm. The samples used for scanning electron microscopy was used for both EDS so care was taken so that specimens does not come in contact with water. After cutting the and polishing when necessary the specimens were cleaned with kerosene.

## **Chapter 5**

### **RESULTS AND DISCUSSION**

This chapter deals with the results of the tests that were performed (chapter 3). Some of the experimental procedures are not sensitive to the exposure of the FRP samples or the corrosive fluid, at least not in this work. But the experimental procedure and test results are reported for the further development of the experimental procedures and apparatus. Some of the tests were done on both FRP material and resin (tensile test ASTM D638, bending test ASTM D790), while some tests were done only on the resin (heat deflection test ASTM D648), and finally the other tests were done only on the FRP material (tensile test for laterally loaded pipe section, compression test for axially loaded pipe section, three point bending test for FRP pipe section, microstructure analysis).

#### **5.1 Tensile Test ASTM D638:**

Tensile stress is calculated by dividing the load by the original cross sectional area and tensile strength is the maximum stress attained during the test. Percent elongation is calculated by dividing the extension for a particular stress by the original gauge length (one inch for this case). The modulus is determined by the “best fit” straight line of the portion of the stress strain curve before failure. The best fit straight line is determined by regression.

### 5.1.1 Repeatability of the Test

The repeatability of the test is done by testing four (UP1 – UP4) unexposed polyester resin specimens. As it appears from the tensile test results that the tensile yield strength and yield stress at fracture varies with the specimen (Table 5-1). This indicates that the repeatability of the test, in terms of the tensile strength is not good. But it appears from the following figure (Figure 5-1) that the graphs follow the same pattern although tensile strengths and strains are different. Moreover, the fracture of the specimens at different tensile strengths may be a consequence of applying different loads at the grips of the apparatus, variability in the amount of hardener and resin, change of thickness of the specimens and defects on the surface of the specimen. The UP3 specimen will be considered as a basis for comparison with the other specimens in Figure 5-1 and Figure 5-2.

Table 5-1 Tensile test results of unexposed polyester for testing repeatability

Test Date	Material	Width (mm)	Thickness (mm)	Load at break (N)	Tensile Strength (MPa)	Strain at fracture	Modulus (MPa)
30-Mar	UP1	12.69	5.50	1694	24	0.041	561
30-Mar	UP2	12.47	6.16	2595	33	0.055	562
12-Apr	UP3	12.75	4.88	1828	29	0.058	470
12-Apr	UP4	12.75	5.75	1412	19	0.047	399

\*Modulus is measured from the “slope” of best fit regression line

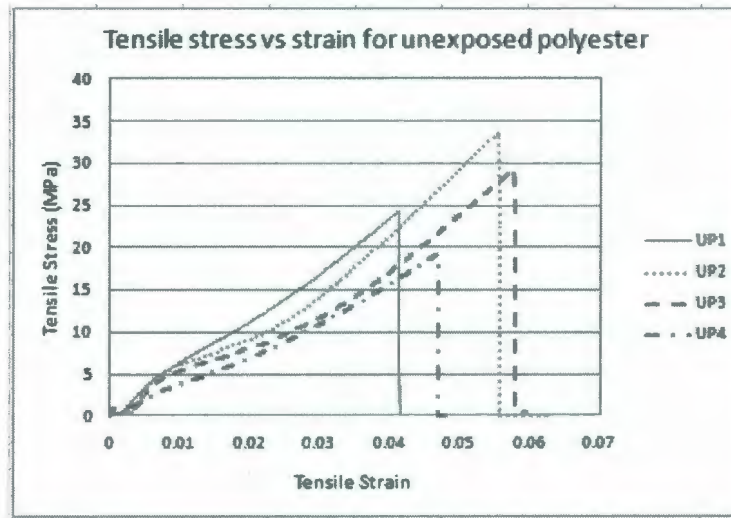


Figure 5-1 Tensile stress versus strain for four polyester specimens

### 5.1.2 Effect of Exposure Duration on Stress Strain Curve

The effect of duration of exposure to the solution was investigated by exposing the specimen up to four weeks. Figure 5-2(a) shows the effect of exposure duration on the tensile stress strain curve when polyester is exposed to 1M H<sub>2</sub>SO<sub>4</sub> at 75°C. It is evident from this figure that the modulus increases when polyester is exposed for 48 hour but the modulus decreases when it was exposed for 1 week and decreases more for 4 week of exposure. When polyester is exposed to cobalt spent electrolyte the modulus remains at about 390 to 440 MPa for both exposed and unexposed test specimens (Figure 5-2 )

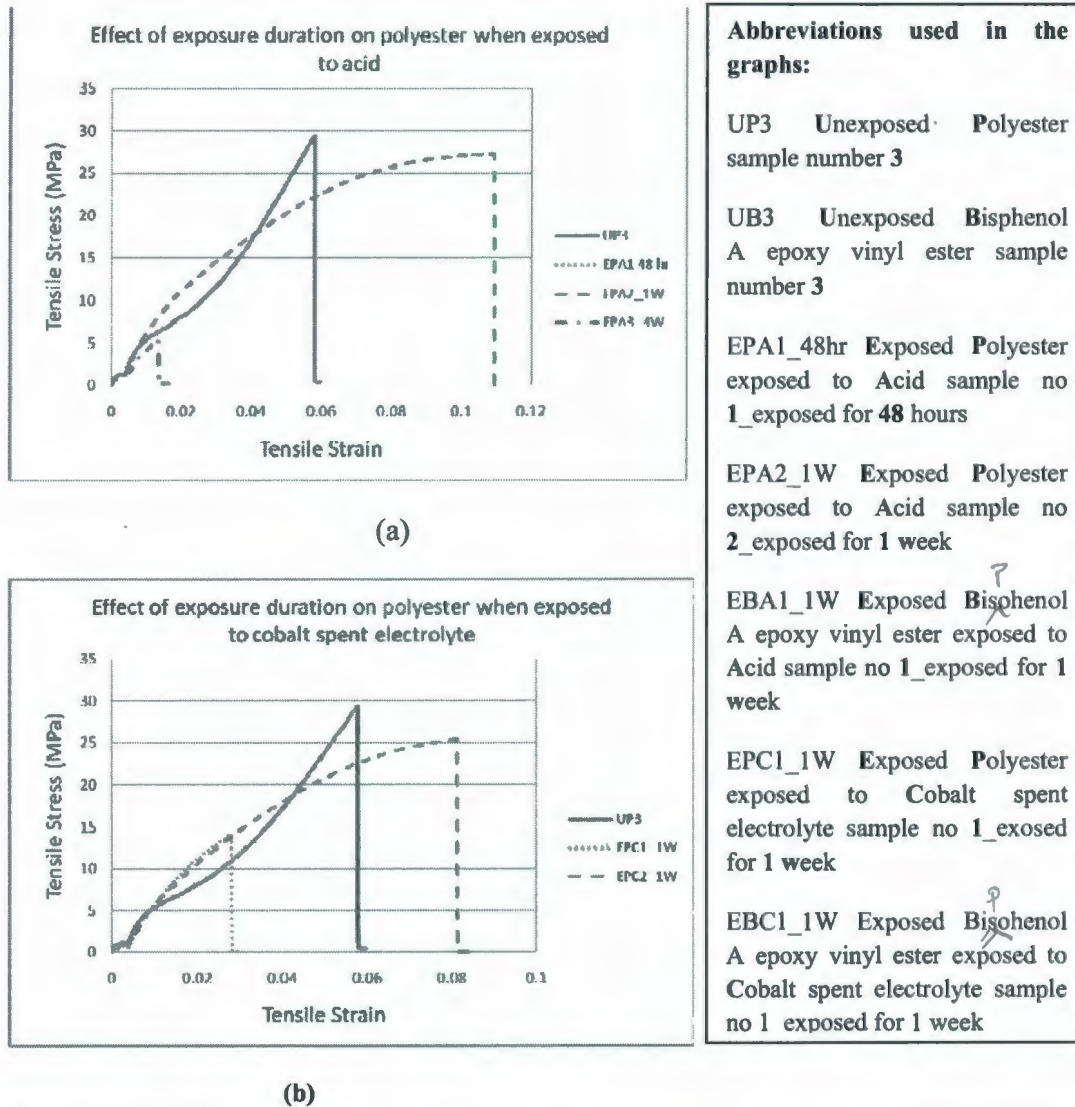
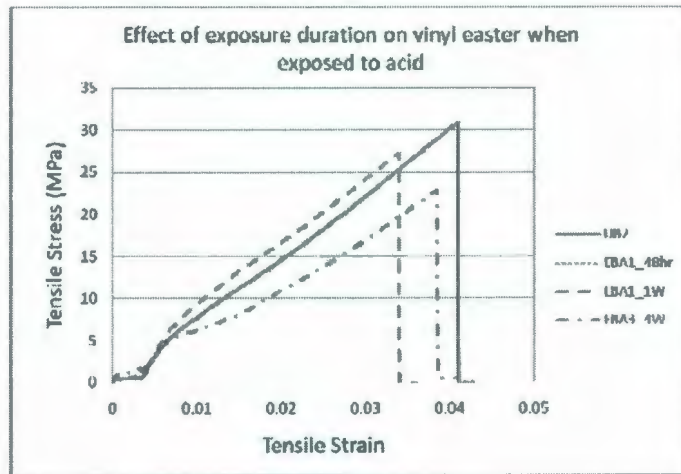


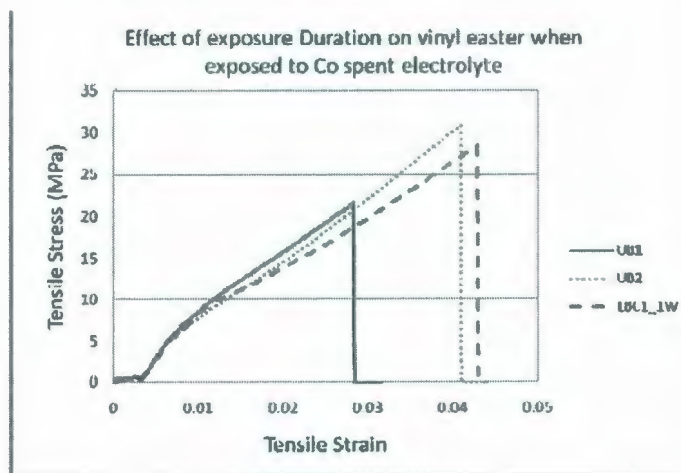
Figure 5-2 Effect of duration of exposure on exposed polyester specimen (a) when exposed to acid (b) when exposed to Cobalt spent electrolyte at 75°C.

Figure 5-3 shows the effect of duration of exposure when bisphenol A epoxy vinyl ester is exposed to 1M H<sub>2</sub>SO<sub>4</sub> (Figure 5-3(a)) and cobalt spent electrolyte (Figure 5-3 (b)) at 75°C. For both cases though the change of slope is evident but the variation of slope among different exposure time is too small to make any comment on the effect of

duration of time. This test procedure to determine the effect of exposure duration for bisphenol A epoxy vinyl ester does not seem to be sensitive enough to pick up the change. The slope of stress strain curve for unexposed and exposed to different solution varies from 440 to 780 MPa.



(a)

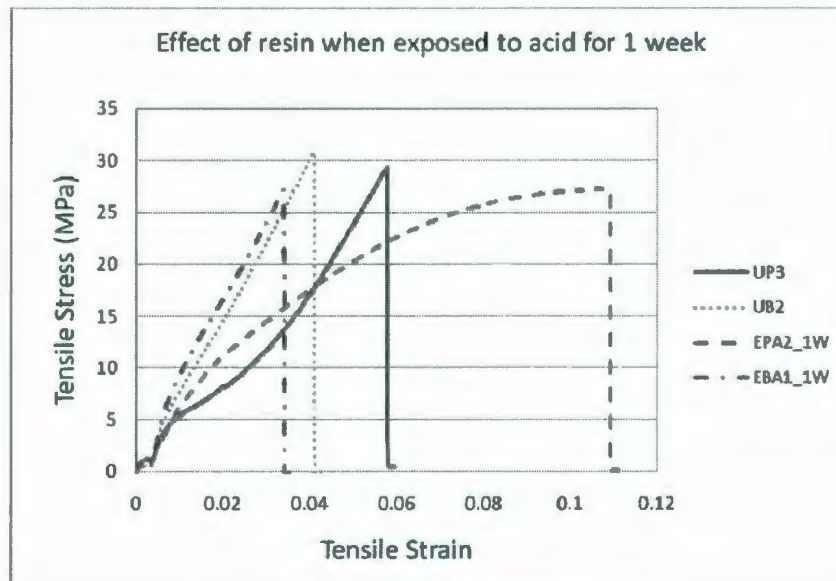


(b)

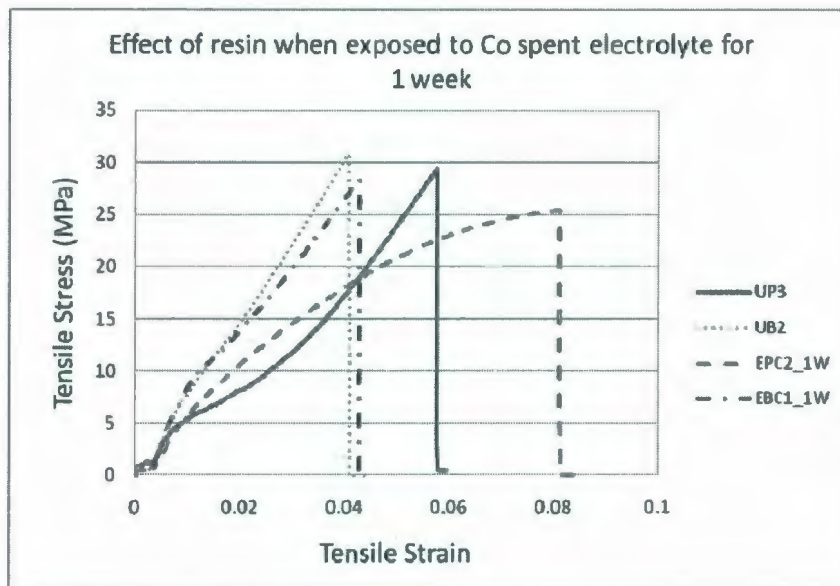
Figure 5-3 Effect of exposure duration on bisphenol A epoxy vinyl ester to (a) 1M  $H_2SO_4$  and (b) Hydrometallurgical solution at  $75^\circ C$ .

### 5.1.3 Effect of Different Resins and Solutions on Stress Strain Curve

The effect of the two resins bisphenol A epoxy vinyl ester and polyester on the stress strain curve were analyzed and will be discussed next. Both the specimens were exposed to 1M H<sub>2</sub>SO<sub>4</sub> and cobalt spent electrolyte and the change of the modulus for using different solution was also tested. Figure 5-4 shows the effect of the resins when it was exposed to different solutions. It is evident from Figure 5-4 that the change of modulus for bisphenol A epoxy vinyl ester is less compared to polyester even after exposure for 1 week to 1M H<sub>2</sub>SO<sub>4</sub> and cobalt spent electrolyte at 75°C.



(a)



(b)

Figure 5-4 Effect of different resins on tensile stress strain curve when the specimens are exposed to (a) 1M H<sub>2</sub>SO<sub>4</sub> and (b) Cobalt spent electrolyte solution at 75°C.

Figure 5-5 shows the effect of resin when it is exposed to 1M H<sub>2</sub>SO<sub>4</sub> at 75°C. It is evident from the figure that 4 weeks of exposure clearly shows the difference of resins if we compare the ultimate tensile strength. Comparing slopes in this case does not show any difference between the resins. It was also observed that crack appears at the surface of polyester after exposing it to acid for four weeks, which reveals its very low ultimate tensile strength.

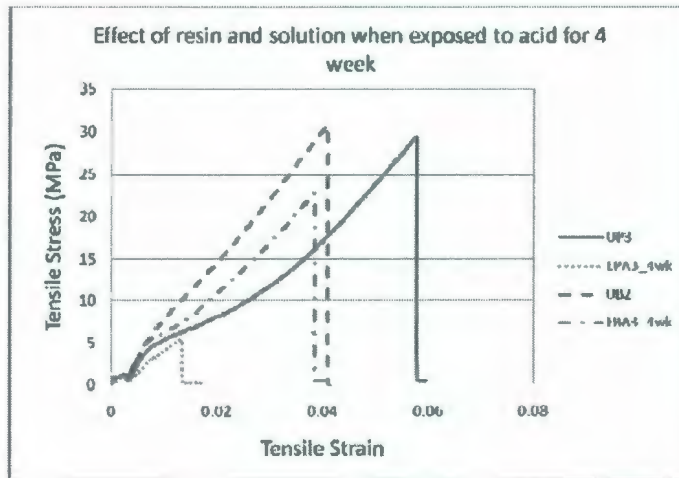


Figure 5-5 Effect of different resins on tensile stress strain curve exposed to 1M H<sub>2</sub>SO<sub>4</sub> at 75°C.

These tests show much variability in extension (i.e. strain to failure) and slope or (modulus) in both unexposed and exposed specimens. Variability in strain is to be expected as brittle materials are very sensitive to surface defects but variability in slope/modulus for similar specimens is also present. Again the difference in modulus for exposed and unexposed specimens are not evident. Though it was evident that this test could differentiate polyester exposed for 4w with the other exposure, it is not sensitive enough to predict the difference between the qualities of the resins. The variation in results in repeated tests is somewhat the same for parameters like resin, time and exposing fluid. Overall tensile tests do not appear to be useful with exposures of a few weeks or less to show or study the effects of exposure. The results of all tensile tests using ASTM D638 are tabulated in table A1-1.

## 5.2 Bending Test (ASTM D790)

The bending test theoretically should be a more sensitive test to any changes on the surface of the material. For a particular deflection at the middle the inner and the outer surface of the specimen experience maximum strain. This ensures the sensitivity to a small change in the surface. The following results also proves this assumption. As it was described earlier two different setups were used to determine the bending stress strain relationship. The first phase, which was also a preliminary phase to determine whether the bending test has sensitivity to exposure conditions or not, did not have a constant rate of loading. After ensuring the effectiveness of bending test the second phase was carried out with an important test apparatus in phase 2 with servo controlled loading. The load and position of the loading cross head was recorded. From these two parameters flexural stress ( $\sigma_f$ ) and strain ( $\epsilon_f$ ) was calculated. Flexural stress ( $\sigma_f$ ) i.e. tensile stress in specimen (i.e. at the surfaces furthest away from the neutral axis) is calculated from the following equation,

$$\sigma_f = \frac{3PL}{2bd^2} \quad \dots \quad \dots \quad \dots \quad \dots \quad (5-1)$$

where, P is the load, L is the distance between the supports, b is the width of the specimens and d is the thickness of the specimen. The strain ( $\epsilon_f$ ), which occurs at the centre of the specimen, halfway between the supports is calculated by the equation

$$\epsilon_f = \frac{6Dd}{L^2} \quad \dots \quad \dots \quad \dots \quad \dots \quad (5-2)$$

where, D is the displacement, d is the thickness of the specimen and L is the distance between the supports.

### 5.2.1 Phase 1 Bending test

Two resins were tested and the effect of exposure on stress strain curve was obtained by exposing a bisphenol A epoxy vinyl ester resin for 1 week in 1 M H<sub>2</sub>SO<sub>4</sub> at 75°C. As seen Figure 5-6 that the highest modulus observed from the two tests observed from the two tests on unexposed specimens was 295 MPa whereas the modulus after exposing bisphenol A epoxy vinyl ester specimens for 1 week was 1574 MPa. It is also clear from the figure that bisphenol A epoxy vinyl ester has higher modulus than unexposed polyester. The following table consists of the same test results as shown in the figure. The increase of modulus due to 1 week exposure may be due to the increase of cross linking as previously reported by Shafeeq (2006). The numerical values of the modulus and flexural stress at different strains can easily be compared.

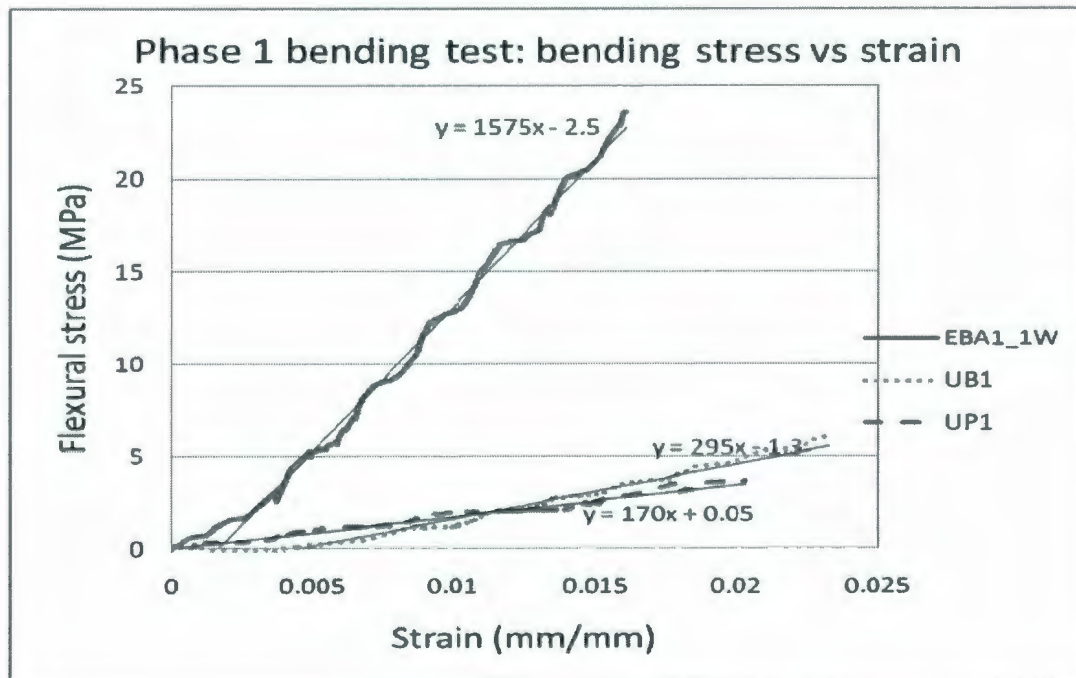


Figure 5-6 Effect of exposure (exposed to 1M H<sub>2</sub>SO<sub>4</sub>) and different resin on flexural stress strain curve

Table 5-2 Bending test result (phase 1)

Material	Width, b (mm)	Thickness, d (mm)	Flexural Stress, $\sigma_f$ at 1% Strain (MPa)	Maximum Measured Stress (MPa)	Strain at Maximum Measured Stress	Modulus* ( <i>MPa</i> )
EB1_1wk	15.00	5.00	13	24	0.016	1575
UB1	15.00	5.00	1	6	0.023	295
UB2	15.00	5.00	3	7	0.024	298
UP1	15.00	5.00	2	4	0.020	170

\*Modulus is determined from the slope of a best fit line.

The following bending test results which will be described were from the phase 2 test results.

### 5.2.2 Repeatability of Test

The repeatability of the test is checked by testing three unexposed polyester test specimens (UP1-UP3) and three exposed bisphenol A epoxy vinyl ester resin exposed for 1 week (EBA1\_1W to EBA3\_1W). Figure 5-7 shows the repeatability of the bending test for different specimens. It is evident that there is up to about 3.5 :1 range in ultimate flexural strength. The modulus varies from 1849 *MPa* to 2649 *MPa* for unexposed polyester specimens and from 2471 to 3423 *MPa* for bisphenol A epoxy vinyl ester exposed to 1M H<sub>2</sub>SO<sub>4</sub> at 75°C for 1 week. This is about 1.4:1 range in modulus for both sets of tests.

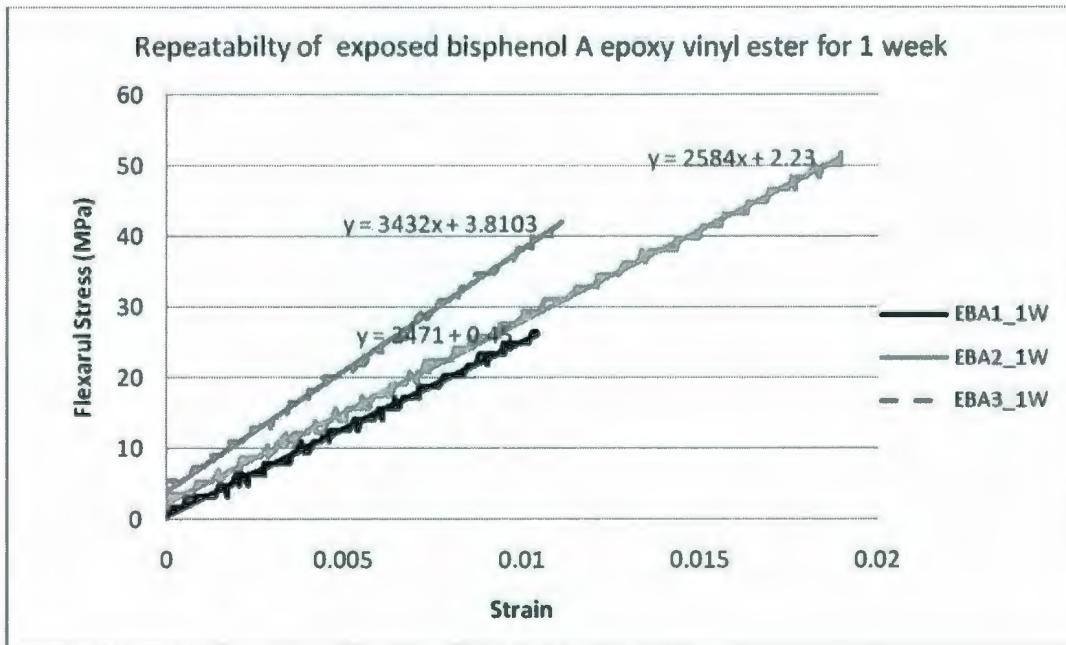
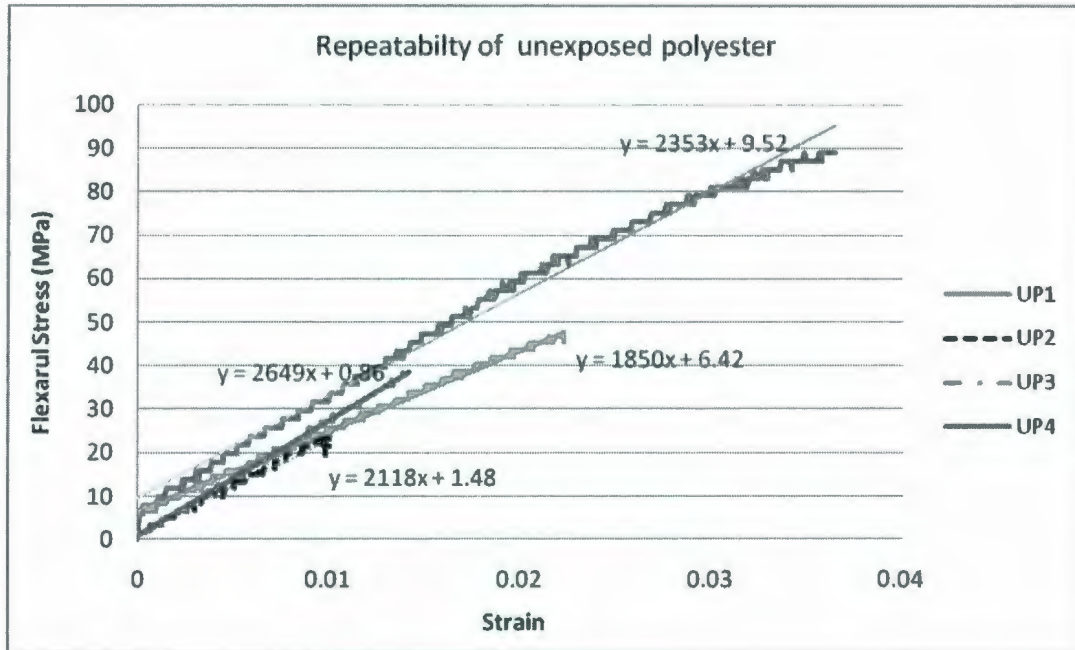


Figure 5-7 Repeatability of bending test specimen for (a) unexposed polyester and (b) bisphenol A epoxy vinyl ester exposed to 1M H<sub>2</sub>SO<sub>4</sub> at 75°C for 1 week.

### 5.2.3 Effect of Exposure Duration

When Figure 5-8 and Figure 5-10 are compared we can analyze the effect of exposure duration on polyester with respect to stress strain parameters (modulus, elongation). Similarly comparison between Figure 5-9 and Figure 5-11 shows the effect of exposure duration on bisphenol A epoxy vinyl ester.

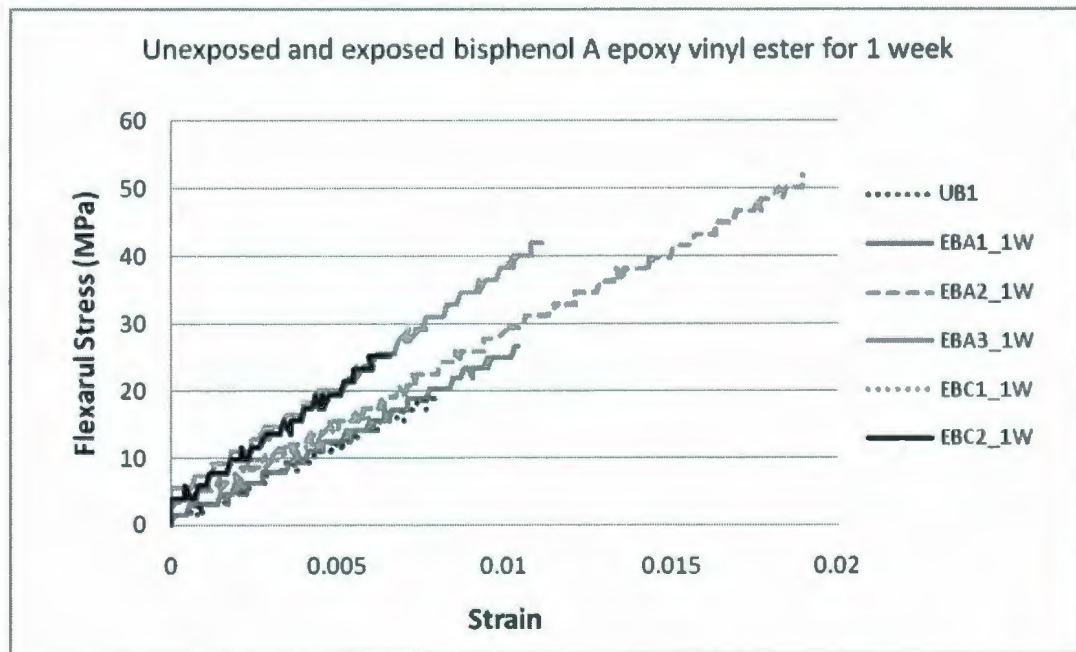


Figure 5-8 Flexural stress strain curve for unexposed and exposed bisphenol A epoxy vinyl ester to 1M H<sub>2</sub>SO<sub>4</sub> and cobalt spent electrolyte

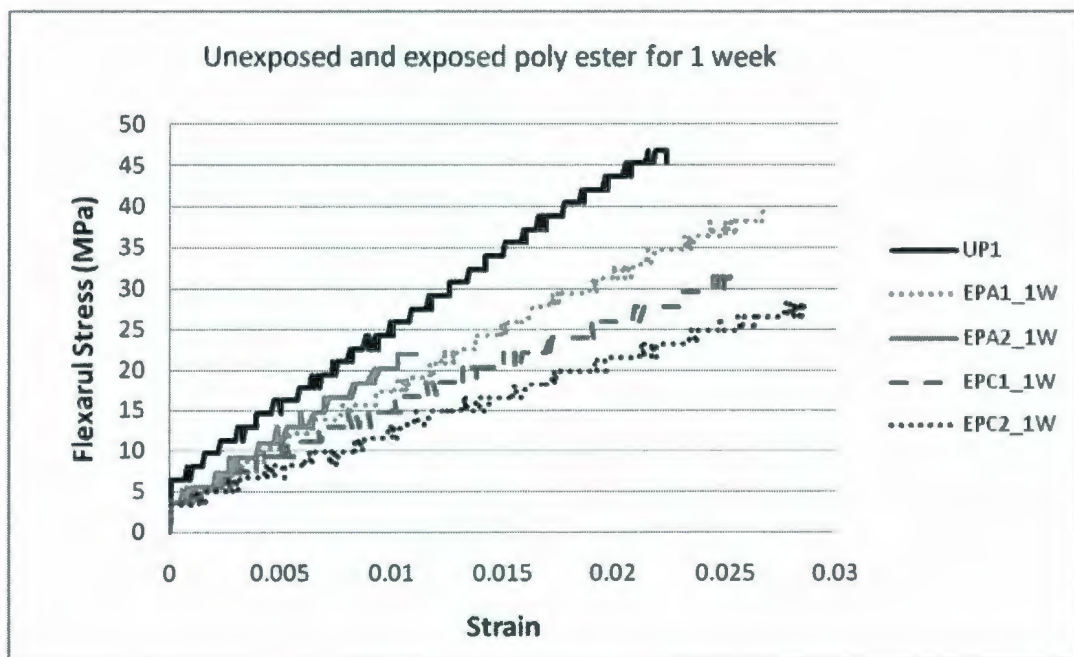


Figure 5-9 Flexural stress strain curve for unexposed and polyester to 1M H<sub>2</sub>SO<sub>4</sub> and cobalt spent electrolyte at 75°C for 1 week

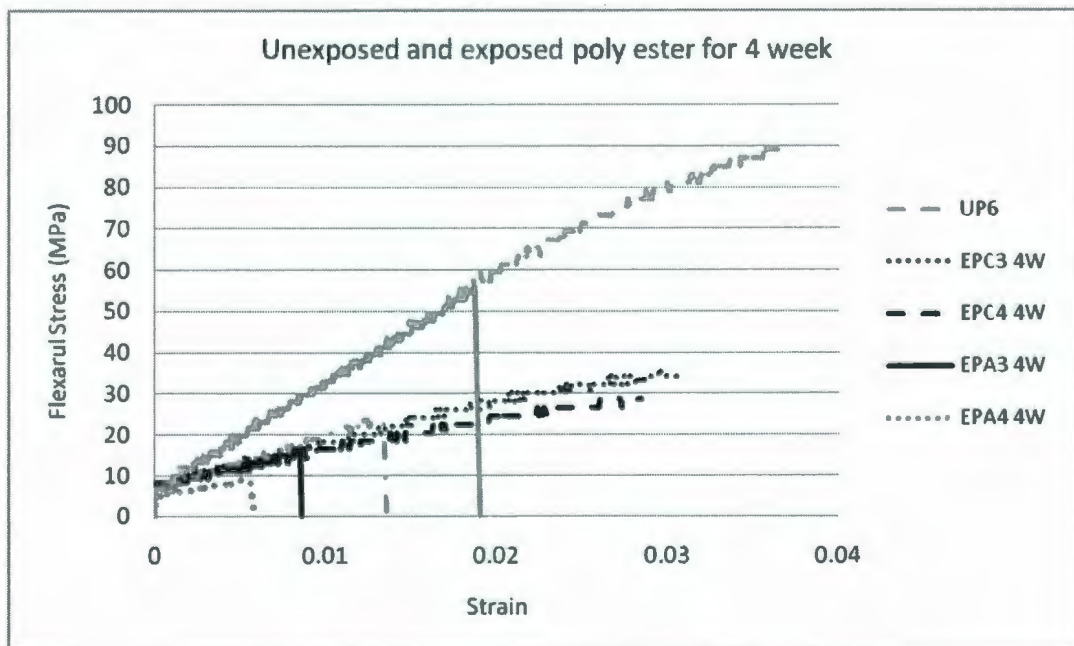


Figure 5-10 Flexural stress strain curve for unexposed and exposed poly ester to 1M H<sub>2</sub>SO<sub>4</sub> and cobalt spent electrolyte at 75°C for 4 week

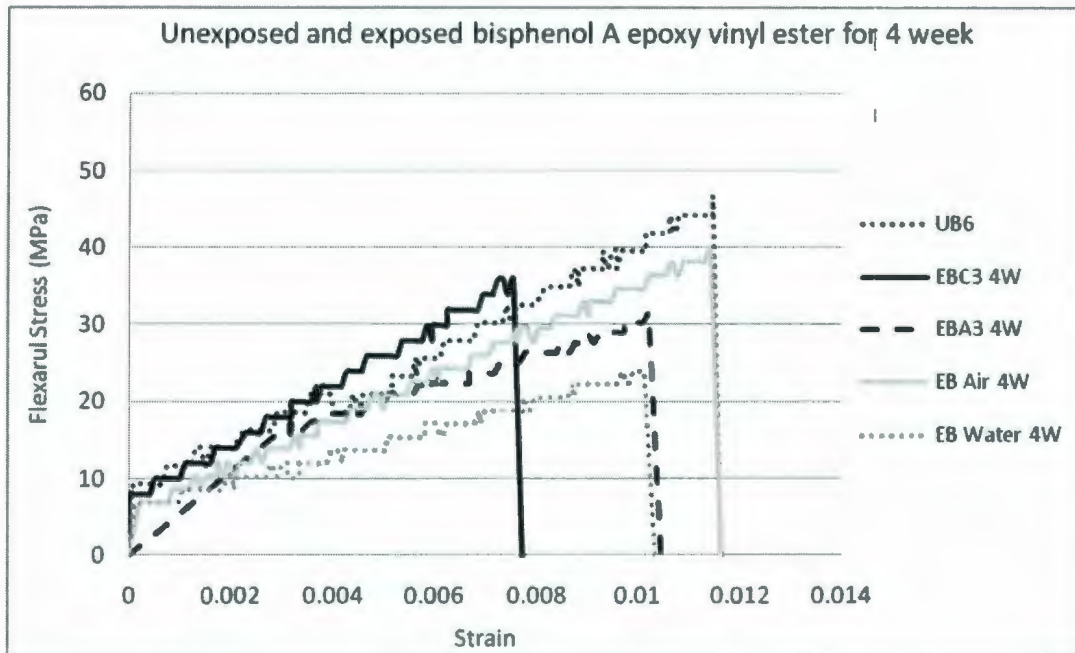


Figure 5-11 Flexural stress strain curve for unexposed and exposed bisphenol A epoxy vinyl ester to 1M H<sub>2</sub>SO<sub>4</sub> and cobalt spent electrolyte

Figure 5-12 shows the effect of exposure duration on the modulus for different resins and exposure. It is evident from the figure that when exposed to 1 M sulphuric acid for both polyester and bisphenol A epoxy vinyl ester the modulus reduces with duration of exposure. Only when bisphenol A epoxy vinyl ester is exposed to cobalt spent electrolyte the modulus increases.

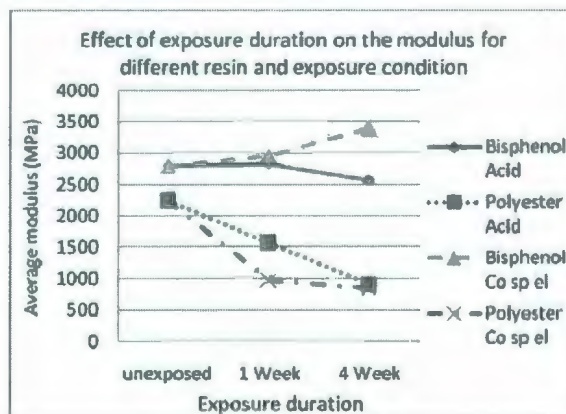


Figure 5-12 Effect of exposure duration on modulus of flexural stress versus strain curve for different resins and exposure condition when exposed to 1 M H<sub>2</sub>SO<sub>4</sub> or Cobalt spent electrolyte at 75°C.

#### 5.2.4 Effect of Resins and Solution

Figure 5-13 shows the effect of resins used and different solution to which the specimens are exposed. In the unexposed condition polyester has a higher modulus but when it is exposed to 1M H<sub>2</sub>SO<sub>4</sub> or cobalt spent electrolyte the modulus decreases. However, different results were found for bisphenol A epoxy vinyl ester where the modulus increases for exposure to 1M H<sub>2</sub>SO<sub>4</sub> or cobalt spent electrolyte.

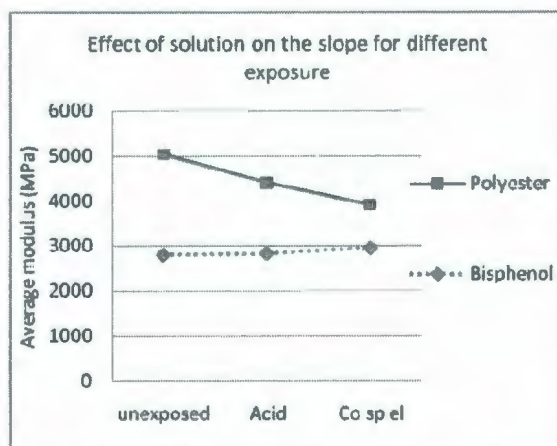
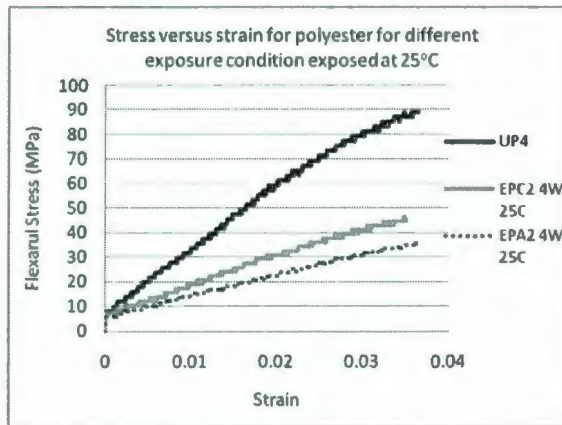


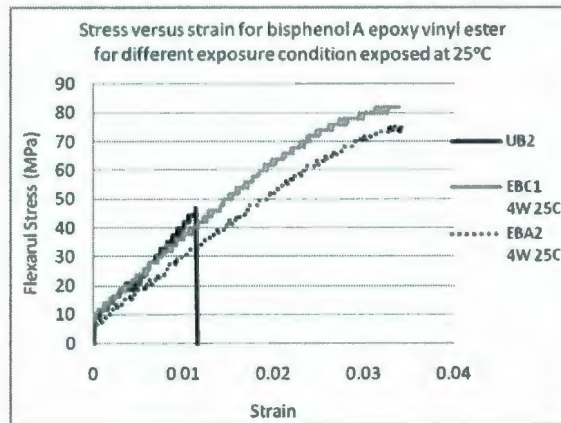
Figure 5-13 Effect of resin and solution on the modulus of stress strain curve when exposed to 1M H<sub>2</sub>SO<sub>4</sub> and cobalt spent electrolyte for 1 week at 75°C.

#### 5.2.5 Effect of Temperature of Exposure

The resins were exposed to different solution at 25°C and 75°C to observe the effect of temperature (however, bending tests were done at room temperature. Figure 5-14 shows the stress versus strain curve for different resins and exposure condition. It is evident from the figure that at even at 25°C the modulus is different from the unexposed specimen.



(a)



(b)

Figure 5-14 Flexural Stress versus strain curve for (a) polyester and (b) bisphenol A epoxy vinyl ester when exposed to 1M H<sub>2</sub>SO<sub>4</sub> and cobalt spent electrolyte at 25°C

The effect of temperature for different resins and exposure conditions are shown in Figure 5-15. For polyester modulus decreases with the increase of exposure temperature but for bisphenol A epoxy vinyl ester the modulus increases.

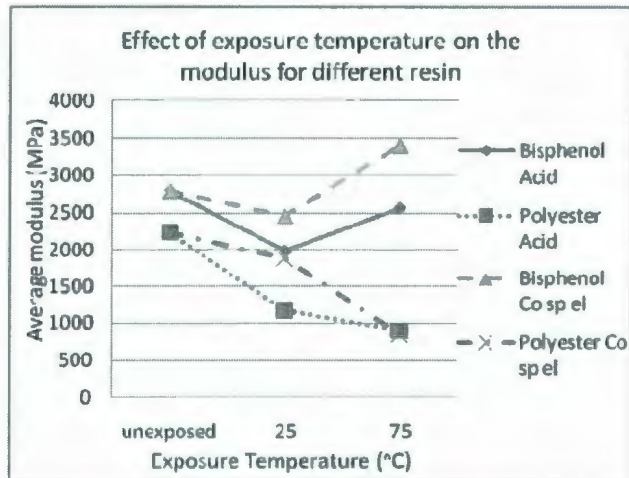


Figure 5-15 Effect of temperature on the modulus for different resins and exposure when exposed for four weeks

The average results after testing at least two samples for each parameter and exposure condition is tabulated in Table 5-3. The results for each of the sample is also recorded and included in table A2-2.

Table 5-3 Results of bending test ASTM D790

Material	Exposed to	Duration of exposure (Week)	Average Flexural Stress, $\sigma_f$ at 1% Strain (MPa)	Average Modulus (MPa)
Polyester	Unexposed	0	26	2242
	1M H <sub>2</sub> SO <sub>4</sub> at 75°C	1	18	1579
	1M H <sub>2</sub> SO <sub>4</sub> at 75°C	4	*	902
	1M H <sub>2</sub> SO <sub>4</sub> at 25°C	4	18	1171
	Co spent electrolyte at 75°C	1	14	980
	Co spent electrolyte at 75°C	4	17	849

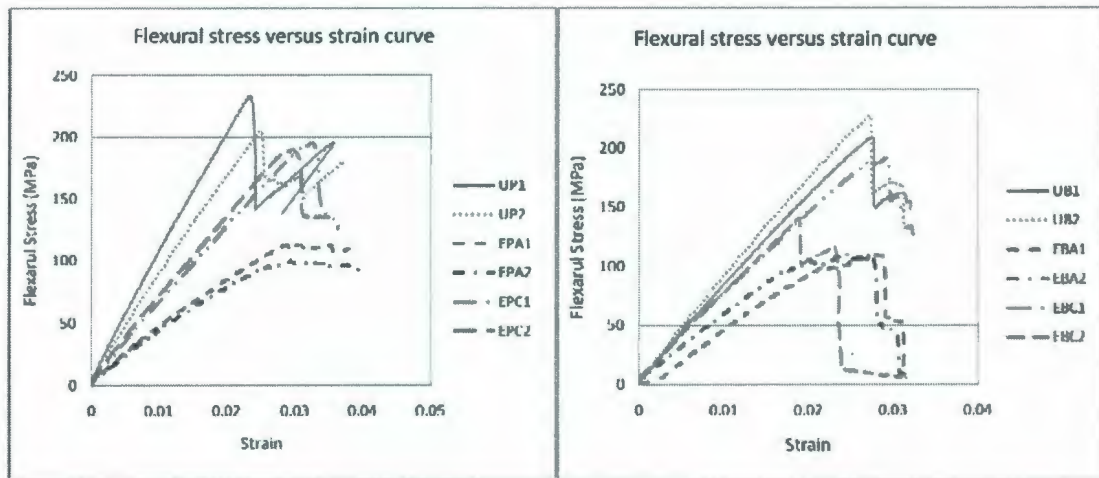
	Co spent electrolyte at 25°C	4	26	1888
Bisphenol A Epoxy Vinyl Ester	Unexposed	0	*	2335
	1M H <sub>2</sub> SO <sub>4</sub> at 75°C	1	30	2829
	1M H <sub>2</sub> SO <sub>4</sub> at 75°C	4	30	2560
	1M H <sub>2</sub> SO <sub>4</sub> at 25°C	4	28	1992
	Co spent electrolyte at 75°C	1	14	980
	Co spent electrolyte at 75°C	4	*	3392
	Co spent electrolyte at 25°C	4	40	2463

\*break before 1% strain

Average values are taken from testing two specimens. The test result for each of the sample is recorded in Table A1-2.

### 5.2.6 Test for FRP Samples

ASTM D790 test was also performed on FRP samples. FRP samples were cut from FRP pipes. Figure 5-16 shows the stress versus strain curve for polyester and bisphenol A epoxy vinyl ester for different exposure conditions. It is evident from the figure that the modulus of the curve as well as the ultimate bending stress is repeatable for most of the cases. Both the parameters were used in the following figures and tables to compare between the FRPs.



(a)

(b)

Figure 5-16 Flexural stress versus strain curve for glass fibre reinforced (a) polyester (b) bisphenol A epoxy vinyl ester for different exposure conditions exposed for four weeks at 75°C.

Figure 5-17 shows the effect of different solutions on the modulus for FRP samples. It is evident from the figure that with the exposure to different solution the modulus reduces for both polyester. After 4 weeks of exposure both of the materials were effected significantly due to exposure to 1M sulphuric acid and cobalt spent electrolyte.

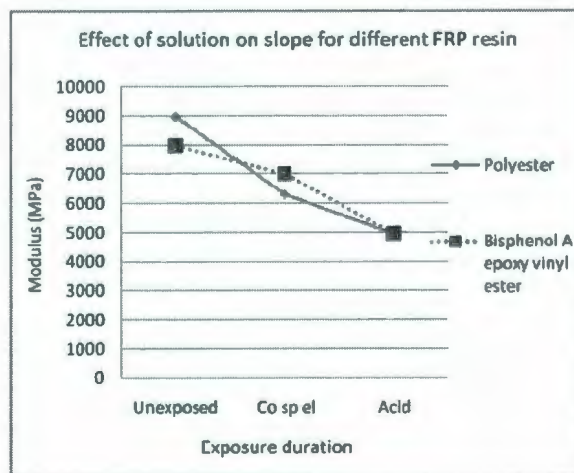


Figure 5-17 Effect of different exposure conditions for different resin on stress versus strain modulus for 4 weeks at 75°C

Average test result for bending test on FRP samples are recorded in Table 5-1 and the test result for each of the samples are tabulated in table A

Table 5-4 Result for ASTM D790 test for fibre reinforced polymers

Material	Average maximum stress (MPa)	Average strain at maximum stress (mm/mm)	Modulus* (MPa)
UP	220	0.025	8968
UB	218	0.027	7978
EPA	106	0.029	3697
EBA	107	0.023	4952
EPC	193	0.030	6299
EBC	167	0.024	7006

\*Modulus is measured from the "slope" of the best fit straight line determined by regression

### 5.3 Micro Hardness Test:

A hardness test is a way to determine the hardness of the surface layer of an object. The thickness of the layer in question is determined by the depth to which the indenter produces plastic deformation. The lower the indenter's load the thinner the layer studied. At loads less than 1000g the hardness test is usually referred to as a micro-hardness test.

However, there are several ways a micro-hardness test may be affected by other variables, Normally the deformation produced by a conical indenter, such as used in the

Vickers test has a similar pattern whatever the size of the indentation and should indicate of the same hardness in a material of uniform hardness, whatever the load applied to the indenter. However the apparent hardness often increases with decreasing load. In some situations the reverse is the case. Various reasons have been proposed for these effects.

The object of the current work was to explore the value off micro hardness test in studying the effect of exposure to acids on resins. The objective of this test was to determine whether the hardness changes at different depth of the specimen due to exposure by increasing the depth of indentation by increasing the weight on the indenter. The diagonal distance ( $d_1$ ) of the rectangular indentation is measured by the microscope. The Vicker's hardness is determined by the equation

$$HV = \frac{1.854 \times P}{d_1^2} \quad \dots \quad \dots \quad \dots \quad \dots \quad (5-3)$$

where, P is the load of the indenter and  $d_1$  is the diagonal distance of the rectangular indentation. The depth of the indentation is determined because the angle between the indenter surfaces is known ( $136^\circ$ ). Average micro hardness was calculated from the hardness values for different loads. The depth of indentation is given by the equation,

$$depth = \frac{d_1}{2 \times \tan 68^\circ} \quad \dots \quad \dots \quad \dots \quad \dots \quad (5-4)$$

where,  $d_1$  is the diagonal distance of the rectangular indentation on the specimen. The test result also differed from each other depending on the surface preparation. Polished or ground surface hardness is higher compared to unpolished surface. So both cases were tested.

Specimens were prepared with polished and unpolished surface are the different surfaces for the micro-hardness test. The unpolished surface refers to the original surface which is very smooth, shiny and transparent. Other surfaces were sanded and polished with fine abrasive paper and diamond paste. The two types of surface gave different hardness values. Hence, the effect of exposure on surfaces prepared both ways was examined.

### **5.3.1 Repeatability of the Test**

Micro hardness of the whole surface cannot be the same because the surface is affected by many conditions like curing period, inclusion of bubbles on the surface, difference of smoothness on the surface and so on. For each of the specimen three readings were taken and averaged. The result of the unexposed and unpolished polyester and epoxy vinyl ester is shown in Figure 5-18 which indicates that the micro hardness tests are repeatable with a very little of variation. But it was also observed as shown in this figure that with the variation of load of the indenter the hardness increases.

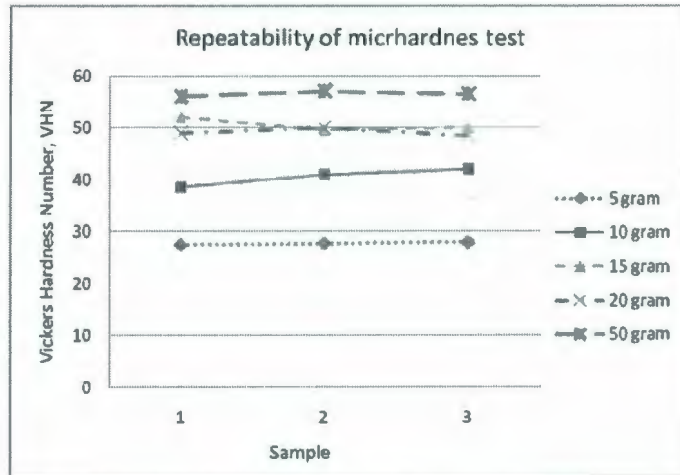
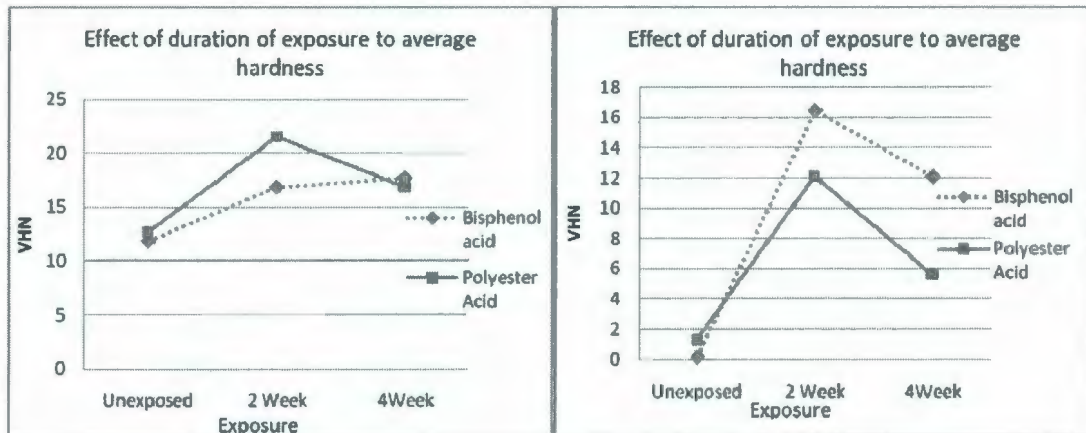


Figure 5-18 Repeatability of micro hardness test of unexposed polished polyester resin for different weights of indentation.

### 5.3.2 Effect of Duration of Exposure and Surface Preparation

Figure 5-19 shows the effect of exposure duration on the average hardness using loads of 5 to 25 (5, 10, 15, 20 and 25) grams when exposed to 1M H<sub>2</sub>SO<sub>4</sub> at 75°C. It is evident from the figure that for both polished and unpolished surfaces the hardness increases for 1 week exposure but later decreases with time. It can also be concluded by comparing (a) and (b) that though the unexposed unpolished surface has much lower hardness, after exposure they tend to attain the same magnitude of hardness after the exposure of 1 week to acid.



(a)

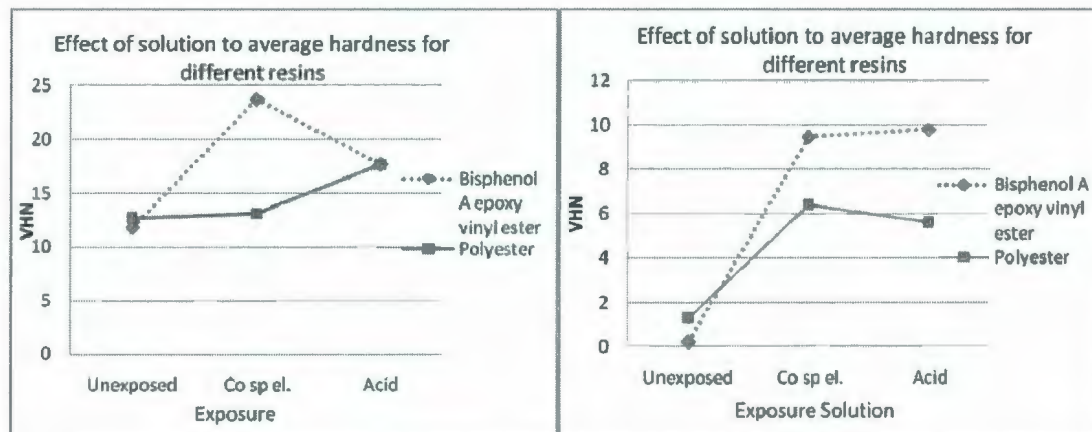
(b)

Figure 5-19 Effect of exposure duration on Vickers hardness when exposed to 1M H<sub>2</sub>SO<sub>4</sub> at 75°C for (a) polished surface and (b) unpolished surface

The change of hardness due to polishing is evident from all the results. This change may occur because of the work hardening of the plastic or it might be due to the non-homogeneity of the plastic material. The outer surface of the casted specimens may have a very low hardness.

### 5.3.3 Effect of Resin and Solution

It is evident from Figure 5-20 that exposing to any solution increases the hardness of both the materials. The magnitude of the increase varies for different resins and solution.



(a)

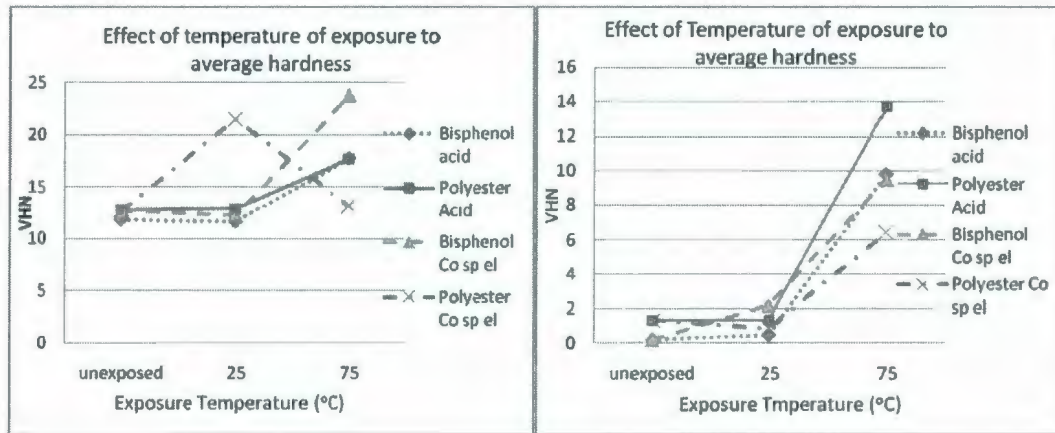
(b)

Figure 5-20 Effect of solution on Vickers average micro hardness at loads 5, 10, 15, 20 and 25 gram for different resins for (a) polished and (b) unpolished surface when exposed at 75°C for 4 weeks

After 4 weeks of exposure at 75°C polished surface has almost the same average Vickers hardness for both cobalt spent electrolyte and 1M H<sub>2</sub>SO<sub>4</sub> and for polished surface again it is different from the unpolished surface.

### 5.3.4 Effect of Temperature

The effect of exposure temperature has a high effect on the hardness. It is evident from Figure 5-21 that exposure at 25°C did not change the hardness much as exposure at 75°C. For all of the specimens, except polyester exposed to Cobalt spent electrolyte, the effect is the same; for polyester exposed to Co spent electrolyte, microhardness increases after 1 week of exposure but when it was exposed for 4 weeks the Vickers hardness decreased.



(a)

(b)

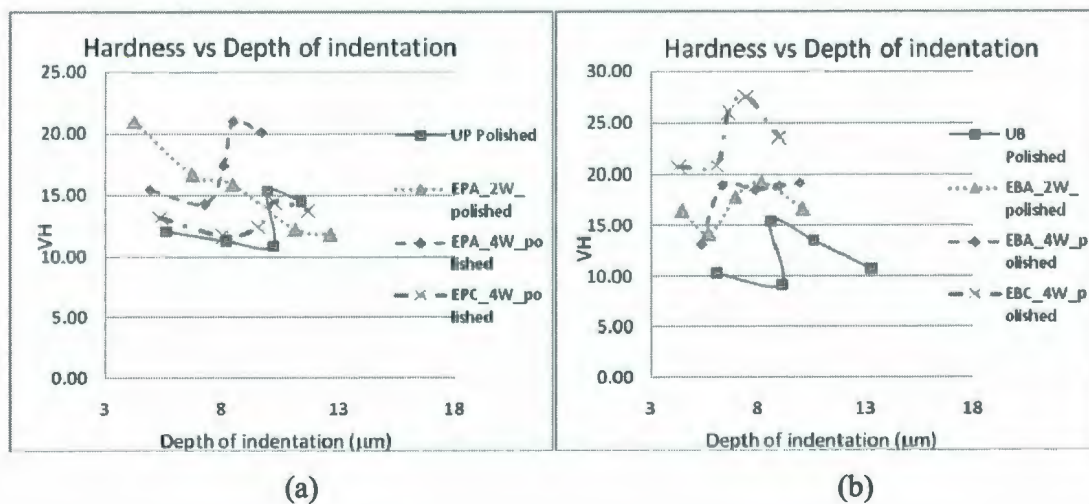
Figure 5-21 Effect of exposure temperature on Vickers hardness for (a) polished and (b) unpolished surface exposed for 4 weeks.

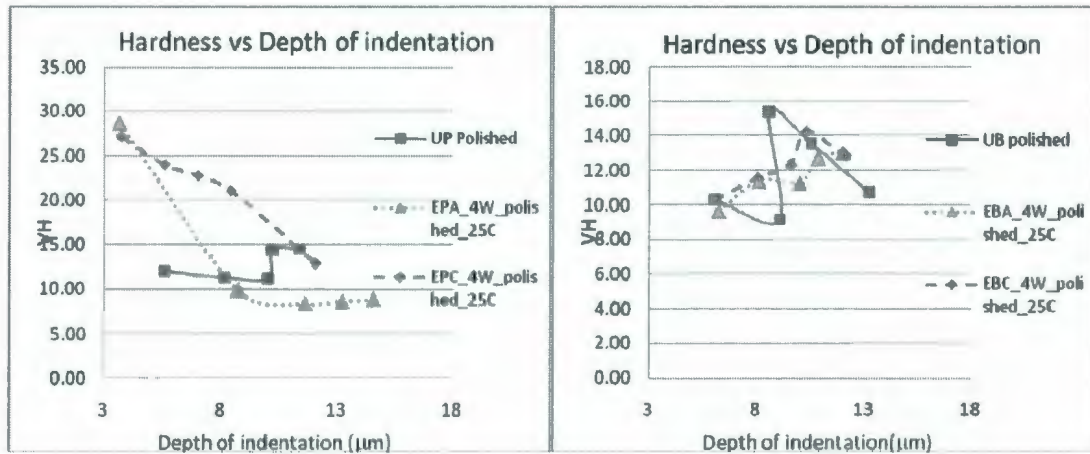
### 5.3.5 Effect of Exposure on Microhardness at Different Depth of Penetration

The main objective of microhardness test was to determine any effect of exposure depending upon depth. It is well known that micro hardness can depend on depth of indentation, i.e., on load, and can either increase or decrease with increasing depth. The load dependence of the micro hardness does not follow a simple law and even for a homogeneous material (Microhardness, 2010). If the micro indenting process is assumed to involve a cutting mechanism, the friction between the indenter and sample surface will govern the indentation depth (Samuels, 1986). An opposing theory for micro indentation is proposed by Mulhearn (1959), which assumes compression of a volume much larger than the indentation. The test results show that the hardness varies with the load or depth of penetration even with the unexposed specimen. It is clear that either the variation is an inherent property of the test or the material itself is non uniform with an effect of

exposure. The comparison of hardness at different depth of indentations (or load of the indenter) for exposed and unexposed specimens reveals an effect of exposure at different depths, i.e. an effect of penetration of the acidic solutions.

Figure 5-22 shows change of hardness with depth of indentation for polished surface for different exposure solutions, exposure durations and exposure temperatures. The hardness of the unexposed resins varies between 10 to 16 for indentation 5 to 13  $\mu\text{m}$ . Except bisphenol A epoxy vinyl ester exposed at 25°C the hardness at very low depth becomes high after exposure and then decreases with indentation depth. For bisphenol A epoxy vinyl ester exposed at 25°C shown in Figure 5-22 (d) the microhardness did not show much variation compared to unexposed specimens. Hardness at a depth of approximately 5  $\mu\text{m}$  for polyester exposed at 75°C to 1M  $\text{H}_2\text{SO}_4$  increases 12 to 21 VHN and then reduces to 15 VHN after 4 weeks of exposure.



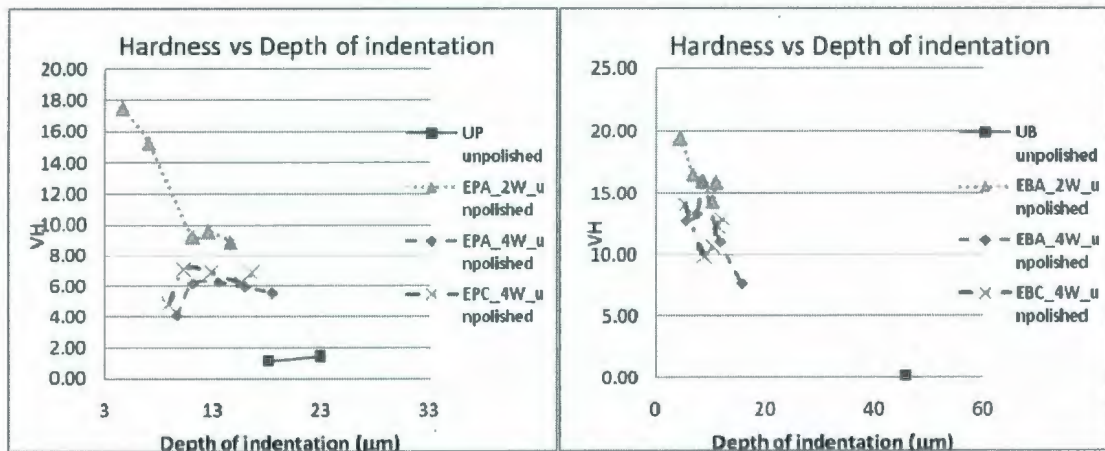


(c)

(d)

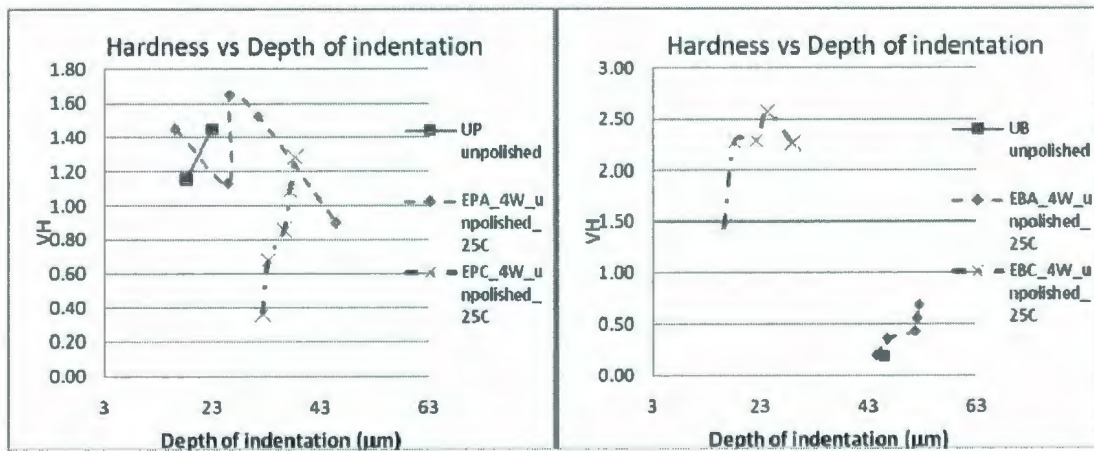
Figure 5-22 Change of hardness of polished surface with depth of indentation for (a) polyester exposed at 75°C (b) bisphenol A epoxy vinyl ester exposed at 75°C (c) polyester exposed at 25°C (d) bisphenol A epoxy vinyl ester exposed at 25°C

Figure 5-23 shows the effect of exposure on hardness for different depth of indentation for unpolished surface. An unpolished surface has a very low hardness. As a result for unpolished surface it was only possible to obtain hardness for very low weight on indentation (5 and 10 gm). However the depth of indentation for this small load was very high. The effect on this surface is obvious from the figures for the specimens exposed at 75°C. For both polyester and bisphenol A epoxy vinyl ester the hardness becomes very high at very low depth when they are exposed for 2 weeks to 1M H<sub>2</sub>SO<sub>4</sub> but after 4 week of exposure the outer surfaces becomes softer.



(a)

(b)



(c)

(d)

Figure 5-23 Change of hardness of unpolished surface with depth of indentation for (a) polyester exposed at 75°C (b) bisphenol A epoxy vinyl ester exposed at 75°C (c) polyester exposed at 25°C (d) bisphenol A epoxy vinyl ester exposed at 25°C

For all the cases it appears that the outer surface is most affected by the exposure (high increase of hardness). As the depth of indentation increases the change of hardness as compared to the unexposed ones reduces.

#### 5.4 Heat Deflection Temperature ASTM D648

Any change in heat deflection temperature due to exposure is not recognizable as the variation of the results for different samples of the same type of exposure is more than the average change of heat deflection temperature. The heat deflection temperatures for different samples are listed below in Table 5-5. The change of average heat deflection is small, but since the variation of HDT for a particular exposure test is large, the average values of four tests results must be recorded in order to see if a trend exists in the data. Otherwise anomalous test result errors would have to be explained.

Table 5-5 Heat deflection temperature results

Material	Exposed to	Duration of exposure (Week)	Average heat deflection temperature (°C)
Polyester	Unexposed	0	45.7
	1M H <sub>2</sub> SO <sub>4</sub>	4	46.0
	Co spent electrolyte	4	47.0
Bisphenol A Epoxy	Unexposed	0	110.0
	1M H <sub>2</sub> SO <sub>4</sub>	4	112.0
Vinyl Ester	Co spent electrolyte	4	115.0

No significant effect of exposure on heat deflection temperature (HDT) is evident.

#### 5.5 Tensile Test on Laterally Loaded Pipe Section

This is one of the four tests that were performed only on FRP pipe sections. Though the tensile load is applied on the pipe sections it acts like a three point bending

test. It will be clear if upper or lower part of the tube section is considered. The result is a similar pattern of stresses and strain in the central portion of the specimen, in both tests.

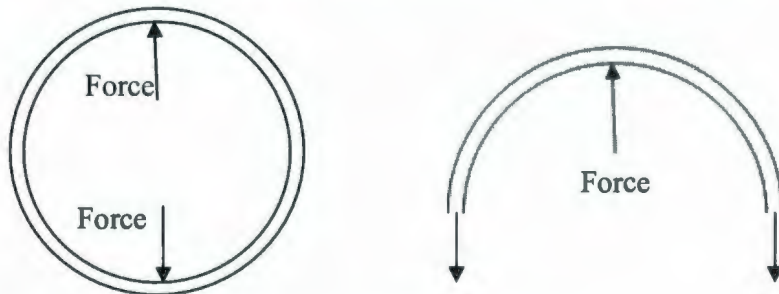


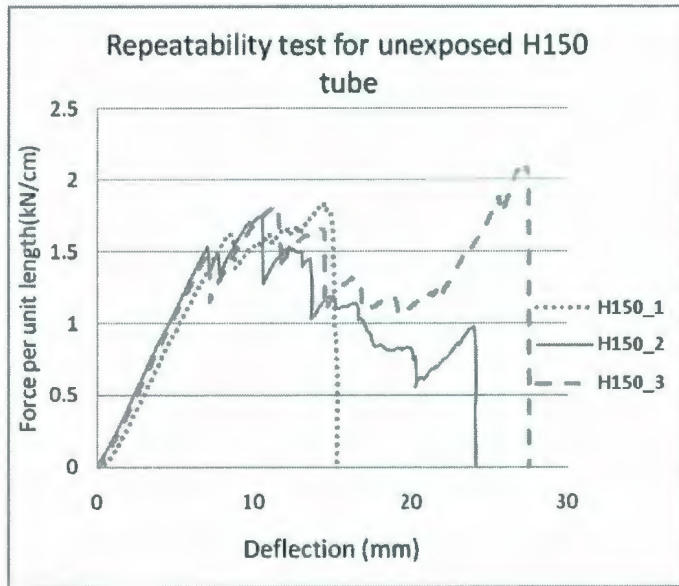
Figure 5-24 Applied force for laterally loaded tube sections.

It should also be mentioned that the pipe diameter and thickness is identical for all the pipe sections. So in this section force per unit length of the pipe section versus displacement was recorded and analyzed instead of stress versus strain analysis.

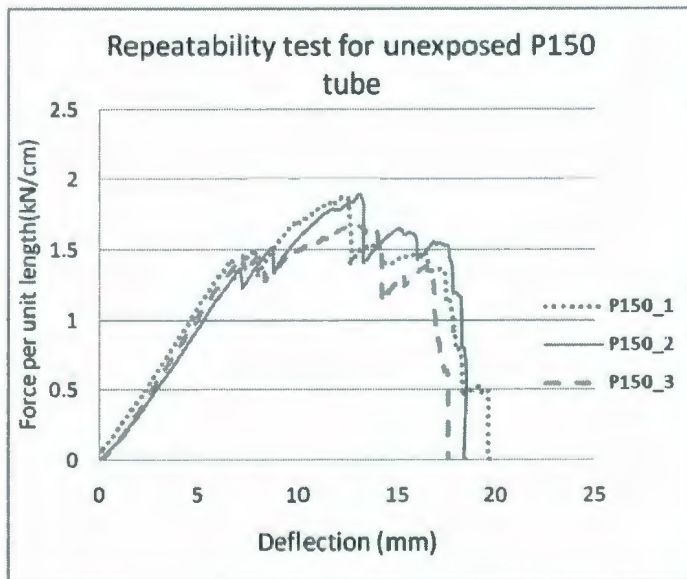
### 5.5.1 Repeatability of Test

For determining the repeatability of the tensile test method more than one test must be performed for each condition. In this case three unexposed H150 and three P150 pipe sections were tested. Figure 5-25 shows the load per unit length versus displacement curve for H150 and P150 pipe sections. From Figure 5-25 and Table 5-6 it is evident that the initial straight line portion of the curve is repeatable. For unexposed H150 specimens the slope varies from 0.0200 to .0225  $\frac{kN}{mm}$  the initial failure occurs at average 1.55 kN/cm which varies from 1.49 to 1.62 kN/cm. For unexposed P150 test specimen average slope is 0.0212  $\frac{kN}{mm}$  which varies from 0.0207 to 0.0215  $\frac{kN}{mm}$  and initial failure

takes place when the average force is 1.494 kN/cm which varies from 1.47 to 1.52 kN/cm.



(a)



(b)

Figure 5-25 Repeatability of laterally loaded tube section for (a) unexposed H150 (bisphenol A epoxy vinyl ester) and (b) unexposed P150 (bisphenol A epoxy novolac vinyl ester) pipe sections

The slope and the maximum force (and the corresponding displacement) required for the first failure are repeatable for this test. The toughness (proportional to the area under a stress versus strain curve and somewhat similar to area under the plots of force per unit length versus deflection) and the ultimate flexural stress (somewhat similar to the maximum force per unit length) are not repeatable. So for comparison of effects of exposure among different resins the slope and maximum force per unit length are used.

Table 5-6 Tube section tensile test results of unexposed H150 and P150 pipe sections for testing repeatability

Material	Force per unit length for initial failure (kN/cm)	Displacement (mm)	Slope of straight portion of curve $(\frac{kN/mm}{mm})$	Max <sup>m</sup> Force per unit length (kN/cm)	Displacement at max <sup>m</sup> force (mm)	Area Under the curve $(\frac{kN}{mm} \times mm)$
H150_1	1.62	8.35	0.020	1.84	15.39	1.76
H150_2	1.54	6.93	0.023	1.75	10.42	2.49
H150_3	1.49	7.00	0.022	1.78	10.83	3.50
P150_1	1.50	7.83	0.021	1.87	12.32	2.30
P150_2	1.52	8.66	0.021	1.89	13.16	2.23
P150_3	1.47	7.20	0.022	1.68	12.82	1.98

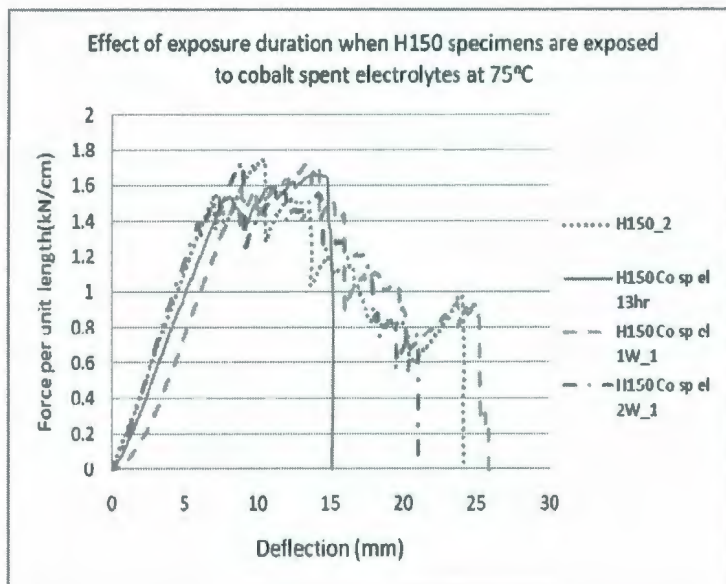
This data is affected critically by displacement measurements. These could be affected by (i) the steel rod's embedding in a softened surface-giving a reduced initial slope (force versus displacement), (ii) a gap between the rods and specimen surface which differs from test to test and (iii) a preload which differs from test to test. To reduce

these effects each of the test was started keeping a very small gap between the steel rod and the specimen. First few data which showed zero force for displacement was not considered. This was also considered by using the initial straight portion of the curve. These effects appears to all of the slope data.

It should be noted that some of the tests (which were not exposed for 1 week or 4 weeks) are not repeated. It is possible that these could be "rogue" results, i.e. a deviation from what would be obtained for most tests at a given condition, due perhaps to experimental error, some unnoticed difference during exposure, a defective specimen (e.g. a crack).

#### **5.5.1 Effect of Exposure Duration**

Figure 5-26 and Figure 5-27 show force per unit length vs deflection for different exposure duration, solution and resins. It is evident from these two figures that the slope and the initial failure force per unit length are very close to one another. In order to determine the effect of exposure duration on the slope and the first failure force per unit length is plotted for different solutions and resins (Figure 5-28). It is evident from Figure 5-28 (a) that the slope reduces with time of exposure the difference between the slope of unexposed and 1 week exposure is more than that 1 week and 4 week of exposure. The reduction of stiffness has a high rate up to 1 week but after that rate of reduction of stiffness (slope) is very low. It is evident form Figure 5-28 (b) that the initial failure force reduces with the increase of exposure duration.



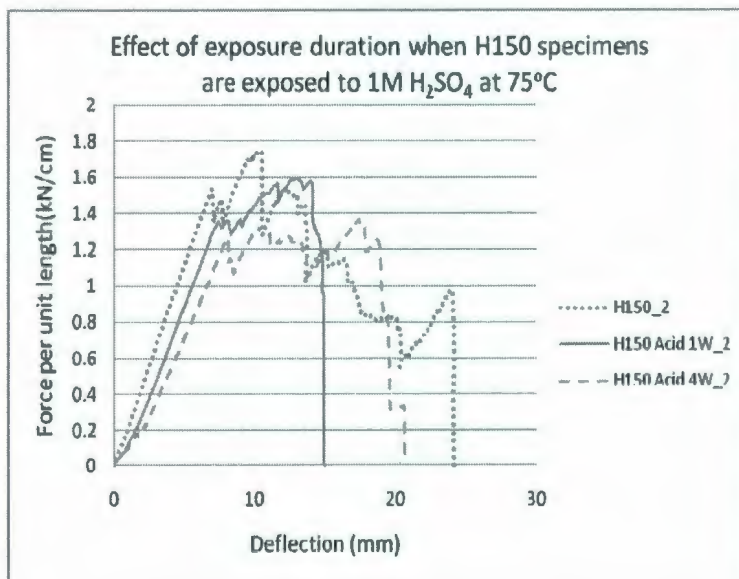
(a)

**Abbreviations:**

H150\_2: unexposed H150 pipe section sample no 2

H150 Co sp el 13hr: H150 pipe section exposed to cobalt spent electrolyte for 13 hrs

H150 Co sp el 2W\_1: H150 pipe section exposed to cobalt spent electrolyte for 2 weeks sample no 2



(b)

Figure 5-26 Force per unit length vs deflection curve for different exposure duration when H150 pipe sections are exposed to (a) cobalt spent electrolyte and (b) 1M H<sub>2</sub>SO<sub>4</sub> at 75°C.

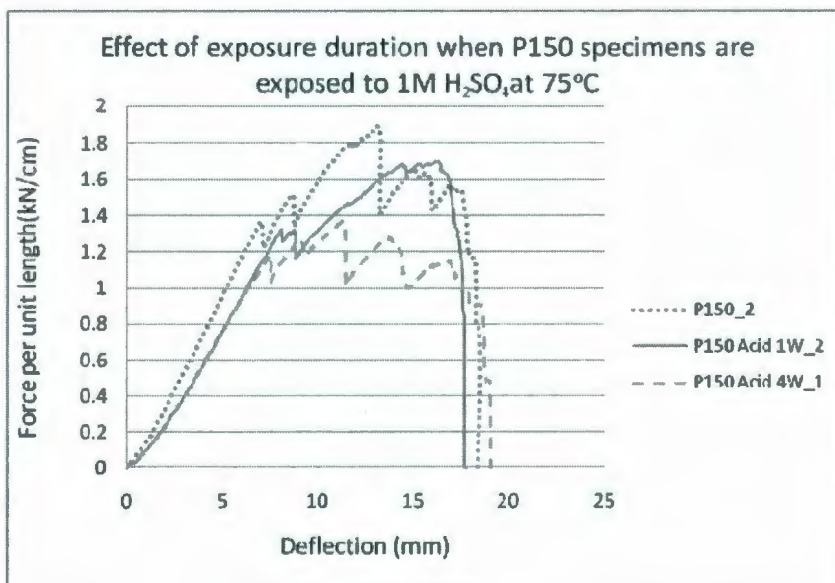
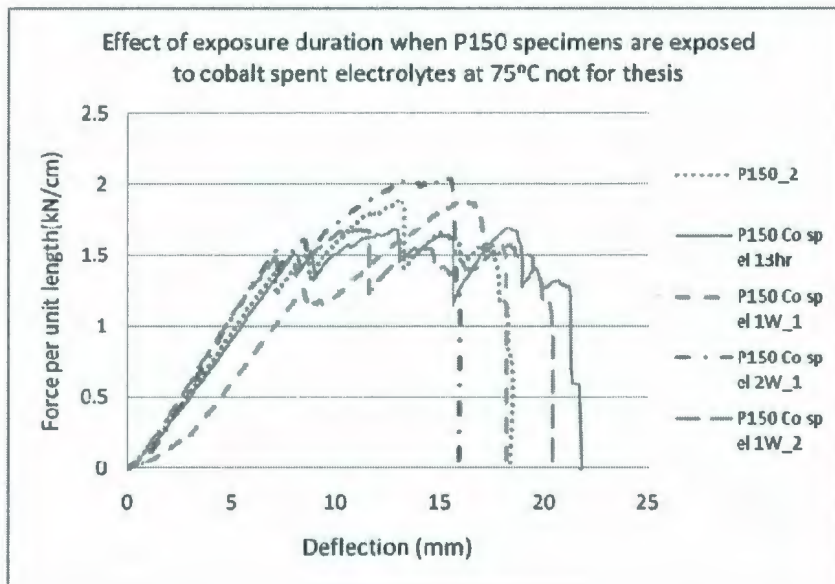


Figure 5-27 Force per unit length vs Deflection curve for different exposure duration when P150 pipe sections are exposed to (a) cobalt spent electrolyte and (b) 1M H<sub>2</sub>SO<sub>4</sub> at 75°C.

### 5.5.1 Effect of Resins and Solution

The same set of data is plotted in Figure 5-28 and Figure 5-29. In Figure 5-28 the effect of different fluids on FRP with the two resins is compared for different exposure times. In Figure 5-29 the effect of exposure duration is compared for different fluids. Evidently for both resins, after 1 week of exposure in both fluids the slope has decreased. Sulphuric acid must have little effect after that. Cobalt spent electrolyte may increase the slope beyond that exposure. Increasing the exposure time appears to decrease the first failure force, especially after one week, though the P150 the one test on FRP at 4 week showed an increase. It is evident from the Figure 5-29 (a) that both the slope and the first failure force decrease if the resins are exposed in acid compared to the unexposed resins. It appears that sulphuric acid consistently decreases the slope for both materials. The same is true after 1 week exposure to cobalt spent electrolyte, but the slope after four weeks exposure is the same as for the unexposed material.

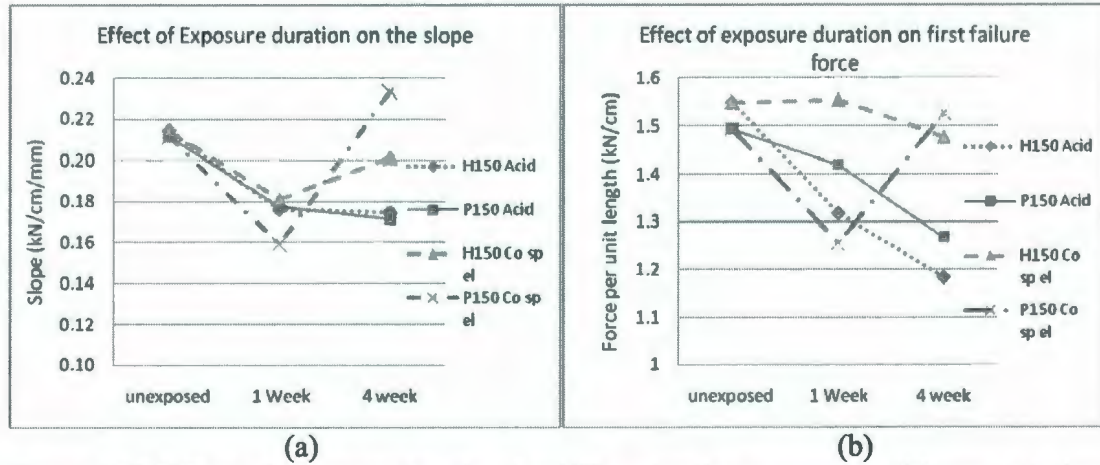


Figure 5-28 Effect of exposure duration for different resins exposed to different solutions at 75°C on (a) slope of force per unit length vs deflection curve and (b) force for the first failure

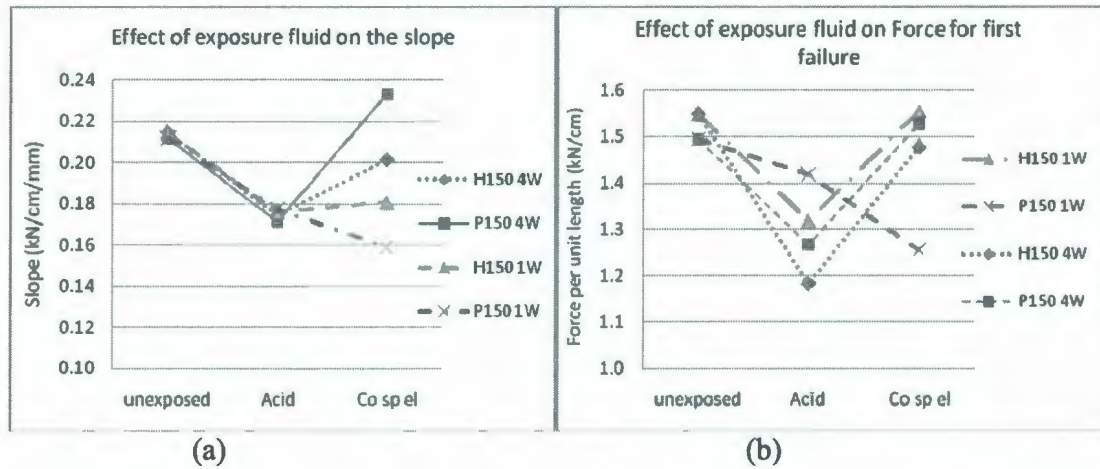


Figure 5-29 Effect of solutions on different resins for different durations of exposure at 75°C on (a) slope of force per unit length vs deflection curve and (b) force per unit length for the first failure

The average test results for laterally loaded pipe sections are tabulated in Table 5-7. The test results for each of the test specimens is recorded in table A

Table 5-7 Result for tensile test on laterally loaded pipe sections

Material	Average Force per unit length for first failure (kN/cm)	Deflection at the first failure (mm)	*Slope of straight line portion of curve ( $\frac{kN/mm}{mm}$ )	Average Deflection at Max <sup>m</sup> . Force (mm)	Average Maxi <sup>m</sup> . Force (kN/cm)	Average Area Under the curve ( $\frac{kN}{mm} \times mm$ )
H150	1.55	7.43	0.022	12.21	1.79	2.5.82
P150	1.49	7.90	0.021	12.77	1.81	2.1.70
H150	1.32	8.10	0.018	13.74	1.60	1.8.45

Acid 1W						
P150 Acid 1W	1.42	8.42	0.018	14.42	1.70	2.0.64
H150 Acid 4W	1.18	7.10	0.018	14.03	1.51	1.7.13
P150 Acid 4W	1.27	7.81	0.017	13.77	1.55	1.8.33
H150 Co sp el 1W	1.56	8.87	0.018	12.95	1.73	2.3.83
P150 Co sp el 1W	1.26	8.49	0.016	16.26	1.89	4.8.58
H150 Co sp el 4W	1.48	8.32	0.020	13.40	1.68	1.9.40
P150 Co sp el 4W	1.53	8.37	0.023	14.37	1.82	2.1.19

\*slope is measured from the slope of the ``best fit line`` determined by regression from the initial straight line portion of the stress strain curve.

## 5.6 Compression Test on Axially Loaded Pipe Section

It was expected that a compression test should be insensitive to any microscopic irregularities on the surface of the tube specimens. Preliminary compression tests were performed to see whether this test had sensitivity to the macroscopic exposure conditions. Preliminary compression tests showed sensitiveness to the exposure of the specimen

when the specimens are exposed only on the inside of the tube specimen. This was an indication that apart from affecting only the surface of the resin, the rate of diffusion of the corrosive solution into the specimen was large enough to show changes in compression test of axially loaded specimens. The stress is obtained from the following equation,

$$\sigma_c = \frac{P}{A} \quad \dots \quad \dots \quad \dots \quad \dots \quad \dots \quad (5-5)$$

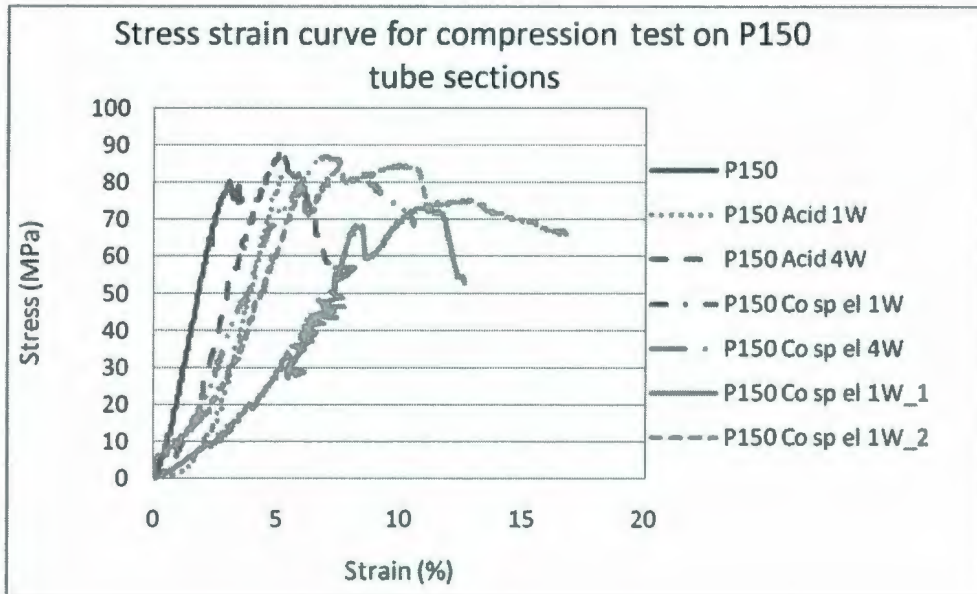
where  $\sigma_c$  is the compressive stress, P is the load and A is the cross sectional area of the pipe. Strain is obtained from the equation

$$\varepsilon = \frac{D}{L} \quad \dots \quad \dots \quad \dots \quad \dots \quad \dots \quad (5-6)$$

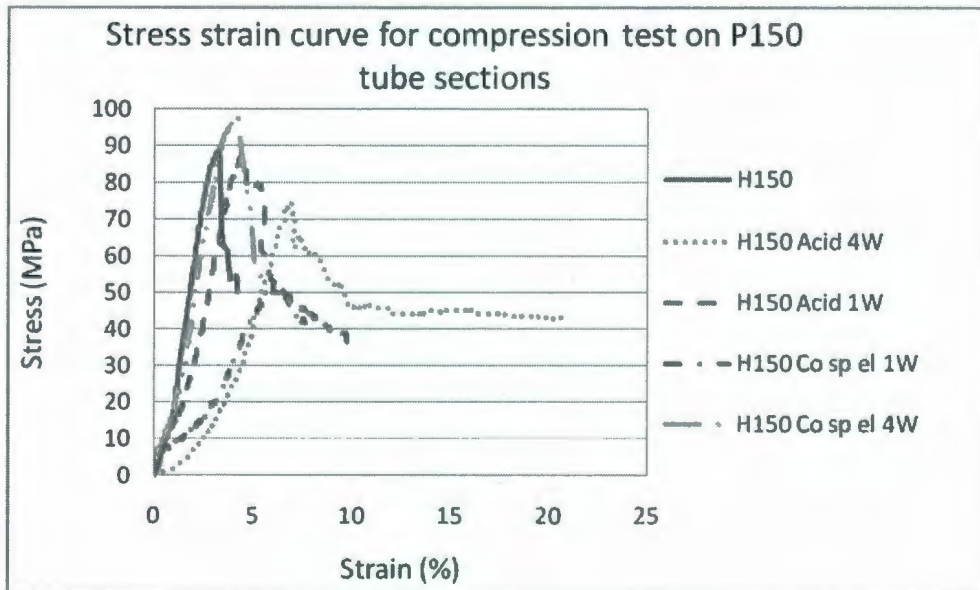
where D is the deflection and L is the length of the pipe section.

### 5.6.1 Repeatability of the Test

P150 FRP pipe exposed to cobalt spent electrolyte for 1 week (P150 Co sp el 1W\_1 and P150 Co sp el 1W\_2) was tested twice to determine the repeatability of the test. It is evident from Figure 5-30 that the modulus and ultimate failure values fall in a large range compared to results from other tests. It is evident from the figure that for P150 specimen the modulus are very close to one another but for H150 specimens it might be sensitive enough to differentiate between exposed and unexposed specimen. As this test method was thought of as insensitive none of the tests are repeated (except P150 Co sp el 1W). Which means ``rogue`` results may be present. Again the two repeated tests show quite different results. These factors seem to make it impossible to conclude much



(a)



(b)

Figure 5-30 Stress versus strain for compression for exposure to 1M H<sub>2</sub>SO<sub>4</sub> and cobalt spent electrolyte exposed for different times for (a) P150 (bisphenol A epoxy novolac

vinyl ester) and (b) H150 (bisphenol A epoxy vinyl ester) FRP pipe sections exposed at 75°C

### 5.6.2 Effect of Duration of Exposure

Figure 5-30 Stress versus strain for compression for exposure to 1M H<sub>2</sub>SO<sub>4</sub> and cobalt spent electrolyte exposed for different times for (a) P150 (bisphenol A epoxy novolac vinyl ester) and (b) H150 (bisphenol A epoxy vinyl ester) FRP pipe sections exposed at 75°C. It is evident from the figure that the modulus and the initial failure force varies. A comparison of modulus and initial failure force is shown in figure 5-31. It appears from the figure that the modulus of the stress strain curve decreases with time for all the specimens and exposure conditions. It is also evident that the magnitude of the initial force did not vary much, if at all with time and fluid with the possible exception of H150 and in that case only in Co spent electrolyte.

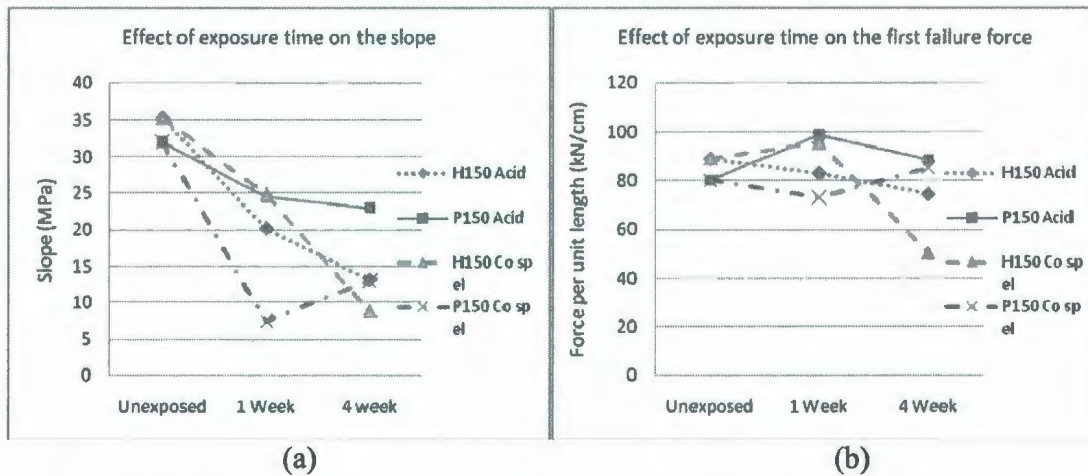


Figure 5-31 Effect of time on (a) slope of stress versus strain and (b) first failure force for different resins exposed to 1M H<sub>2</sub>SO<sub>4</sub> and cobalt spent electrolyte.

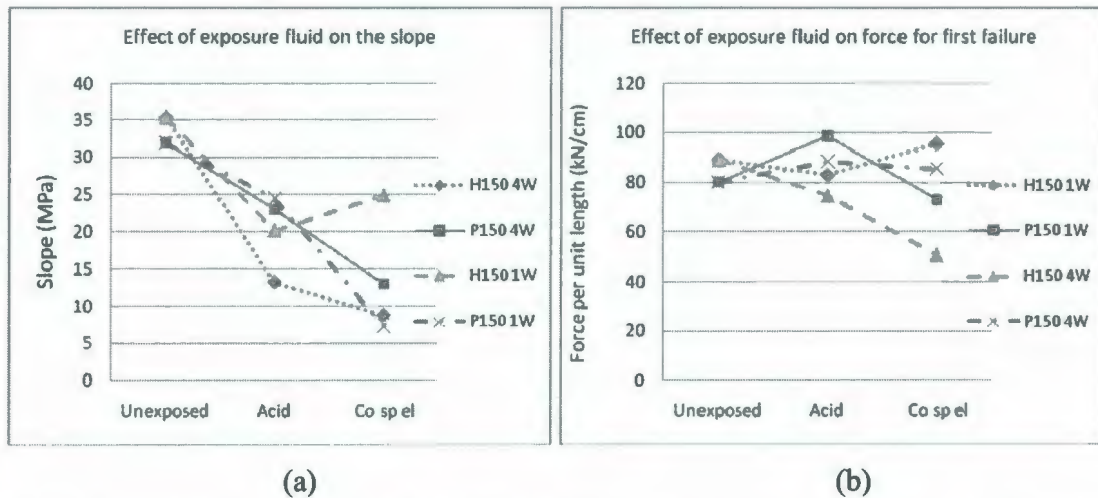


Figure 5-32 Effect of resins for different duration of exposure and resins on the modulus of stress versus strain curve for (a) modulus of stress versus strain curve and (b) force per unit length for the first failure

The compression test result are recorded in the Table 5-8.

Table 5-8 Compression test result for the on axially loaded pipe

Material	Average Maximum Stress (MPa)	Average Strain at Max <sup>m</sup> stress (%)	*Average Modulus of straight line (MPa)	Average area under the curve (MPa)	Average Length of the pipe sections (mm)
P150	80	3.09	32	125	39.98
P150 Acid 1W	99	6.82	24	294	39.00
P150 Acid 4W	89	5.26	23	217	39.47
P150 Co sp el 1W	77	5.90	13	1026	38.91
P150 Co sp el 4W	85	6.58	13	600	38.60
H150	89	3.27	35	146	38.10
H150 Acid 1W	83	4.12	20	204	40.42

H150 Acid 4W	75	6.92	13	182	38.10
H150 Co sp el 1W	96	3.84	25	302	39.53
H150 Co sp el 4W	51	5.75	9	226	37.77

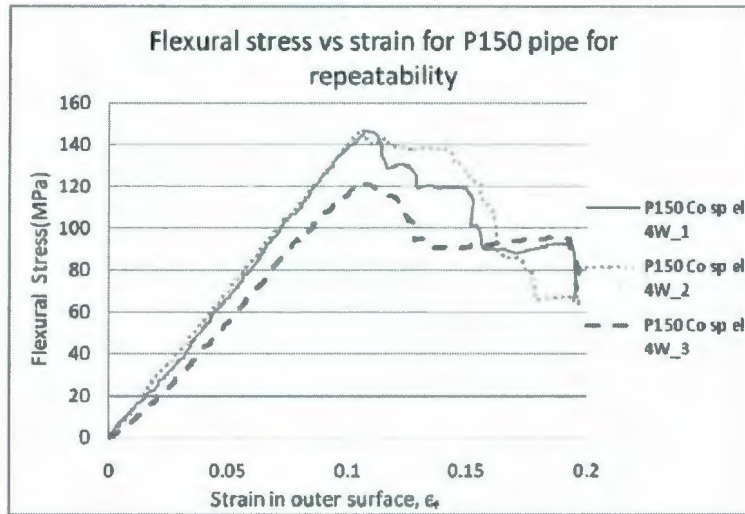
\*modulus is measured from the slope of the ``best fit line`` determined by regression from the initial straight line portion of the stress strain curve.

## 5.7 Three Point Bending Test on FRP Pipe Section

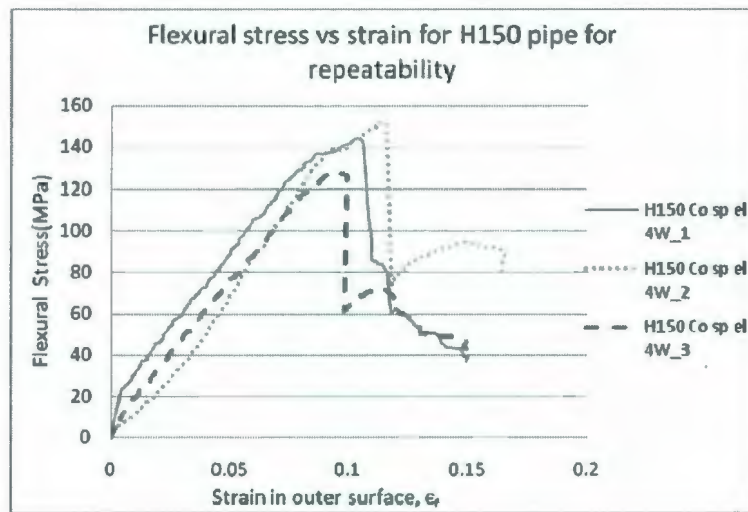
Similar to the ASTM bending test, pipe sections were tested to determine flexural stress versus strain relationship and check whether this test distinguishes between qualities of FRPs for exposed and unexposed FRPs. Though the ASTM D790 bending test deals with the flat FRP and plastic bars similar procedure and calculations were used to compare among the test results.

### 5.7.1 Repeatability of the Test

In order to assess the repeatability of the test for exposed P150 and H150 specimens three measurements were taken. It is evident from the following stress versus Figure 5-33 that for P150 the modulus varies between 1146 to 1389 MPa with an average value of 1300 MPa. Flexural stress at 5% strain varies between 54.6 to 70.9 MPa and maximum flexural stress varies between 121 to 147 MPa. For H150 the modulus varies between 1341 to 1403 MPa with an average value of 1380 MPa. Flexural stress at 5% strain varies between 68 to 89 MPa and maximum flexural stress varies between 127 to 150 MPa. Due to the variation of the results at least two specimens were tested for each case (exposure, temperature, duration of exposure) and the average values are reported.



(a)



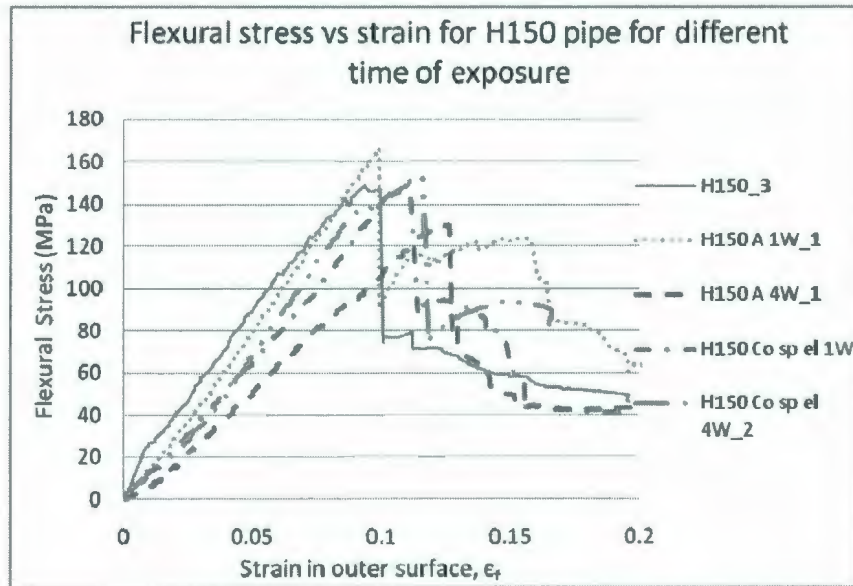
(b)

Figure 5-33 Repeatability test of the results for 3 point bending test for FRP pipe section made of (a) P150 material and (b) H150 material

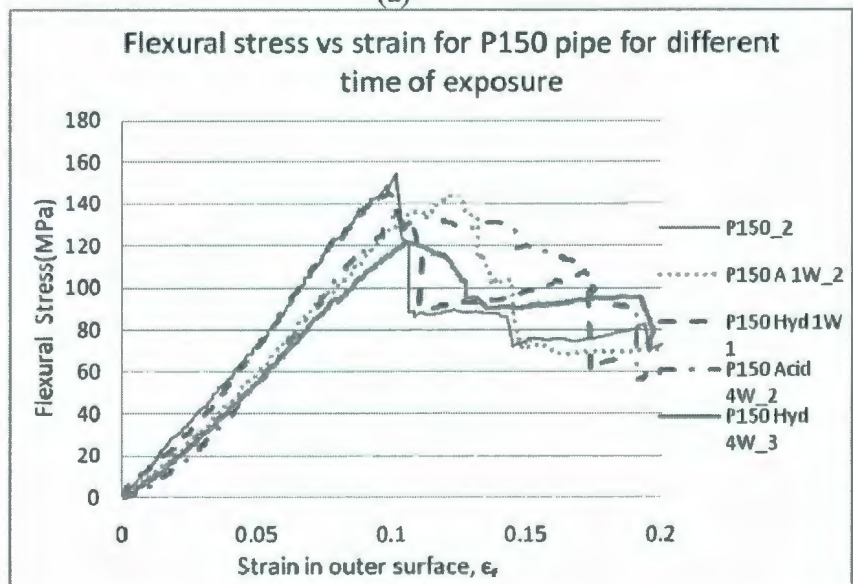
### 5.7.2 Effect Exposure Duration

As it has been mentioned before that the specimens were exposed for one week and four weeks and was compared to determine the effect of exposure. It is evident from

the Figure 5-34 that both the modulus and the maximum stress varies with time and resin and the change in these parameters are clear from the following figures.



(a)



(b)

Figure 5-34 Flexural stress versus strain curve for different duration and exposure condition for (a) H150 and (b) P150 pipe sections

Figure 5-35 shows the effect of the exposure duration on the modulus and the flexural stress at 5% strain. For P150, both modulus and stress at 5% strain decrease with

duration of exposure. For H150, there appear to be a little change, perhaps a tendency for both parameters to increase with duration of exposure.

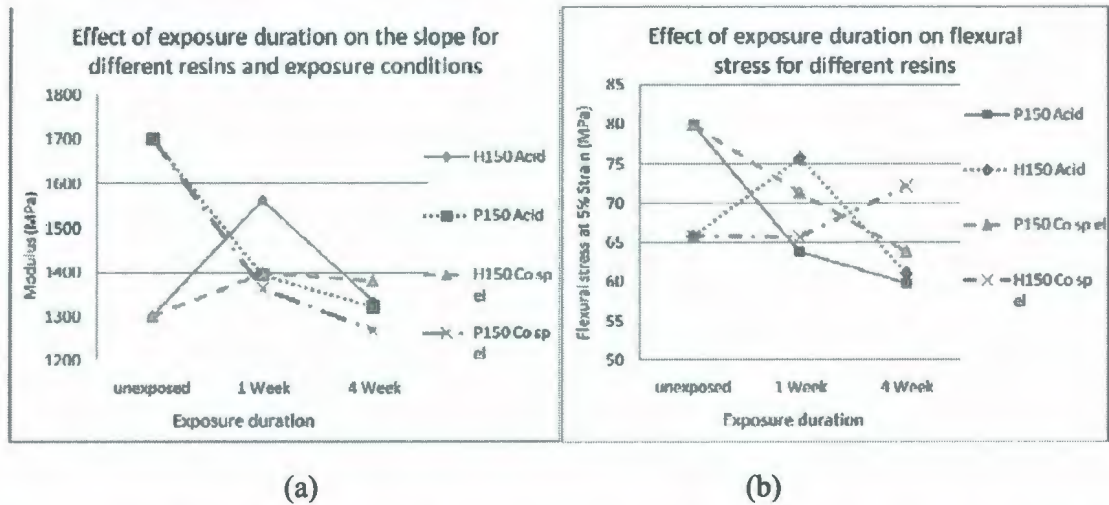
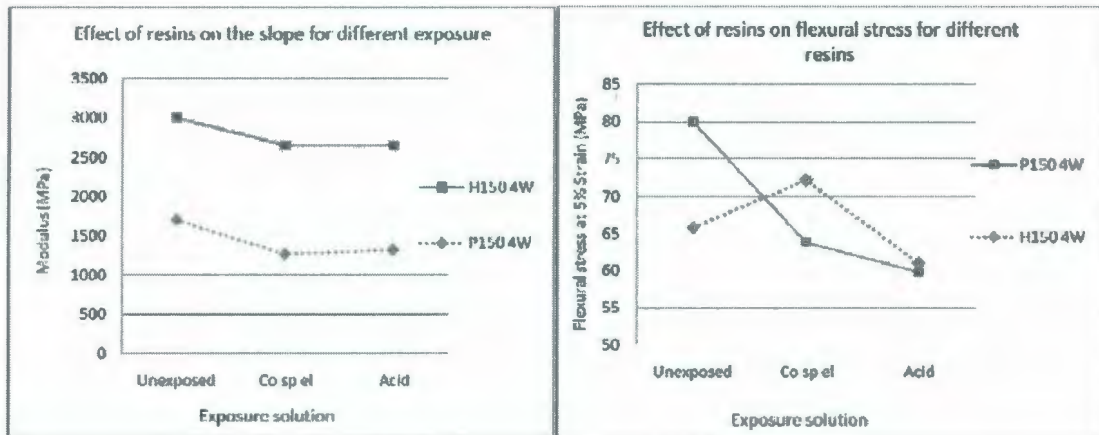


Figure 5-35 Effect of exposure duration on (a) modulus of stress strain curve and (b) flexural stress at 5% strain for specimens exposed at 75°C to cobalt spent electrolyte and 1M H<sub>2</sub>SO<sub>4</sub>

### 5.7.3 Effect of Resins and Solution

Figure 5-36 shows the effect of exposure solution for different resins for just 4 week exposed. It is evident from the figure that the exposure solution has an effect on the modulus and flexural stress. Exposure to sulphuric acid reduces the modulus and the flexural stress at 5% strain. H150 has a higher modulus and flexural stress when compared to that for P150 specimens.



(a)

(b)

Figure 5-36 Effect of resins on (a) modulus of stress strain curve and (b) flexural stress at 5% strain for different resins exposed at 75°C for four weeks

Both solutions reduced modulus by same amount and both materials are affected by the same amount. For P150 the flexural stress at 5% strain is reduced more by the acid than Co spent electrolyte. The effect of both the solution is less on the H150, possibly in opposite direction with Co spent electrolyte increasing the stress and the acid decreasing it.

#### 5.7.4 Effect of Temperature and Exposure

In order to observe the effect of temperature the specimens were exposed to both the solution at 25°C for 4 weeks and were compared to the results of unexposed specimens and exposed specimens at 75°C. Figure 5-37 shows the stress strain curve of the specimens exposed to different conditions for four weeks at 25°C. It is evident from the figure that the modulus of exposed samples are lower than the modulus of the unexposed specimens. The following Figure 5-38 shows the effect on the modulus and the flexural stress reduces with exposure temperature for P150 specimen but less so far

H150 specimens. It is also evident that when exposed to cobalt spent electrolyte the modulus of stress versus strain reduces. When the samples are exposed to acid the modulus increased for 25°C compared to unexposed and reduced for 75°C exposure.

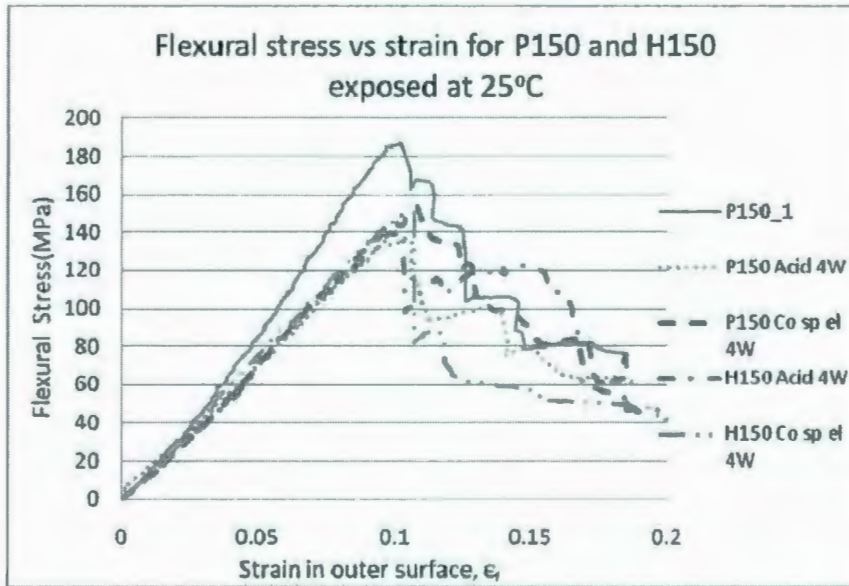
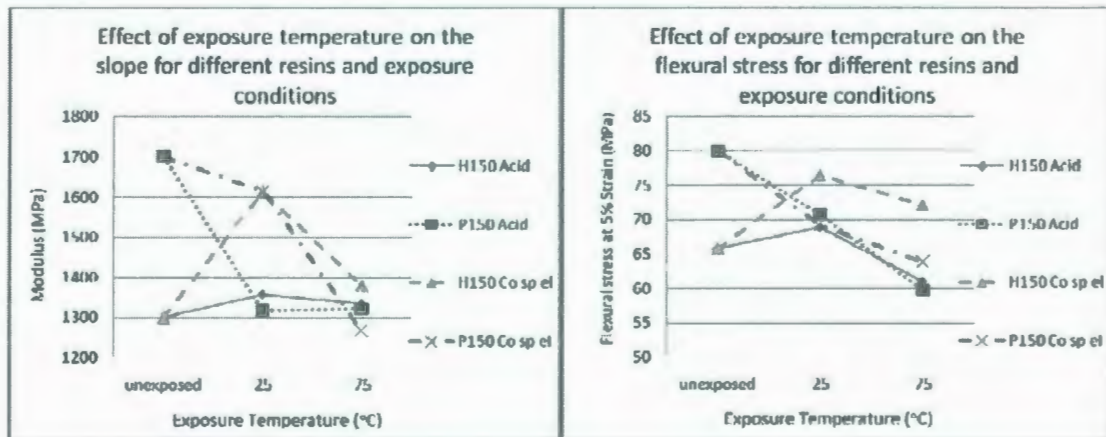


Figure 5-37 Flexural stress versus strain curve for different material exposed to cobalt spent electrolyte and 1 M H<sub>2</sub>SO<sub>4</sub> for four week at 25°C



(a)

(b)

Figure 5-38 Effect of exposure temperature on (a) flexural stress at 5% strain and (b) modulus of stress strain curve for specimens exposed to cobalt spent electrolyte and 1M H<sub>2</sub>SO<sub>4</sub>

Table 5-9 Three point bending test results for FRP pipe sections

Material	Average Width (mm)	Average flexural stress at 5% strain (MPa)	For the straight portion of stress strain curve		*Modulus (MPa)
			Maximum Stress (MPa)	Strain at maxm. Stress	
P150	38.31	80	170	0.100	1700
P150 Acid 1W	39.40	64	154	0.117	1394
P150 Acid 4W	38.97	60	154	0.132	1322
P150 Co sp el 1W	39.54	66	146	0.110	1363
P150 Co sp el 4W	39.41	64	138	0.110	1268
H150	38.10	39	137	0.139	1066
H150 Acid 1W	40.04	76	148	0.096	1563
H150 Acid 4W	39.38	61	130	0.107	1334
H150 Co sp el 1W	39.40	66	151	0.110	1398
H150 Co sp el 4W	39.60	72	140	0.100	1380

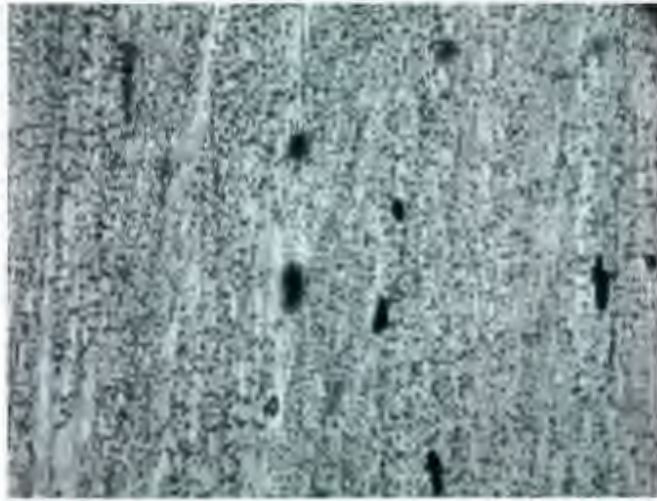
- Modulus is measured form the slope of the best fit line determined by regression of the initial straight line portion of the stress strain curve

## **5.8 Microstructure Assessment**

The microstructures of the specimens of FRP and also samples of resin in unexposed and exposed condition were examined by optical microscopy, scanning electron microscopy (SEM) and energy dispersive spectroscopy (EDS) in order to further understand their microstructure and composition. Although it is clear from the data for the commercially available FRP pipe that glass fibres are the reinforcement material and various resins are the matrix material provided by the manufacturer, some interesting observations were made.

### **5.8.1 Optical Microscopy**

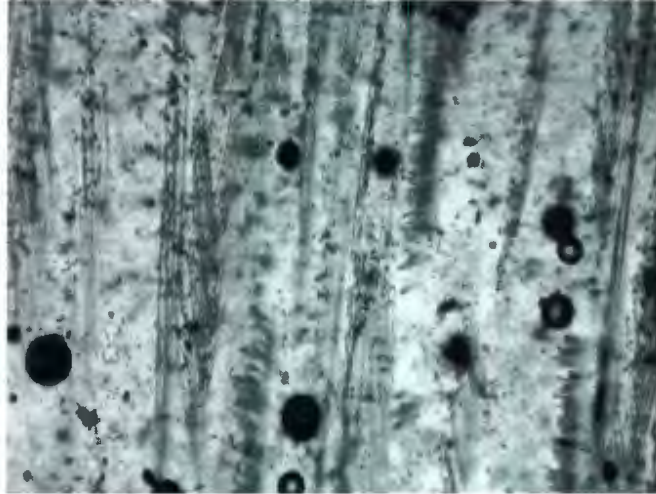
It is difficult to find any difference between exposed and unexposed condition because both the glass and the resin phases are transparent. Figure 5-39 shows the microstructure of different layers of an FRP pipe. The small black stripes are the glass phase and the white or brown portions are the matrix resins. It is evident from this figure that the inner section of the FRP pipe has much less glass fibres compared to outer layer of the pipe. This design feature ensures that the acidic hydrometallurgical solution will come in contact with a resin rich layer. It is anticipated that the solution will eventually come in contact with the glass fibre after diffusing through the resin rich layer. This observation not only gave us an insight into the manufacturing process of the FRP pipe but also it led us to investigate the effect of the hydrometallurgical solution on the resin phase more than on the glass phase.



(a)



(b)



(c)

Figure 5-39 Microstructure of commercially available FRP pipes by optical microscopy at 100X magnification of (a) outer layer, (b) interphase interface between inner and outer layer and (c) inner layer. All images are of area 10 mm by 15 mm wide in the original.

All the resins lost their original color and transparency after exposure. While bisphenol A epoxy vinyl ester showed good resistance to acidic exposure, polyester specimens did not. Figure 5-40 shows the effect of exposure on a polyester specimen to sulphuric acid. Cracks, visible to the naked eye, developed on the surface of polyester resins. Figure 5-41 shows the unexposed and exposed bisphenol A epoxy vinyl ester. No crack is visible even with the help of microscope. It is evident from these figures that the polyester is not suitable for use in acidic solution whereas in case of bisphenol A epoxy vinyl ester resin only the color and the transparency of the specimens are affected.

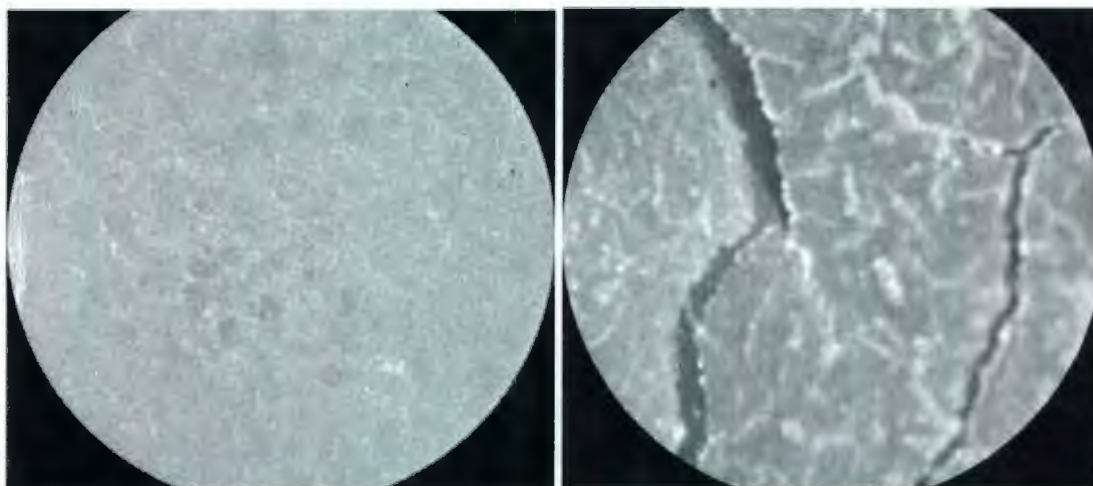


Figure 5-40 Polyester specimens: unexposed (left) and exposed to 1M H<sub>2</sub>SO<sub>4</sub> for four weeks at 75°C. (Magnification 32X)

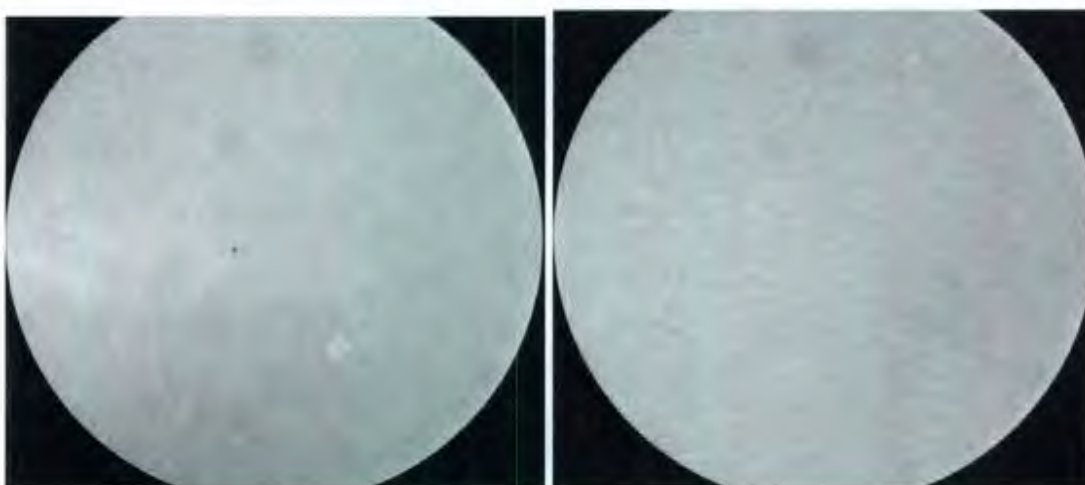


Figure 5-41 Bisphenol A epoxy vinyl ester resin: unexposed (left) and exposed to 1M H<sub>2</sub>SO<sub>4</sub> for four weeks at 75°C (Magnification 32X).

Figure 5-42 Unexposed (left) and exposed (right) surfaces of H150 pipe section. It is evident from the figure that the exposed pipe section has changed color. But with higher magnification (above 100x) no fracture surface damage is evident. Physical damage was visible only in the case when polyester resin was exposed to sulphuric acid for longer duration.



Figure 5-42 Unexposed (left) and exposed (right) surfaces of H150 pipe section.

### 5.8.2 Scanning Electron Microscopy

To further analyse the effect of exposure on the resins, images were taken with the help of a scanning electron microscope (SEM) and energy dispersive spectroscopy (EDS). SEM images of the fibre pull out on bending test specimens are seen in Figure 5-43. Alternating bands of the glass phase appears much like their original matte format when formed in resin. The individual glass fibres has fractured in a brittle manner since no discernable bending (ductility) is present in the pictures. Also, the interface between the glass and epoxy resin phases is relatively free of macroscopic surface discontinuities such as pores, voids, and scratches. However some small particles of debris (glass, resin) from fracture surface remains in the surface.



Figure 5-43 Fibre pull out of a bending test specimen after the test.

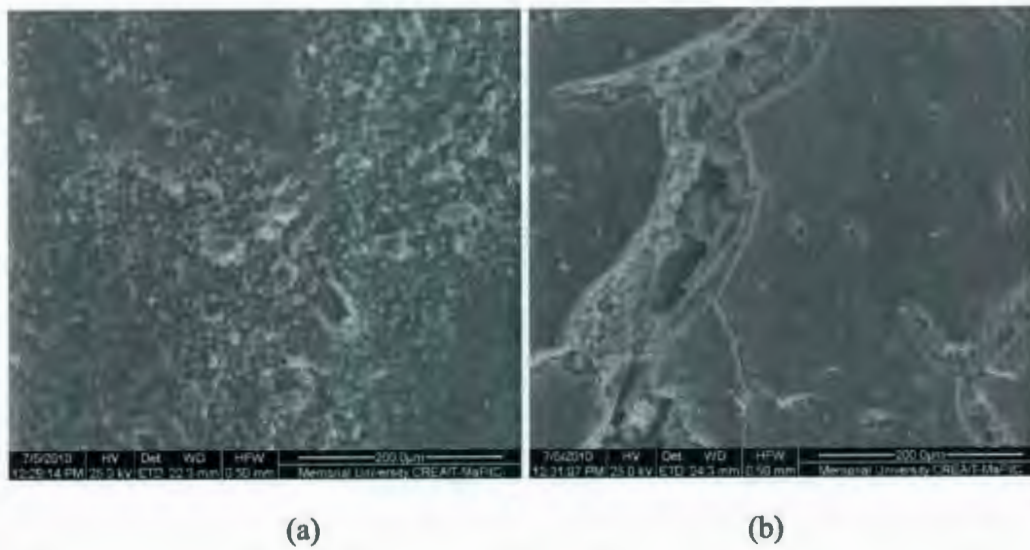


Figure 5-44 (a) Polyester Unexposed surface and (b) Polyester exposed surface (exposed to 1M H<sub>2</sub>SO<sub>4</sub> for four weeks)

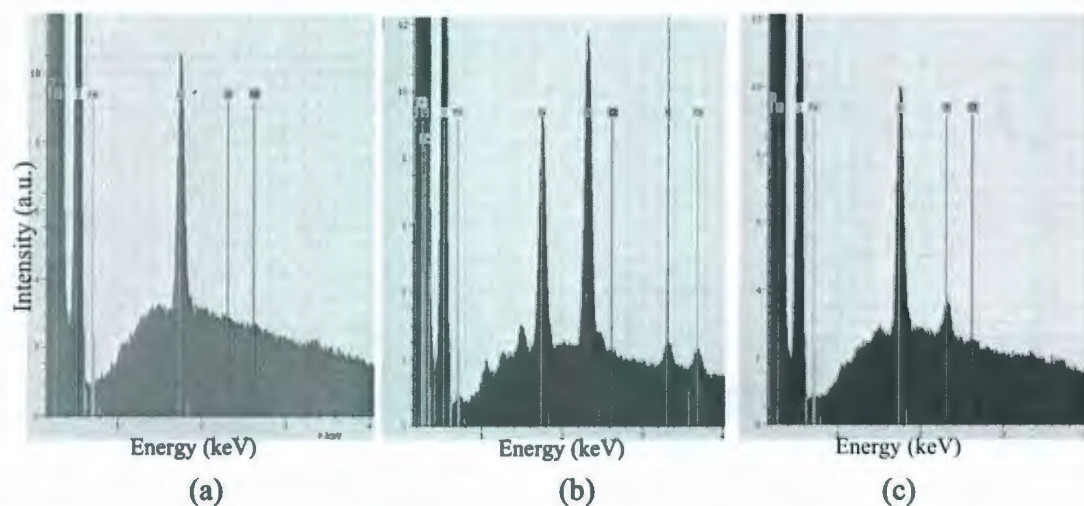


Figure 5-45 Energy dispersive spectra of a cross-section of (a) unexposed polyester (a) exposed polyester on crack (b) exposed polyester not on a crack 0.1 mm away from surface

The above two figures show the SEM image and EDS of unexposed and exposed polyester resin (exposed to 1M H<sub>2</sub>SO<sub>4</sub> for 4 weeks). It is evident from Figure 5-44 and Figure 5-45 that large crack has been formed in the surface and the dissipation of sulphur (at 2.3 keV) through the polyester resin is present while the sulphur content on a crack is much higher because it has come directly in contact with sulphuric acid.

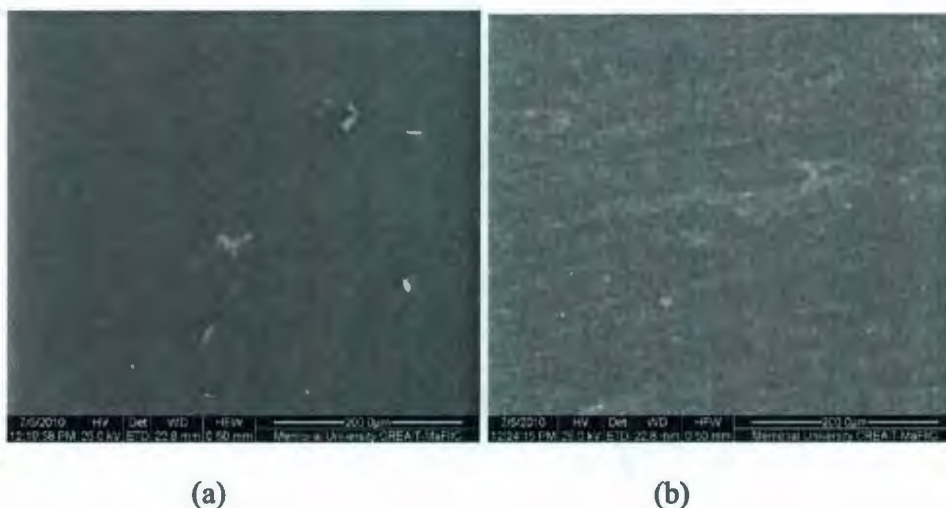


Figure 5-46 SEM image of bisphenol A epoxy vinyl ester for (a) unexposed and (b) exposed surface to 1M H<sub>2</sub>SO<sub>4</sub> for 4 weeks

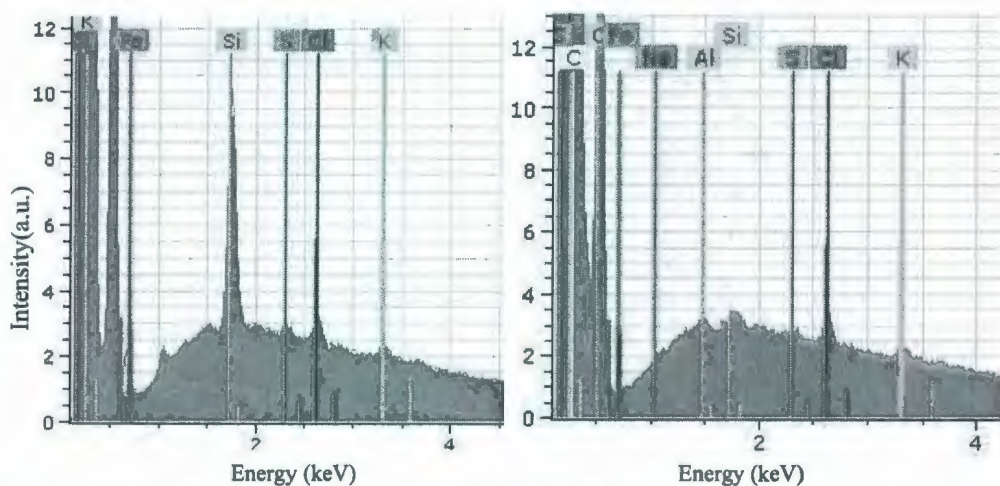
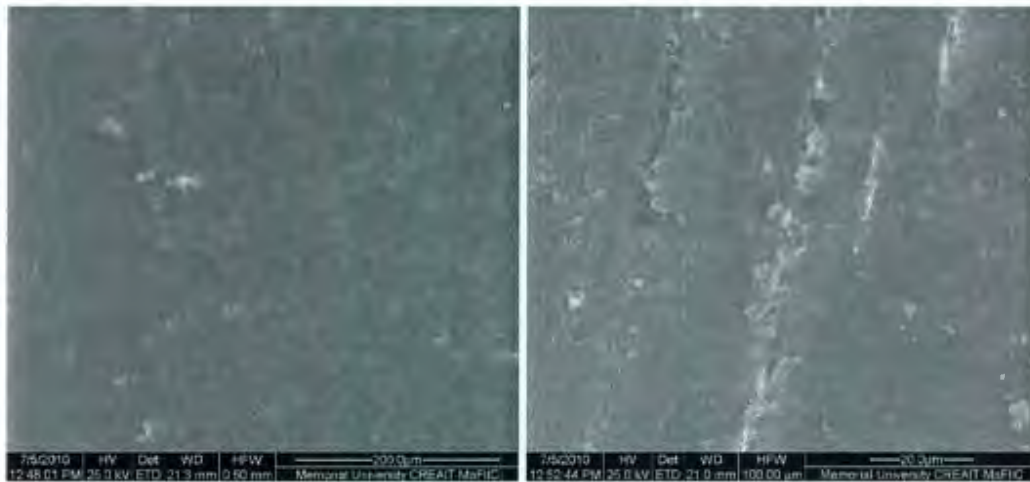


Figure 5-47 Energy dispersive spectra of unexposed (left) and exposed (right) bisphenol A epoxy vinyl ester at 0.1 mm inside of outer surface.

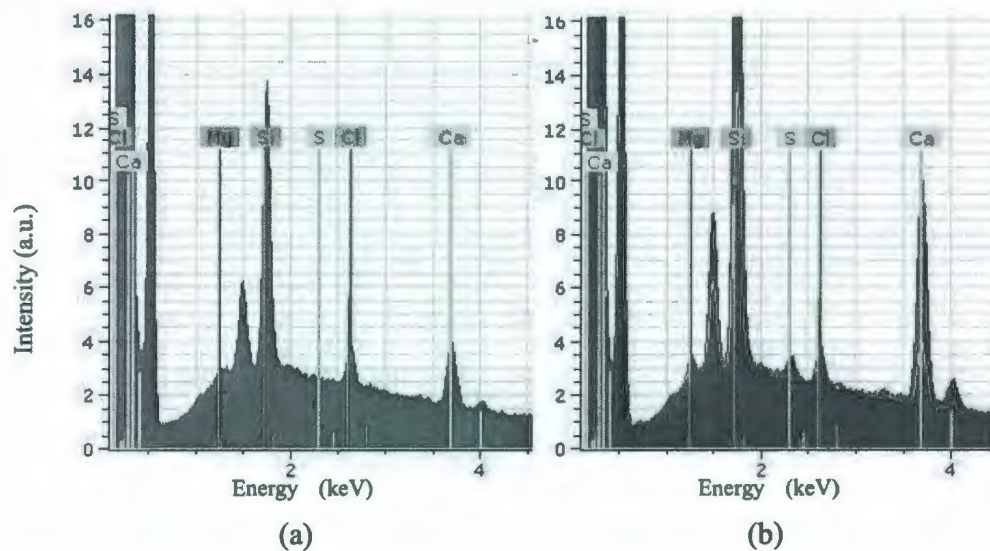
Figure 5-46 and Figure 5-47 show the SEM image and EDS of unexposed and exposed bisphenol A epoxy vinyl ester resin (exposed to 1M H<sub>2</sub>SO<sub>4</sub> for 4 weeks). It is evident from the figure that very smooth unexposed surface becomes rough after exposure for four weeks which is also an indication of small crack development. The unexposed EDS spectra has a high amount of Si compared to the exposed ones. But the dissipation of sulphuric acid (sulphur) through this resin is not evident.



(a)

(b)

Figure 5-48 SEM image of H150 pipe inner surface for (a) unexposed and (b) exposed surface to 1M H<sub>2</sub>SO<sub>4</sub> for 4 weeks



(a)

(b)

Figure 5-49 Energy dispersive spectra of (a) unexposed and (b) exposed H150 pipe section (bisphenol A epoxy vinyl ester) at 0.1 mm away from surface.

Figure 5-48 and Figure 5-49 show the SEM image and EDS of unexposed and exposed (exposed to 1M H<sub>2</sub>SO<sub>4</sub> for 4 weeks) H150 inner surface. It is evident from the figure that very small cracks developed parallel to each other. It is also evident that the

sulphur content of the exposed specimen is little higher than that of unexposed ones. To observe sulphuric acid dissipation X ray maps were generated (next figure) for exposed H150 pipe. It is evident from the figure that sulphur (lighter grey) has dissipated about 0.3 mm through the cross-section of the H150 pipe.

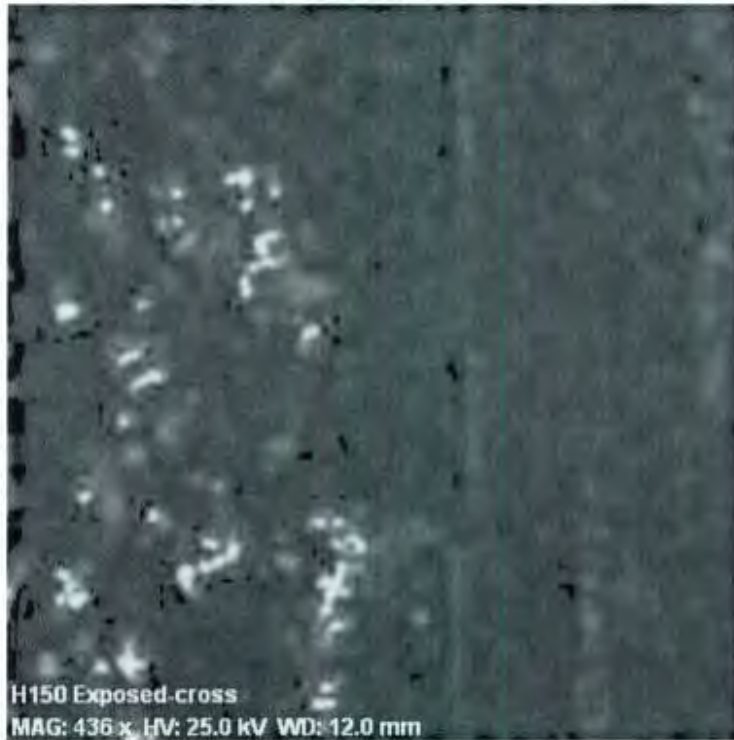


Figure 5-50 X-Ray MAP of H150 inner pipe section exposed for 4 week to 1 M H<sub>2</sub>SO<sub>4</sub>. The left side of the figure is the inner surface (total width 0.62 mm)

## **Chapter 6**

### **CONCLUSIONS**

Conclusion were found from the following three areas (i) tests on resins, (ii) test on FRP tube sections and (iii) examination of micro structure.

#### **6.1 Test on Resins**

From the two materials (resins) studied, the polyester resin was affected more by exposure than the bisphenol A epoxy vinyl ester. The ASTM D638 test (tensile test) on resins can only determine the difference of exposure if the effect of the solution on the resin is high. For example it can predict the difference of tensile property when polyester is exposed to 1M sulphuric acid for four weeks.

ASTM D790 test (bending test) was the test most sensitive to the change of exposure conditions. It is evident that the bisphenol A epoxy vinyl ester has less effect of exposure than polyester. Polyester resin has lower slope when exposed to higher temperature or higher exposure duration, and also shows sensitivity to solutions when exposed for longer time (four weeks). When used only as resin bisphenol A epoxy vinyl ester has a little effect due to time, temperature and solutions. But when used as a matrix in glass fibre reinforced plastic it shows the similar effect as polyester. This happens due to the fact that the standard specimen was cut from a large FRP plate where along all the cut off surface glass fibre was exposed to the solution.

ASTM D648: heat deflection temperature did not show any sensitivity to exposure.

Microhardness test on the resins was sensitive to exposure duration and exposure temperature. With increasing exposure duration the average hardness increased up to 2 weeks and when it was exposed for four weeks the hardness decreased. With the increase of temperature average micro hardness increases with an exception of polyester when exposed to cobalt spent electrolyte. Micro hardness testing of plastic material shows a relationship between the hardness and depth of indentation which is also an indication how deep the exposure has affected in terms of hardness.

Among the tests done on only resins the bending test shows more sensitivity to the exposure. For example the average modulus of unexposed polyester is approximately 2250 MPa and the modulus reduced to 900 MPa when it was exposed to 1M H<sub>2</sub>SO<sub>4</sub> for four weeks, whereas for the same exposure and material the tensile test modulus reduced from approximately 5080 MPa to 4380 MPa. The bending test is better in terms of repeatability and sensitivity compared to the tensile test, but the bending test results have a very high range of flexural strength values. For example bisphenol A epoxy vinyl ester exposed for 1 week fractures at 25, 42 and 52 MPa for different specimens. This is due to the fact that the failure loads differ have occurred due to the difference in defects on the initial specimens. Micro hardness test have clearly indicated that the outer surface of the exposed specimen is more affected than inner portions and the test is very sensitive to the exposure. The hardness at the outer surface of unpolished polyester and bisphenol A epoxy vinyl ester specimens increased when exposed to 1 M H<sub>2</sub>SO<sub>4</sub> for 2 weeks but after four weeks of exposure the hardness of the outer surface reduced.

## 6.2 Tests on FRP Tube Sections

Tests on laterally loaded tube sections show that both P150 and H150 pipe sections are affected more by the acid, compared to cobalt spent electrolyte. For both materials the modulus (measured from the slope of the initial straight line portion) reduces from approximately 21 MPa (unexposed) to 17 MPa (exposed to 1M H<sub>2</sub>SO<sub>4</sub> for four weeks). The force for first failure also follows same pattern for this test. Compression test also shows reduction in modulus (determined from the slope of initial straight line). But the lack of repeatability of this test prohibits the opportunity of any valid comment. Bending test on tube sections shows a consistent difference in result for two materials. Modulus of P150 pipe sections reduced from 1700 MPa (unexposed) to 1300 MPa (exposed to acid and cobalt spent electrolyte for 4 weeks) where as modulus of H150 pipe sections increased from 1300 MPa (unexposed) to 1350 MPa (exposed to acid and cobalt spent electrolyte for 4 weeks). The flexural stress at 5% strain for bending test also provided similar results.

## 6.3 Study of Microstructure

The optical microscopy provided us some vital information which changed the approach of this study and introduced test only on resins. But SEM images and EDS are much more useful for the detection of penetration of acid and cobalt spent electrolyte. EDS could detect diffusion of sulphur into the polyester (exposed to 1M H<sub>2</sub>SO<sub>4</sub> for four weeks) and showed higher amounts of sulphur in the cracks developed during exposure. The X-Ray map was able to detect the penetration of sulphur into an H150 specimen exposed to 1 M H<sub>2</sub>SO<sub>4</sub> for four weeks.

## **Chapter 7**

### **RECOMMENDATION FOR FUTURE WORK**

The measurement the chemical composition (i.e. FTIR and XRD etc) of the material before and after exposure is warranted from a research point of view to establish any basic changes in structure and chemical composition.

The effect of defects on surface, especially on bending test specimens, is huge. Very small defect on a surface of the specimen leads to a premature failure during the test. For this study the top surface was smoothed to remove meniscus after casting. This, in turn, left polishing mark/indentations. A process must be developed to avoid meniscus (might be round cornered mould).

Exposing small tube sections to acidic solutions involved high rate of evaporation. Instead of cutting off and exposing; tubes should be filled, sealed and then exposed after that it could be cut to suitable size.

More EDS and X-ray scan tests to have to be performed to determine penetration into the specimens. EDS should be done at different depth of specimen to compare the amount of sulphur dissipated at different depth.

Further test on resins should also include bending and microhardness test. Bending test specimens with a uniform thickness and with no surface flaw is necessary to compare results among specimens with different exposure conditions. In the case of micro hardness tests hardness was measured changing the load on indenter. Depth of indentation was different for different exposures conditions even the load of indenter was

the same. It was difficult to present or interpret the effect on hardness with the change of depth of penetration of the indenter. Micro hardness should be measured changing the load in such a way that the same depth of penetration may be achieved for each of the exposure condition.

Among the tests carried out on FRP tubes bending test and tensile test laterally loaded tube section test should be done for further investigation. Apart from increasing the exposure duration care should be taken to make the length of the tube exactly the same for each specimen.

## REFERENCES

- Bansal, R. K., Mittal, J., & Singh, P., (1989). Thermal-stability and degradation studies of polyester resins. *Journal of Applied Polymer Science* 37,1901-1913.
- Bunsell, A. R., & Renard, J., (2005). *Fundamentals of fibre reinforced composite material*. Bristol: Institute of Physics publishing.
- Barkatt, A. (2001). *Environmental effects on engineered materials*. New York: Mercel Dekker.
- Caddock, B. D., Evans, K. E. & Hull, D., (1987). The diffusion of hydrochloric acid in polyester thermosetting resins. *Journal of Material Science*, 22, 3368-3372.
- Caddock, B. D., Evans, K. E. & Hull, D., (1989). Diffusion of aqueous hydrochloric acid into polyester resin, part 2, Effect of applied stress on diffusion behaviour. *Journal of Material Science*, 24, 1005-1010.
- Callister, D. Jr., (2005). *Material science and engineering: an integrated approach*, 2<sup>nd</sup> Edition. Hoboken, N. J.: John Wiley & Sons.
- Composite Material*. (2010). Retrieved March 23, 2010, from Wikipedia website [http://en.wikipedia.org/wiki/Composite\\_material](http://en.wikipedia.org/wiki/Composite_material).
- Cook, J. & Gordon, J. E., (1964). A mechanism for control of crack propagation in all brittle systems. *Proceedings of the Royal Society*, A282, 308-314.

- Curry, B., (2005). New high temperature resistant vinyl ester. Retrieved on 13<sup>th</sup> March 2010, from the official website of AOC, <http://www.aoc-resins.com>
- Feih, S., Mouritz, A. P., Mathys, Z., & Gibson, A. G. Tensile Strength Modeling of Glass Fiber-Polymer Composites in Fire, *Journal of Composite Materials* 41, 2387-2396.
- Hammami, A., & Al-Ghuilani, N. (2004). Durability and environmental degradation of glass-vinyl ester composite. *Polymer Composites* , 609-616.
- Harris, C. E., & Morris, D. H., (1985). A damage tolerant design parameter for graphite or epoxy laminated composite, *Journal of Composites Technology Research* 7, 77-89.
- Hofirek, Z. & Halton, P. (1990), *Production of High Quality Electrowon Nickel at Rustenburg Base Metal Refiners (PTY.) LTD.*, Electrometallurgical Plant Practice, Claessens P.L. and Harris G.B. ., Proceedings 20th Annual Hydrometallurgy Meeting, CIM, Montreal, Quebec, 85-93.
- Hogg, P. J., & Hull, D., (1983). *Developments in GRP Technology - 1*, edited by B. Harris (Applied Science, London).
- Hydrometallurgy-Vale-Inco New Caledonia*, (2010). Retrieved on 3<sup>rd</sup> April 2010 from Vale Inco (New Caledonia Plant) website: <http://www.valeinco.nc/pages-eng/geologie/hydrometallurgie.htm#etapes>
- Ingits, C., (1913). Stress in a plate due to the presence of cracks and sharp corners. *Transactions Institute Naval Architecture, Vol. 55, 2019-2025.*

*Instruction for Micromet hardness tester (manual).*

Jones, F. R., Mulheron, M., & Bailey, J. E., (1983). Generation of thermal strains in GRP. *Journal of Material Science. Vol. 18, 1012-1019.*

Kulshershta, A. K., & Vasile, C. (Eds.). (2002). *Handbook of polymer blends and composites*, UK: Rapra Technology Limited. Retrieved from: <http://books.google.ca/>

Mahmoud, M. K., Tantawi, S. H., (2003). Effect of strong acids on mechanical properties of glass/polyester GRP pipe at normal and high temperatures. *Polymer - Plastics Technology and Engineering*, Vol. 42, No. 4, 677-688.

Mallik, P. K. (1988). *Fiber-reinforced composites: material manufacturing and design*, New York: Marcel Dekker, p. 96.

Mallison, J. H. (1982). Abrasion of fiber-reinforced plastics in corrosive environments. *Chemical Engineering, vol. 89, no. 11, .5413-5423*

Metacalfe, A. G., & Schmitz, G. K., (1972). Mechanism of stress corrosion in E glass filaments, *Glass Technology, Vol. 13, 589-598.*

Marsh Jr., H.N., (1992). *Standard for reinforced plastic corrosion-resistant equipment*. *Journal of Pressure Vessel Technology*, Vol. 114, No. 3, 369-375.

Marshal, J. P., (1982). The diffusion of water and hydrochloric acid into glass reinforced vinyl ester laminates. *S. A. M. P. E Quarterly, Vol. 13, no. 4, 87-95.*

Marshall, J. P., Marshall, G. P., & Pinzell, R. F. (1982). The diffusion of liquids into resins and composites. *Polymer composites, Vol. 3, 131-137.*

*Micro hardness (Manual)*. Retrieved 15<sup>th</sup> March 2010 from the manual of micro hardness tester manufactured by Reinchert Optische Werke, Austria.

Mills, N. J. (1993). Environmental effects in: Plastics, microstructure and engineering applications (2nd ed.), London, UK: Edward Arnold.

Ngoy, E. K., Campbell, I. M. D., Reid, G. R., & Paskaramoorthy (2009), Modelling and prediction of the chemical and physical degradation of fibre reinforced plastics. *Journal of Material Science, Vol. 44, 2393-2407.*

Mulhearn, T. O., (1959). *Journal of Mechanics and Physics of Solids*, vol. 7, pp 85-96.

Price, J. N. & Hull, D., (1983). Propagation of stress corrosion cracks in aligned glass fibre composite materials. *Journal of Material Science, Vol. 18, 514-521.*

Proctor, B. A., (1984). *Glass Current Issues*. Proceedings of NATO Advanced Study Institute, Puerto De La Cruz, Tenerife, Canary Islands, Spain.

*Product information Vipel F010 Series Bisphenol Vinyl Ester Resins, (Brochure)*, Retrieved 15<sup>th</sup> March 2010 from: <http://www.aoc-resins.com/images/uploads/F010.pdf>

- Ramamurthy, H. (1988). An Experimental Investigation into the Thermophysical Properties of Decomposing Polymer Composites. (M.S. thesis, University of Rhode Island).
- Rashed, M. (2010). Removal of impurities from electrolyte solution to produce pure metals. M.S. thesis, Memorial University of Newfoundland, Canada.
- Reinforced plastic system Inc (2010). FRP Equipment Designer and Manufacturer, (Brochure).*
- Regester, R. F. (1969). Behaviour of fibre reinforced plastic materials in chemical service, *Corrosion – NACE*, 25, 157-167.
- Samuels, L. E. (1986). Microindentation in Metals, Microindentation Techniques in Materials Science and Engineering, pp 5-25.
- Scrimshaw, G. (1980), *Large Diameter Glass Reinforced Pipes*, Paper presented at Pipecon Conference, London, UK. Abstract retrieved from <http://www.sciencedirect.com/>
- Severov, G. F., Posyosoeva, A. P., & Litvinenko, A. F. (1982). The use of plastics and glass-reinforced plastics in place of stainless steels and nonferrous metals in chemical plant. *Chemical and Petroleum Engineering*, Vol. 35, 137-140.
- Sjogren, B. A., Gamstedt, E.K. (1999). Micromechanisms in tension-compression fatigue of composite laminates containing transverse plies. *Composite Science Technology*, 59(2):167–178.

- Shafeeq, M. (2006). *Effect of environment on the fatigue and tensile properties of glass fibre reinforced vinyl ester and epoxy thermoset*, MS Thesis, King Fahd University of Petroleum and Mineral (KFUPM), Dhahran, Saudi Arabia.
- Snow, G. (2005). *Evaluation of the corrosion performance of 316 l stainless steel for hydrometallurgical processing of Voisey's Bay nickel concentrate*, MS Thesis, Memorial University of Newfoundland, St. John's, Canada.
- Sprague, P. A. Hira, P.E., Ahluwalia, S. (2000), Corrosion barrier deterioration and detection, NACE conference online proceeding and retrieved 16 March 2010 from, <http://web.nace.org/departments/store/product.aspx>
- Springer, G. S. (1988). *Environmental effect on composite material, Vol. 3*. Westport: Technomic Publishing Co.
- Sullivan, R. M. (1993). A coupled solution method for predicting the thermostructural response of decomposing, expanding polymeric composites. *Journal of Composite Material*, 27, 408-434.
- System Engineering Portfolio: Environmental sensors for military and consumer goods*. (2010). Retrieved March 22, from, <http://www.crgp.net/technology/systemsportfolio/environmental-sensors.shtml>.
- Vipel corrosion resistance resin guide* (Brochure). Retrieved on 2010 from: <http://www.aoc-resins.com/>

Weng, A., Hiltner, T., & Baer, E. (1989). Failure process in fibre reinforced liquid crystalline polyester composites. *Journal of Macromolecular Science, Part A, Chemistry A* 26, 273-307

Yakoyuma, H., & Takayanagi, T., (1993). Japan Patent No. JP05148379. Tokyo: Japan Patent office.

## APPENDIX 1: TEST RESULT

Table A1 1: Tensile test result (ASTM D638)

Material	Width (mm)	Thickness (mm)	Tensile stress at break (MPa)	Elongatio n at break	Modulu s (MPa)	Change of modulus compared to unexposed specimens %	Exposure Temperat ure (°C)
UP1	12.69	5.50	24	0.041	561	19.3	N/A
UP2	12.47	6.16	34	0.055	562	19.5	N/A
UP3	12.75	4.88	29	0.058	470	0.0	N/A
UP4	12.75	5.75	19	0.047	399	-15.1	N/A
EP1_48 hr	12.51	6.29	21	0.029	746	58.7	75
EPA1_1 week	12.60	5.00	18	0.059	237	-49.7	75
EPA2_1 week	12.70	5.00	27	0.109	300	-36.2	75
UB1	12.70	5.93	21	0.028	801	6.0	N/A
UB2	13.50	5.46	31	0.041	755	0.0	N/A
EBA1_48 hr	13.05	6.45	18	0.038	436	-42.3	75
EBA2_48 hr	12.80	6.90	13	0.021	605	-19.9	75
EBA1_1 week	12.70	5.00	27	0.034	810	7.26	75
EBA2_1 week	12.50	4.75	47	0.068	615	-18.6	75

EPA3_4W	12.55	5.0	5	0.013	419	-11.0	75
EBA3_4W	12.55	4.90	23	0.038	564	-25.3	75
EBA4_4W	13.11	5.00	22	0.033	655	-13.3	75
EPC1_1W	12.53	5.50	14	0.028	544	15.6	75
EPC2_1W	12.76	5.44	25	0.081	315	-33.0	75

Table A1 2: Results for bending test: ASTM D790

Material	Width (mm)	Thickness (mm)	Flexural Stress, $\sigma_f$ at 1% Strain (MPa)	Maximum Measured Stress (MPa)	Strain at Maximum Measured Stress	Modulus (MPa)
UP1	5.00	14.50	24	45	0.022	1850
UP2	5.00	14.20	21	21	0.010	2118
UP3	5.00	14.60	27	36	0.015	2649
UB1	5.00	15.00	*	18	0.008	2335
EBA1_1W	5.00	13.40	25	**26	0.010	2471
EBA2_1W	4.60	16.00	29	**51	0.019	2584
EBA3_1W	4.58	15.30	38	**41	0.011	3432
EBC1_1W	4.43	15.33	*	**17	0.006	2370
EBC2_1W	4.40	15.63	38	42	0.011	3530
EPA1_1W	4.65	15.64	17	39	0.027	1374
EPA2_1W	4.53	15.56	20	**22	0.011	1784
EPC1_1W	4.50	15.66	16	31	0.025	1087

EPC2_1W	4.62	15.62	11	28	0.029	873
EBC3 4W	4.33	15.72	*	**35	0.007	3834
EBC4 4W	4.87	15.35	*	27	0.007	2949
EPC3 4W	4.31	15.64	18	34	0.030	944
EPC4 4W	4.21	16.25	16	28	0.028	755
EBA3 4W	5.30	15.82	30	31	0.010	2003
EBA4 4W	4.73	15.61	*	**41	0.009	3117
EPA3 4W	4.47	15.93	*	**14	0.008	995
EPA4 4W	5.30	16.30	*	**9	0.006	808
EBC1 4W 25°C	4.31	15.81	39	82	0.003	2424
EBC2 4W 25°C	4.37	14.97	41	44	0.011	2502
EBA1 4W 25°C	4.17	16.37	25	62	0.029	1895
EBA2 4W 25°C	4.60	16.25	30	73	0.033	2089
EPA1 4W 25°C	4.10	16.02	23	48	0.027	1490
EPA2 4W 25°C	5.03	16.51	14	35	0.036	852
EPC1 4W 25°C	4.81	15.52	33	36	0.011	2628
EPC2 4W 25°C	4.71	15.43	18	45	0.034	1148

\*specimens broke before 1% strain

\*\*specimen fractured at maximum measured stress

Table A1 3: Bending test result for FRP specimens (ASTM D790)

Material	Width (mm)	Thickness (mm)	Flexural Stress, $\sigma_f$ at 1% Strain (MPa)	Maximum Measured Stress (MPa)	Strain at Maximum Measured Stress	Modulus (MPa)
UP1	14.55	7.40	108	234	0.023	9843
UP2	13.70	7.80	92	207	0.027	8092
UB1	16.70	6.70	84	208	0.027	7636
UB2	16.40	6.50	93	227	0.027	8311
EBA1	16.45	6.90	46	110	0.028	4809
EBA2	16.80	6.70	60	104	0.020	5094
EPA1	14.70	8.15	48	113	0.028	3796
EPA2	14.20	8.15	43	100	0.029	3597
EBC1	16.35	6.60	78	192	0.029	6759
EBC2	15.60	6.60	78	141	0.019	7253
EPC1	14.20	7.60	68	196	0.032	6143
EPC2	14.50	7.40	72	190	0.029	6455

Table A1 4 Tensile test results for laterally loaded pipe sections

Material	Force per unit length for first failure (kN/cm)	Deflection at the first failure (mm)	Slope of straight line portion of curve ( $\frac{kN/mm}{mm}$ )	Deflection at Max <sup>m</sup> . Force (mm)	Maxi <sup>m</sup> . Force (kN/cm)	Area Under the curve (kN)
H150_1	1.62	8.35	0.020	15.39	1.84	1.8
H150_2	1.54	6.93	0.023	10.42	1.75	2.5
H150_3	1.49	7.00	0.022	10.83	1.78	3.5
H150Acid1W_1	1.28	8.83	0.016	14.57	1.60	2.1
H150 Acid 1W_2	1.35	7.37	0.019	12.91	1.60	1.5
H150 Acid 4W_1	1.10	6.15	0.018	10.69	1.66	1.5
H150 Acid 4W_2	1.27	8.05	0.017	17.36	1.37	1.9
H150 Co sp el 13H	1.54	8.12	0.021	13.77	1.68	1.7
H150 Co sp el 2W	1.39	5.92	0.025	21.00	1.73	2.0
H150 Co sp el 1W_1	1.59	8.86	0.018	13.33	1.73	2.5
H150 Co sp el 1W_2	1.52	8.88	0.018	12.57	1.73	2.2
P150_1	1.50	7.83	0.021	12.32	1.87	2.3
P150_2	1.52	8.66	0.021	13.16	1.89	2.2
P150_3	1.47	7.20	0.022	12.82	1.68	2.0
P150 Co sp el 13H 20C	1.64	8.22	0.022	11.97	1.77	2.6
P150 Co sp el 13H	1.50	8.02	0.020	18.30	1.69	2.6

P150 Air 13H	1.83	8.15	0.024	15.05	2.37	
P150 Water 13H 80C	1.87	8.66	0.023	12.18	2.00	3.0
P150 Co sp el 1W_1	1.40	6.19	0.024	14.40	1.77	2.0
P150 Co sp el 1W _2	1.48	7.13	0.022	10.14	1.68	2.5
P150 Co sp el 2W	1.55	7.13	0.023	15.35	2.03	2.1
P150 Acid 1W_1	1.52	8.72	0.018	12.65	1.69	2.2
P150 Acid 1W_2	1.32	8.13	0.017	16.19	1.70	1.9
P150 Acid 4W_1	1.18	7.54	0.017	11.40	1.37	1.7
P150 Acid 4W_2	1.35	8.08	0.017	16.14	1.73	1.9
P150 Co sp el 1W_3	1.26	8.49	0.016	16.26	1.89	4.9

## APPENDIX 2: SAMPLE RAW DATA

Sample of raw data (partial) from test result of fibre reinforced bisphenol A epoxy vinyl ester exposed to cobalt spent electrolyte for four weeks

NI VI Logger

Created: 5/31/2010 3:54:31.146 PM Newfoundland Daylight Time

Number of scans: 546

Scan rate: 0.2 seconds

Row,Time,Deflection mm(Voltage),Applied Load kN(Voltage)

1,3:32:41.234 PM,22.8271,-0.0244141
2,3:32:41.434 PM,22.8271,-0.0244141
3,3:32:41.634 PM,22.8271,-0.0244141
4,3:32:41.834 PM,22.8271,-0.0244141
5,3:32:42.034 PM,22.8271,-0.0244141
6,3:32:42.234 PM,22.8271,-0.0244141
7,3:32:42.434 PM,22.8271,-0.0244141
8,3:32:42.634 PM,22.8516,-0.0244141
9,3:32:42.834 PM,22.8271,-0.0244141
10,3:32:43.034 PM,22.8271,-0.0244141
11,3:32:43.234 PM,22.8271,-0.0244141
12,3:32:43.434 PM,22.8271,-0.0244141
13,3:32:43.634 PM,22.8516,-0.0244141
14,3:32:43.834 PM,22.8271,-0.0244141
15,3:32:44.034 PM,22.8271,-0.0244141

16,3:32:44.234 PM,22.8027,-0.0292969  
17,3:32:44.434 PM,22.7783,-0.0292969  
18,3:32:44.634 PM,22.7539,-0.0341797  
19,3:32:44.834 PM,22.7051,-0.0390625  
20,3:32:45.034 PM,22.7051,-0.0390625  
21,3:32:45.234 PM,22.7051,-0.0390625  
22,3:32:45.434 PM,22.6807,-0.0390625  
23,3:32:45.634 PM,22.6563,-0.0439453  
24,3:32:45.834 PM,22.6318,-0.0439453  
25,3:32:46.034 PM,22.6074,-0.0439453  
26,3:32:46.234 PM,22.6074,-0.0488281  
27,3:32:46.434 PM,22.583,-0.0488281  
28,3:32:46.634 PM,22.5586,-0.0537109  
29,3:32:46.834 PM,22.5342,-0.0537109  
30,3:32:47.034 PM,22.5098,-0.0585938  
31,3:32:47.234 PM,22.5098,-0.0585938  
32,3:32:47.434 PM,22.4854,-0.0585938  
33,3:32:47.634 PM,22.4609,-0.0634766  
34,3:32:47.834 PM,22.4365,-0.0634766  
35,3:32:48.034 PM,22.4365,-0.0683594  
36,3:32:48.234 PM,22.3877,-0.0683594  
37,3:32:48.434 PM,22.3633,-0.0683594  
38,3:32:48.634 PM,22.3633,-0.0732422  
39,3:32:48.834 PM,22.3389,-0.0732422  
40,3:32:49.034 PM,22.3145,-0.078125  
41,3:32:49.234 PM,22.3145,-0.078125

42,3:32:49.434 PM,22.2656,-0.0830078  
43,3:32:49.634 PM,22.2656,-0.0830078  
44,3:32:49.834 PM,22.2168,-0.0878906  
45,3:32:50.034 PM,22.1924,-0.0878906  
46,3:32:50.234 PM,22.2168,-0.0878906  
47,3:32:50.434 PM,22.1924,-0.0878906  
48,3:32:50.634 PM,22.1191,-0.0927734  
49,3:32:50.834 PM,22.1436,-0.0927734  
50,3:32:51.034 PM,22.1436,-0.0927734  
51,3:32:51.234 PM,22.0947,-0.102539  
52,3:32:51.434 PM,22.0703,-0.102539  
53,3:32:51.634 PM,22.0459,-0.102539  
54,3:32:51.834 PM,22.0215,-0.107422  
55,3:32:52.034 PM,22.0215,-0.107422  
56,3:32:52.234 PM,21.9971,-0.107422  
57,3:32:52.434 PM,21.9727,-0.112305  
58,3:32:52.634 PM,21.9482,-0.112305  
59,3:32:52.834 PM,21.9238,-0.117188  
60,3:32:53.034 PM,21.9238,-0.117188  
61,3:32:53.234 PM,21.8994,-0.117188  
62,3:32:53.434 PM,21.875,-0.12207  
63,3:32:53.634 PM,21.8506,-0.12207  
64,3:32:53.834 PM,21.8506,-0.12207  
65,3:32:54.034 PM,21.8262,-0.126953  
66,3:32:54.234 PM,21.8018,-0.126953  
67,3:32:54.434 PM,21.7773,-0.131836

68,3:32:54.634 PM,21.7529,-0.131836  
69,3:32:54.834 PM,21.7529,-0.136719  
70,3:32:55.034 PM,21.7285,-0.136719  
71,3:32:55.234 PM,21.7041,-0.136719  
72,3:32:55.434 PM,21.6797,-0.141602  
73,3:32:55.634 PM,21.6553,-0.141602  
74,3:32:55.834 PM,21.6309,-0.141602  
75,3:32:56.034 PM,21.6064,-0.146484  
76,3:32:56.234 PM,21.6064,-0.146484  
77,3:32:56.434 PM,21.582,-0.151367  
78,3:32:56.634 PM,21.5576,-0.151367  
79,3:32:56.834 PM,21.5332,-0.15625  
80,3:32:57.034 PM,21.5332,-0.15625  
81,3:32:57.234 PM,21.5088,-0.15625  
82,3:32:57.434 PM,21.4844,-0.161133  
83,3:32:57.634 PM,21.46,-0.161133  
84,3:32:57.834 PM,21.4355,-0.161133  
85,3:32:58.034 PM,21.4355,-0.166016  
86,3:32:58.234 PM,21.4111,-0.170898  
87,3:32:58.434 PM,21.3867,-0.170898  
88,3:32:58.634 PM,21.3623,-0.170898  
89,3:32:58.834 PM,21.3379,-0.175781  
90,3:32:59.034 PM,21.3135,-0.175781  
91,3:32:59.234 PM,21.3135,-0.180664  
92,3:32:59.434 PM,21.2891,-0.180664  
93,3:32:59.634 PM,21.2646,-0.180664

94,3:32:59.834 PM,21.2402,-0.180664  
95,3:33:00.034 PM,21.2158,-0.185547  
96,3:33:00.234 PM,21.1914,-0.185547  
97,3:33:00.434 PM,21.1914,-0.19043  
98,3:33:00.634 PM,21.167,-0.19043  
99,3:33:00.834 PM,21.1426,-0.195313  
100,3:33:01.034 PM,21.1182,-0.195313  
101,3:33:01.234 PM,21.1182,-0.195313  
102,3:33:01.434 PM,21.0938,-0.200195  
103,3:33:01.634 PM,21.0693,-0.200195  
104,3:33:01.834 PM,21.0449,-0.205078  
105,3:33:02.034 PM,21.0205,-0.205078  
106,3:33:02.234 PM,20.9961,-0.205078  
107,3:33:02.434 PM,20.9717,-0.209961  
108,3:33:02.634 PM,20.9717,-0.214844  
109,3:33:02.834 PM,20.9229,-0.214844  
110,3:33:03.034 PM,20.9229,-0.214844  
111,3:33:03.234 PM,20.8984,-0.214844  
112,3:33:03.434 PM,20.874,-0.219727  
113,3:33:03.634 PM,20.8496,-0.219727  
114,3:33:03.834 PM,20.8496,-0.224609  
115,3:33:04.034 PM,20.8252,-0.224609  
116,3:33:04.234 PM,20.8008,-0.229492  
117,3:33:04.434 PM,20.7764,-0.229492  
118,3:33:04.634 PM,20.752,-0.229492  
119,3:33:04.834 PM,20.752,-0.234375

120,3:33:05.034 PM,20.7275,-0.234375  
121,3:33:05.234 PM,20.7031,-0.234375  
122,3:33:05.434 PM,20.6787,-0.234375  
123,3:33:05.634 PM,20.6543,-0.239258  
124,3:33:05.834 PM,20.6543,-0.244141  
125,3:33:06.034 PM,20.6299,-0.244141  
126,3:33:06.234 PM,20.6055,-0.244141  
127,3:33:06.434 PM,20.5811,-0.249023  
128,3:33:06.634 PM,20.5566,-0.249023  
129,3:33:06.834 PM,20.5322,-0.253906  
130,3:33:07.034 PM,20.5078,-0.253906  
131,3:33:07.234 PM,20.5078,-0.253906  
132,3:33:07.434 PM,20.4834,-0.258789  
133,3:33:07.634 PM,20.459,-0.258789  
134,3:33:07.834 PM,20.4346,-0.263672  
135,3:33:08.034 PM,20.4102,-0.263672  
136,3:33:08.234 PM,20.3857,-0.263672  
137,3:33:08.434 PM,20.3857,-0.268555  
138,3:33:08.634 PM,20.3613,-0.268555  
139,3:33:08.834 PM,20.3369,-0.268555  
140,3:33:09.034 PM,20.3125,-0.273438  
141,3:33:09.234 PM,20.2881,-0.273438  
142,3:33:09.434 PM,20.2637,-0.27832  
143,3:33:09.634 PM,20.2637,-0.27832  
144,3:33:09.834 PM,20.2393,-0.27832  
145,3:33:10.034 PM,20.2148,-0.283203